

ANALYSIS OF THE DUAL-EXCITED SYNCHRONOUS MACHINE
WITH SPECIAL REFERENCE TO ITS DYNAMIC STABILITY

A Thesis Submitted to
the Faculty of Graduate Studies
in Partial Fulfilment of the Requirements for
the Degree of Master of Science
in The Department of
Electrical Engineering
University of Saskatchewan

by
Mohamad Abd El-Raheim Badr

November 1971

The author claims copyright. Use shall not be made of the material contained herein without proper acknowledgement, as indicated on the following page.

The author has agreed that the Library, University of Saskatchewan, may make this thesis freely available for inspection. Moreover, the author has agreed that permission for extensive copying of this thesis for scholarly purposes may be granted by the professor or professors who supervised the thesis work recorded herein or, in their absence, by the Head of the Department or the Dean of the College in which this thesis work was done. It is understood that due recognition will be given to the author of this thesis and to the University of Saskatchewan in any use of the material in this thesis. Copying or publication or any other use of the thesis for financial gain without approval by the University of Saskatchewan and the author's written permission is prohibited.

Requests for permission to copy or to make other use of material in this thesis or in part should be addressed to:

Head of the Department of Electrical Engineering
University of Saskatchewan
Saskatoon, Canada.

ACKNOWLEDGEMENT

The author wishes to express his gratitude to Dr. A. M. El-Serafi for the assistance and encouragement which he gave during the course of this work.

Acknowledgement of financial support given by the National Research Council of Canada under Grants No. A-7115 and No. C-0343 is made.

UNIVERSITY OF SASKATCHEWAN

Electrical Engineering Abstract 71A141

"ANALYSIS OF THE DUAL-EXCITED SYNCHRONOUS MACHINE
WITH SPECIAL REFERENCE TO ITS DYNAMIC STABILITY"

Student: M. A. Badr

Supervisor: Dr. A. M. El-Serafi

M.Sc. Thesis Presented to the College of Graduate Studies November 1971.

ABSTRACT

In the recent past, attention has been directed towards the possibility of using properly controlled dual-excited synchronous machines to overcome the existing stability limitation of the conventional ones.

This thesis presents a generalized analysis for the dual-excited synchronous machine, in which the two field windings are not necessarily located on the rotor-axes, and may not have equal number of turns or equal inclination angles to the direct-axis of the pole structure. In deriving the general equations, the external connection is considered in a general form so as to allow for studying the machine performance when it is connected to an infinite-bus through a general transmission system. The small displacement equations are then derived and arranged in a form suitable for investigating the dynamic stability when different excitation control schemes are used.

The improved dynamic stability of the dual-excited synchronous generator is demonstrated by studying a simple power system. For this, a digital computer program has been established. The results show that this machine has superior dynamic stability boundaries compared with those of a conventional synchronous machine especially at no load as well as at low power demand.

This research has been supported by the National Research Council of Canada Grants No. A-7115 and No. C-0343.

TABLE OF CONTENTS

	Page
Copyright	ii
Acknowledgement	iii
Abstract	iv
Table of Contents	v
List of Figures	viii
List of Symbols	xii
<u>1. INTRODUCTION</u>	<u>1</u>
<u>2. STABILITY PROBLEM OF SYNCHRONOUS MACHINES</u>	<u>3</u>
2.1 Introduction	3
2.2 Transient Stability	3
2.2.1 Methods for improving transient stability	6
2.2.2 Improving transient stability by the dual-excitation of synchronous generators	6
2.3 Steady-State Stability	10
2.3.1 Methods for improving steady-state stability	13
2.3.2 Improvement of dynamic stability by the dual-excitation of synchronous generators	16
2.4 Application of the Dual-Excitation to Turbo-Generators	18
2.5 Purpose of the Thesis	20
<u>3. ANALYSIS OF THE DUAL-EXCITED SYNCHRONOUS MACHINE</u>	<u>23</u>
3.1 Introduction	23
3.2 Mathematical Representation	25
3.2.1 Inductance equations	25
a) Stator self-inductances	25
b) Stator mutual-inductances	26
c) Mutual-inductances between stator and rotor circuits	27
d) Rotor self- and mutual-inductances	29
3.2.2 Flux linkage equations	29
3.2.3 Park's transformation	31
3.2.4 Voltage equations	32
3.2.5 Torque Equations	32
3.3 Per-Unit System for the Dual-Excited Synchronous Machine	33
3.3.1 Stator base values	34
3.3.2 Rotor base values	35
a) Power equality constraint	35
b) Inductance relations	36
c) Rotor base currents	37

TABLE OF CONTENTS (continued)

	Page
3.3.3 Per-unit time, speed and torque	38
3.4 Normalized Equations	40
3.4.1 Flux linkage equations	40
3.4.2 Voltage equations	41
3.4.3 Torque equations	41
3.4.4 The operational equations	42
3.5 Dual-Excited Synchronous Machine Connected to an Infinite-Bus Through a General Transmission System	44
3.5.1 Analysis of the transmission system	44
3.5.2 Equations of the machine in connection with the system.	48
3.5.3 Steady-state equations	49
3.5.4 Simplified transient equations	50
3.5.5 Application to a simple power system	51
a) Steady-state equations	52
b) Simplified transient equations	52
<u>4. SMALL DISPLACEMENT EQUATIONS OF THE DUAL-EXCITED SYNCHRONOUS MACHINE</u>	<u>53</u>
4.1 Introduction	53
4.2 Possible Techniques for Dynamic Stability Studies	54
4.3 Small Displacement Equations	56
4.4 Machine Regulation	60
4.5 Application to a Simple Power System	67
<u>5. EXTENSION OF THE UNDER-EXCITED STABLE REGION OF THE DUAL-EXCITED SYNCHRONOUS GENERATOR</u>	<u>71</u>
5.1 Introduction	71
5.2 Method of Investigation	74
5.3 Static Stability Boundaries and Capability Diagram	77
5.4 Dynamic Stability Boundaries	81
5.4.1 Effect of voltage regulators	81
5.4.2 Effect of rotor-angle regulators	86
a) Control of field winding 1	86
b) Control of field winding 2	88
c) Control of both field windings	95
5.4.3 Operation with fixed rotor-angle	95
a) Control of field winding 2	98
b) Control of field winding 1	102
c) Control of both field windings	102

TABLE OF CONTENTS (continued)

	Page
<u>6. CONCLUSIONS</u>	108
6.1 General	108
6.2 Analysis	108
6.3 Static-Stability Boundaries and Capability Diagram	109
6.4 Dynamic Stability Boundaries	110
6.5 Recommendations for Future Work	113
<u>7. REFERENCES</u>	114
<u>8. APPENDICES</u>	117
Appendix A - Limitations of the Conventional Synchronous Machine Excitation Control at No Load	117
Appendix B - Limitations of the Dual-Excited Synchronous Machine Excitation Control at No Load	123
Appendix C - Expressions for the Operational Functions of the Dual-Excited Synchronous Machine	130
Appendix D - Steady-State Vector Diagram of the Dual- Excited Synchronous Machine	133
Appendix E - Power/Angle Characteristic of the Dual- Excited Synchronous Machine	138
Appendix F - Flow Chart of the Dual-Excited Synchronous Machine Dynamic Stability Program	142
Appendix G - Typical Computer Results	145

LIST OF FIGURES

Figure		Page
2.1	Vector Diagram of a Nonsalient-pole Synchronous Generator Connected to an Infinite-Bus through a Series Reactance	4
2.2	Transient Power/Angle Characteristic of a Conventional Synchronous Generator	5
2.3	Field Windings Arrangement in Synchronous Machines	8
2.4	Steady-state Power/Angle Characteristics of a d-q Synchronous Generator	9
2.5	Static Stability Boundaries of a Nonsalient-Pole Conventional Synchronous Generator	12
2.6	Static Stability Boundaries of a Salient-Pole Conventional Synchronous Generator	12
2.7	Approximate Cost of Increasing Short Circuit Ratio of Typical Large Waterwheel Generators	14
2.8	Effect of Excitation Control on the Steady-State Stability Boundary of a Nonsalient-Pole Conventional Synchronous Generator	15
2.9	Vector Diagram of a d-q Synchronous Generator	17
2.10	Divided-Winding Rotor of a Turbo-Alternator	19
2.11	Schematic Layout of a Dual-Excited Synchronous Machine	21
3.1	Schematic Layout of an Idealized Dual-Excited Synchronous Machine	24
3.2	A Simple Power System	51
4.1	Single line Block Diagram for the Excitation Control of a Dual-Excited Synchronous Machine	61
5.1	Schematic Single Line Diagram of the Studied System	72
5.2	Block Diagram of the Regulator used for each Field Winding	73
5.3	Steady-State Capability Diagram of the Unregulated Dual-Excited Synchronous Generator	78
5.4	Static Stability Boundaries of the Dual-Excited Synchronous Machine for Different Ratios of Excitation Currents	79

LIST OF FIGURES (continued)

Figure	Page
5.5 Total Field Copper Losses of the Dual-Excited Synchronous Generator for Different Ratios of Excitation Currents (P=1.0 p.u.)	80
5.6 Distribution of Copper Losses between the two field windings of the Dual-Excited Synchronous Generator for Different Ratios of Excitation Currents (P=1.0 p.u.)	82
5.7 Dynamic Stability Boundaries of the Dual-Excited Synchronous Generator for Operation with Equally Excited Field Windings (Field Winding 1 is Controlled by a Voltage Regulator)	84
5.8 Dynamic Stability Boundaries of the Dual-Excited Synchronous Generator for Operation with Equally Excited Field Windings (Field Winding 2 is Controlled by a Voltage Regulator)	85
5.9 Dynamic Stability Boundaries ($Q-\mu_a$) of the Dual-Excited Synchronous Generator for Operation with Equally Excited Field Windings (Field Winding 1 is Controlled by a Rotor-Angle Regulator)	87
5.10 Vector Representation of the Dual-Excited Synchronous Machine at No Load (Field Winding 1 is Controlled)	89
5.11 Dynamic Stability Boundaries (P-Q) of the Dual-Excited Synchronous Generator for Operation with Equally Excited Field Windings (Field Winding 1 is Controlled by a Rotor-Angle Regulator)	90
5.12 Dynamic Stability Boundaries ($Q-\mu_a$) of the Dual-Excited Synchronous Generator for Operation with Equally Excited Field Windings (Field Winding 2 is Controlled by a Rotor-Angle Regulator)	91
5.13 Vector Representation of the Dual-Excited Synchronous Machine at No Load (Field Winding 2 is Controlled)	93
5.14 Dynamic Stability Boundaries (P-Q) of the Dual-Excited Synchronous Generator for Operation with Equally Excited Field Windings (Field Winding 2 is Controlled by a Rotor-Angle Regulator)	94
5.15 Steady-State Vector Diagram of the Dual-Excited Synchronous Generator ($\delta=\alpha_1$, resistance neglected)	97
5.16 Dynamic Stability Boundaries of the Dual-Excited Synchronous Generator for Operation with Fixed Rotor-Angle (Field Winding 2 is Controlled by a Rotor-Angle Regulator, $\delta=\alpha_1$)	99

LIST OF FIGURES (continued)

Figure	Page
5.17 Dynamic Stability Boundaries of the Dual-Excited Synchronous Generator for Operation with Fixed Rotor-Angle ($P=0.0$, Field Winding 2 is Controlled by a Rotor-Angle Regulator)	100
5.18 Dynamic Stability Boundaries of the Dual-Excited Synchronous Generator for Operation with Fixed Rotor-Angle ($P=1.0$ p.u., Field Winding 2 is controlled by a Rotor-Angle Regulator)	101
5.19 Total Field Copper Losses of the Dual-Excited Synchronous Generator for Different Rotor-Angles. ($P=1.0$ p.u.)	103
5.20 Distribution of Copper Losses between the two Field Windings of the Dual-Excited Synchronous Generator for Different Rotor Angles ($P=1.0$ p.u.)	104
5.21 Dynamic Stability Boundaries of the Dual-Excited Synchronous Generator for Operation with Fixed Rotor-Angle ($P=0.0$, Field Winding 1 is Controlled by a Rotor-Angle Regulator)	105
5.22 Dynamic Stability Boundaries of the Dual-Excited Synchronous Generator for Operation with Fixed Rotor-Angle ($P=0.0$, Field Winding 1 is Controlled by a Voltage Regulator while Field Winding 2 is Controlled by a Rotor-Angle Regulator, $\delta=\alpha_1$)	106
8.1 Transfer Functions of the Conventional Synchronous Machine	120
8.2 Transfer Functions of the Dual-Excited Synchronous Machine	126
8.3 Armature Current and Voltage Representation in a Complex Plane	133
8.4 Steady-State Vector Diagram of the Dual-Excited Synchronous Machine	137
8.5 Steady-State Vector Diagram of a Dual-Excited Synchronous Machine Connected to an Infinite-Bus Through a Simple Tie-Line	139
8.6 Steady-State Power/Angle Characteristics of the Dual-Excited Synchronous Machine	141

LIST OF FIGURES (continued)

Figure		Page
8.7	Typical Computer Results for the Dynamic Stability Boundaries (P-Q) of the Dual-Excited Synchronous Generator when Operated with Equally Excited Field Windings (Field Winding 2 is Controlled by a Rotor-Angle Regulator, $C_{2\delta}=1$)	145
8.8	Typical Computer Results for the Dynamic Stability Boundaries (P-Q) of the Dual-Excited Synchronous Generator when Operated with Equally Excited Field Windings (Field Winding 2 is Controlled by a Rotor-Angle Regulator, $C_{2\delta}=-1$)	146
8.9	Typical Computer Results for the Dynamic Stability Boundaries (Q- μ^a) of the Dual-Excited Synchronous Generator for Operation with Fixed Rotor-Angle (Field Winding 2 is Controlled by a Rotor-Angle Regulator, $\delta=90^\circ$)	147

LIST OF SYMBOLS

e	resultant electromotive force before disturbance
e_d, e_q	d- and q-axis component of e respectively
E	r.m.s. value of e
E_d, E_q	d- and q-axis component of E respectively
e_1	resultant electromotive force when field winding 1 only is excited
e_2	resultant electromotive force when field winding 2 only is excited
E_1, E_2	r.m.s. value of e_1 and e_2 respectively
$g_D(p)$	governor transfer function
$g_{R1}(p), g_{R2}(p)$	field winding 1 and 2 regulator transfer function respectively
$G(p)$	field operational function (in a conventional synchronous machine)
H	inertia constant of the machine and its prime mover in seconds
$\text{Im} [\]$	imaginary part of []
i	infinite-bus current
i_d, i_q	d- and q-axis component of i respectively
i_{ta}, i_{tb}, i_{tc}	phase a, phase b and phase c armature current respectively
i_{td}, i_{tq}	d- and q-axis component of armature current respectively
i_o	infinite-bus current before disturbance
i_{do}, i_{qo}	d- and q-axis component of i_o respectively
i_{to}	phase a armature current before disturbance
i_{tdo}, i_{tqo}	d- and q-axis component of i_{to} respectively

I_o	r.m.s. value of i_o
I_{do}, I_{qo}	d- and q-axis component of I_o respectively
I_{to}	r.m.s. value of i_{to}
I_{tdo}, I_{tqo}	d- and q-axis component of I_{to} respectively
i_{f1}, i_{f2}	field winding 1 and 2 current respectively
i_{f1o}, i_{f2o}	field winding 1 and 2 current before disturbance respectively
i_{fd}, i_{fq}	d- and q-axis field winding current respectively (in a d-q machine)
i_{kd}, i_{kq}	d- and q-axis damper winding current respectively
I_{f1B}, I_{f2B}	field winding 1 and 2 base current respectively
I_{kdB}, I_{kqB}	d- and q-axis damper winding base current respectively
I_{sB}	stator base current
J	inertia constant of the machine and its prime mover in $K_g \cdot m^2$
K_e	exciter constant
K_f	ratio between field winding 1 and 2 exciting currents
L_{aa}, L_{bb}, L_{cc}	phase a, phase b and phase c self-inductance respectively
$L_{ab} = L_{ba}$	mutual-inductance between phase a and phase b
$L_{ac} = L_{ca}$	mutual-inductance between phase a and phase c
$L_{bc} = L_{cb}$	mutual-inductance between phase b and phase c
L_{ad}, L_{aq}	d- and q-axis magnetizing-inductance respectively
$L_{akd} = L_{kda}$	mutual-inductance between d-axis damper winding and phase a of stator

$L_{bkd} = L_{kdb}$	mutual-inductance between d-axis damper winding and phase b of stator
$L_{ckd} = L_{kdc}$	mutual-inductance between d-axis damper winding and phase c of stator
$L_{akq} = L_{kqa}$	mutual-inductance between q-axis damper winding and phase a of stator
$L_{bkq} = L_{kqb}$	mutual-inductance between q-axis damper winding and phase b of stator
$L_{ckq} = L_{kqc}$	mutual-inductance between q-axis damper winding and phase c of stator
L_{akdo}	maximum mutual-inductance between q-axis damper winding and phase a of stator
L_{akqo}	maximum mutual-inductance between q-axis damper winding and phase a of stator
L_d, L_q	d- and q-axis synchronous inductance respectively
L_{ff1}, L_{ff2}	self-inductance of field winding 1 and 2 respectively
$L_{f1f2} = L_{f2f1}$	mutual-inductance between field winding 1 and 2
L_{kkd}, L_{kkq}	self-inductance of d- and q-axis damper winding respectively
L_{kdf1}, L_{kdf2}	mutual-inductance between d-axis damper winding and field winding 1 and 2 respectively
L_{kqf1}, L_{kqf2}	mutual-inductance between q-axis damper winding and field winding 1 and 2 respectively
L_{f1B}, L_{f2B}	field winding 1 and 2 base inductance respectively
L_{kdB}, L_{kqB}	d- and q-axis damper winding base inductance respectively
L_{sB}	stator base inductance
L_{σ}	armature leakage inductance
N_{f1}, N_{f2}	field winding 1 and 2 effective number of turns respectively
N_{kd}, N_{kq}	d- and q-axis damper winding effective number of turns respectively

N_s	stator effective number of turns per phase
n_p	number of pole pairs
P	active power delivered to the infinite-bus
p	differential operator $\frac{d}{dt}$
Q	reactive power delivered to the infinite bus
$\text{Re}[\]$	real part of []
R_e	external resistance
r	armature resistance
r_{f1}, r_{f2}	field winding 1 and 2 resistnace respectively
r_{fd}	d-axis field winding resistance (in a conventional machine)
r_{kd}, r_{kq}	d- and q-axis damper winding resistance respectively
t	time in seconds
T_i	shaft torque
v_{f1}, v_{f2}	field winding 1 and 2 exciting voltage respectively
v_{fd}	d-axis field winding exciting voltage (in a conventional machine)
v_{f10}, v_{f20}	field winding 1 and 2 exciting voltage before disturbance respectively
v, v_t	bus-bar and machine terminal voltage respectively
v_a, v_b, v_c	phase a, phase b and phase c bus-bar voltage respectively
v_{ta}, v_{tb}, v_{tc}	phase a, phase b and phase c machine terminal voltage respectively
v_d, v_q	d- and q-axis component of v respectively
v_{td}, v_{tq}	d- and q-axis component of v_t respectively
v_{d0}, v_{q0}	d- and q-axis component of v before disturbance respectively

v_{to}	phase a terminal voltage before disturbance
v_{tdo}, v_{tqo}	d- and q-axis component of v_{to} respectively
V_d, V_q	r.m.s. value of v_d and v_q respectively
V_{to}	r.m.s. value of v_{to}
V_{tdo}, V_{tqo}	d- and q-axis component of V_{to}
V_{f1B}, V_{f2B}	field winding 1 and 2 base voltage respectively
V_{kdB}, V_{kqB}	d- and q-axis damper winding base voltage respectively
V_{sB}	stator base voltage
x_e	external reactance
x_{ad}, x_{aq}	d- and q-axis magnetizing reactance respectively
x_d, x_q	d- and q-axis synchronous reactance respectively
\dot{x}_d	d-axis transient reactance
x_{ff1}, x_{ff2}	field winding 1 and 2 self reactance respectively
x_{f1f2}	mutual reactance between field winding 1 and 2
x_{kkd}, x_{kkq}	d- and q-axis damper winding self reactance respectively
$x_{a\sigma}$	armature leakage reactance
$x_{f1\sigma}, x_{f2\sigma}$	field winding 1 and 2 leakage reactance respectively
x_{kdo}, x_{kqo}	d- and q-axis damper winding leakage reactance respectively
T_a	amplifier time constant
T_e	exciter time constant

T_R	measuring devices time constant
T_s	feed-back stabilizing loop time constant
μ_a	amplifier gain
μ_s	feed-back stabilizing loop gain
δ	rotor angle
δ_e	power-angle
δ_o	rotor angle before disturbance
λ_d, λ_q	d- and q-axis equivalent permeance
α_1	angle between the axis of field winding 1 and the d-axis of the rotor
α_2	angle between the axis of field winding 2 and the d-axis of the rotor.
ψ_d, ψ_q	d- and q-axis armature flux linkage respectively
ψ_{f1}, ψ_{f2}	field winding 1 and 2 flux linkage respectively
ψ_{kd}, ψ_{kq}	d- and q-axis damper winding flux linkage respectively
$p\theta$	speed of the machine (elect. radians/sec)
$p\theta_o$	speed of the machine before disturbance (elect. radians/sec)
$p\theta_m$	speed of the machine (mech. radians/sec)
$p\theta_{mB}$	base mechanical speed
\textcircled{H}	inertia constant of the machine and its prime mover in per-unit
Δ	prefix to denote small changes about the initial operating point

1. INTRODUCTION

The rate of increase in production of electrical energy is such as to double the amount of installed plants each nine or ten years in all the highly developed, industrialized countries of the world. In the underdeveloped countries, the rate of plants installation and growth of consumption is even more rapid. This has resulted in greater inter-connection and larger systems, since this alone can ensure stability, continuity of supply, the most efficient use of plant and the most economical use of national resources. Accordingly, long high voltage transmission lines are needed to connect the remote electrical energy resources to the load centers. Moreover, for safety reasons and because of environmental accommodation, overhead transmission lines are now replaced by high voltage underground cables for power distribution in large towns.

As a consequence of the erection of such long high voltage transmission lines and the widespread use of underground cables, situation can arise in which the loads of synchronous machines become capacitive and they should operate in the under-excited region. The extent to which this is possible is severely limited by the stability of synchronous machines.

The present tendency towards building larger synchronous machines, which is dictated by economical reasons has made the stability problem more acute. Such large machines have higher reactances, which result in reducing appreciably their stability limits.

Many well-known techniques have been applied to improve these stability limits, but it appears that a situation has been reached beyond which further improvements are not seen for conventional synchronous machines especially at no load as well as at light loading. In the recent past, attention has been directed to the possibility of using properly controlled dual-excited synchronous machines to improve further the stability of power systems. The general analysis for such machines with special reference to their dynamic stability is the main concern of this thesis.

2. STABILITY PROBLEM OF SYNCHRONOUS MACHINES

2.1 Introduction

The stability of synchronous machines can be generally defined as their ability to remain in synchronism with other machines in the power system without excessive oscillations and to be able at the same time to supply all connected consumers without interruption. To simplify the handling of such a problem, it is a common practise to divide it into two main categories.

2.2 Transient Stability²⁻⁴

Power systems are often subjected to sudden large disturbances such as: sudden increments of load, faults, switching one or several lines out of the system, a combination of a fault and the subsequent isolation of the faulted part. For a certain fault occurring at a given location and cleared in a definite manner, there is a power limit which the loading cannot exceed without the system being exposed to a loss of synchronism. For this power limit, known as the transient stability limit, and a certain reactive power flow, there is definite phase difference between the electromotive force of the synchronous machine and the voltage at the terminals (Fig. 2.1). The phase of the terminal voltage is related to the resultant rotating field, while the phase of the electromotive force is related to the exciting field produced by the field winding.

For a simple system consisting of a conventional synchronous generator connected to an infinite-bus through a simple tie line, the transient power angle characteristic is given by Fig. 2.2. Neglecting

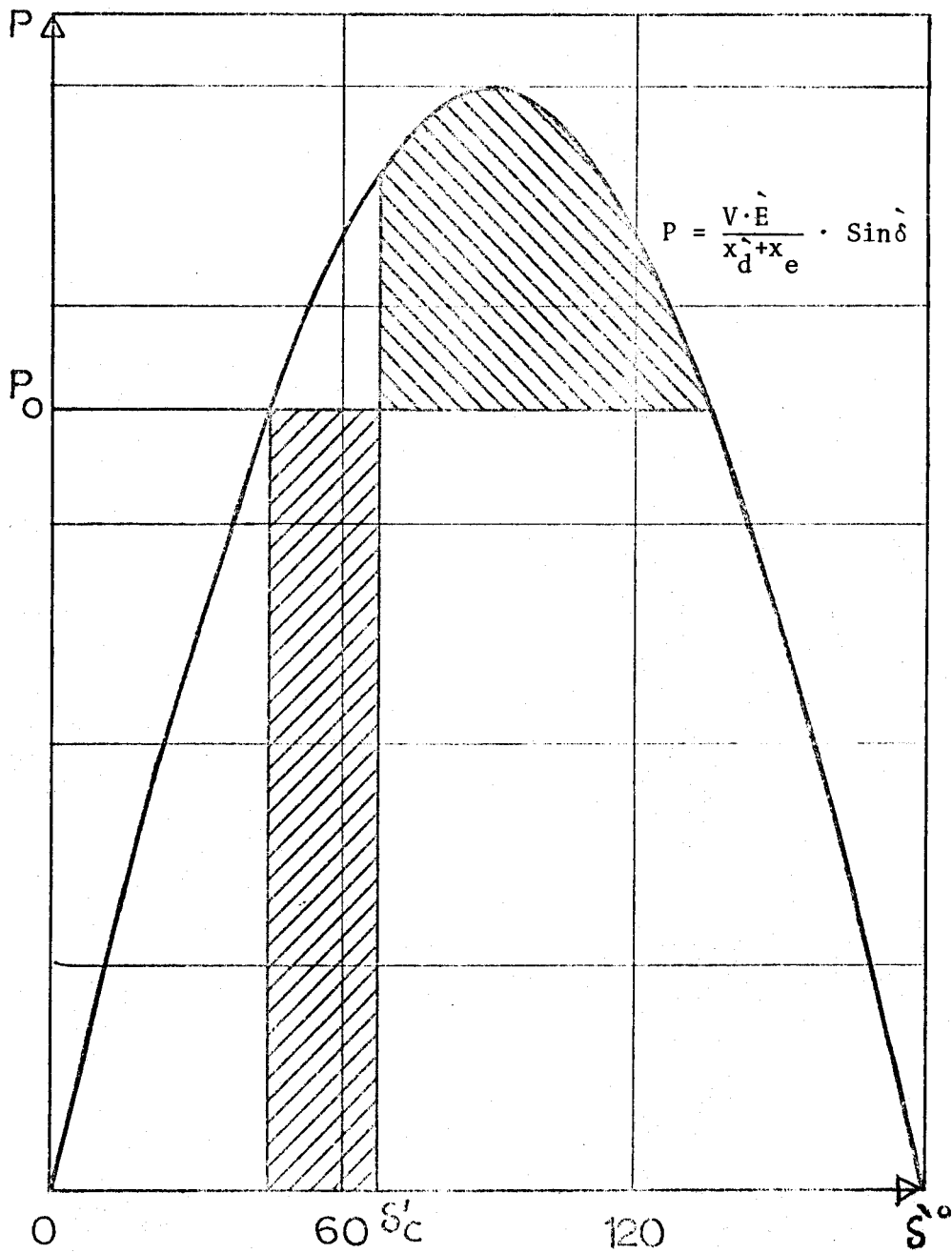


Fig. 2.2 Transient Power/Angle Characteristic of a Conventional Synchronous Generator (Transient Saliency Neglected)

transient saliency, the characteristic is approximately a sine wave having its crest equal to $V \cdot \hat{E} / (\hat{x}_d + x_e)$, where \hat{E} is the voltage of the machine behind its transient reactance. If a short circuit occurs on the tie line, the power output from the generator will be interrupted either completely or partly. Owing to the inertia inherent in the power regulation of the prime mover, the driving mechanical power cannot adapt itself to the new conditions without time lag. It follows that, for a short time, there is a surplus mechanical torque which tends to accelerate the rotor of the synchronous generator and so the transient load-angle δ increases. If the short circuit is not cleared before δ reaches a certain critical value δ_c , the generator will fall out of step.

2.2.1 Methods for improving transient stability

The most obvious method for improving the transient stability of power systems is to reduce the transfer reactance between synchronous machines, as this increases the synchronizing power that may be interchanged between them. High-speed circuit breakers and relays constitute a very important measure for increasing the transient stability by clearing the fault in the shortest time interval, and so limiting the effect of the disturbance. Control of the excitation of synchronous machines helps also to improve the transient stability by partially overcoming the demagnetizing effect within the machine through positively increasing the machine fluxes and terminal voltages^{5,6}.

2.2.2 Improving transient stability by the dual-excitation of synchronous generators

Among the methods used for improving the transient stability, it is noticed that there is no one dealing with a direct action on the load-

angle. The problem as seen from the machine point of view is that the magnetic-axis of the exciting field is attached to the physical-axis of the pole structure, and so it follows its movement. If this magnetic-axis is set free during the fault period, a situation can be reached at which the phase angle of the electromotive force in respect to the terminal voltage is maintained at values consistent with the synchronous operation.

Sapen²⁵ suggested the decoupling of the magnetic-axis of the exciting field from the physical-axis of the pole structure by providing the machine with an additional field winding acting on the quadrature-axis (Fig. 2.3). The d-q synchronous generator in this case has two identical field windings, one is continuously excited (direct-axis), while the other is excited only after the occurrence of a disturbance. To demonstrate the stabilizing effect of the quadrature-axis field winding, a simple power system is considered. As shown in Fig. 2.4, the system consists of a d-q generator connected to an infinite bus through two parallel transmission lines. On the occurrence of a three phase short circuit at point F, the change of the rotor angle due to the fault and the subsequent variations of the machine excitation is shown in Fig. 2.4. Curve 1 represents the power-angle characteristic for steady-state operation with only the direct-axis field winding excited. Curve 6 is the same as Curve 1 but with the quadrature-axis field winding only excited. Curves 2 - 5 represent different operating conditions. On the occurrence of a disturbance, the sequence of operation can be explained as follows:

Point A represents the steady-state operating point before the occurrence of the short circuit.

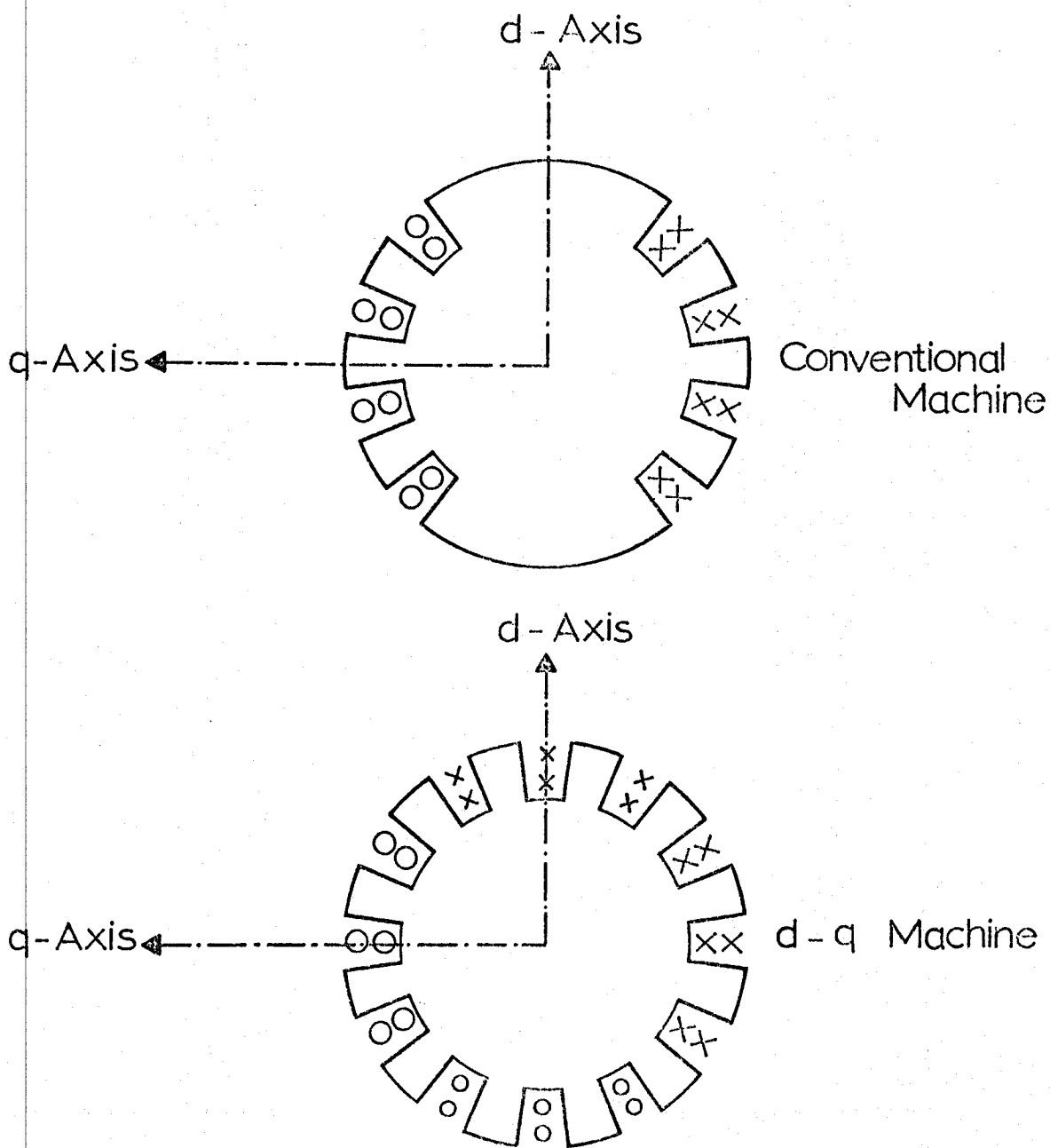


Fig. 2.3 Field Windings Arrangement in Synchronous Machines

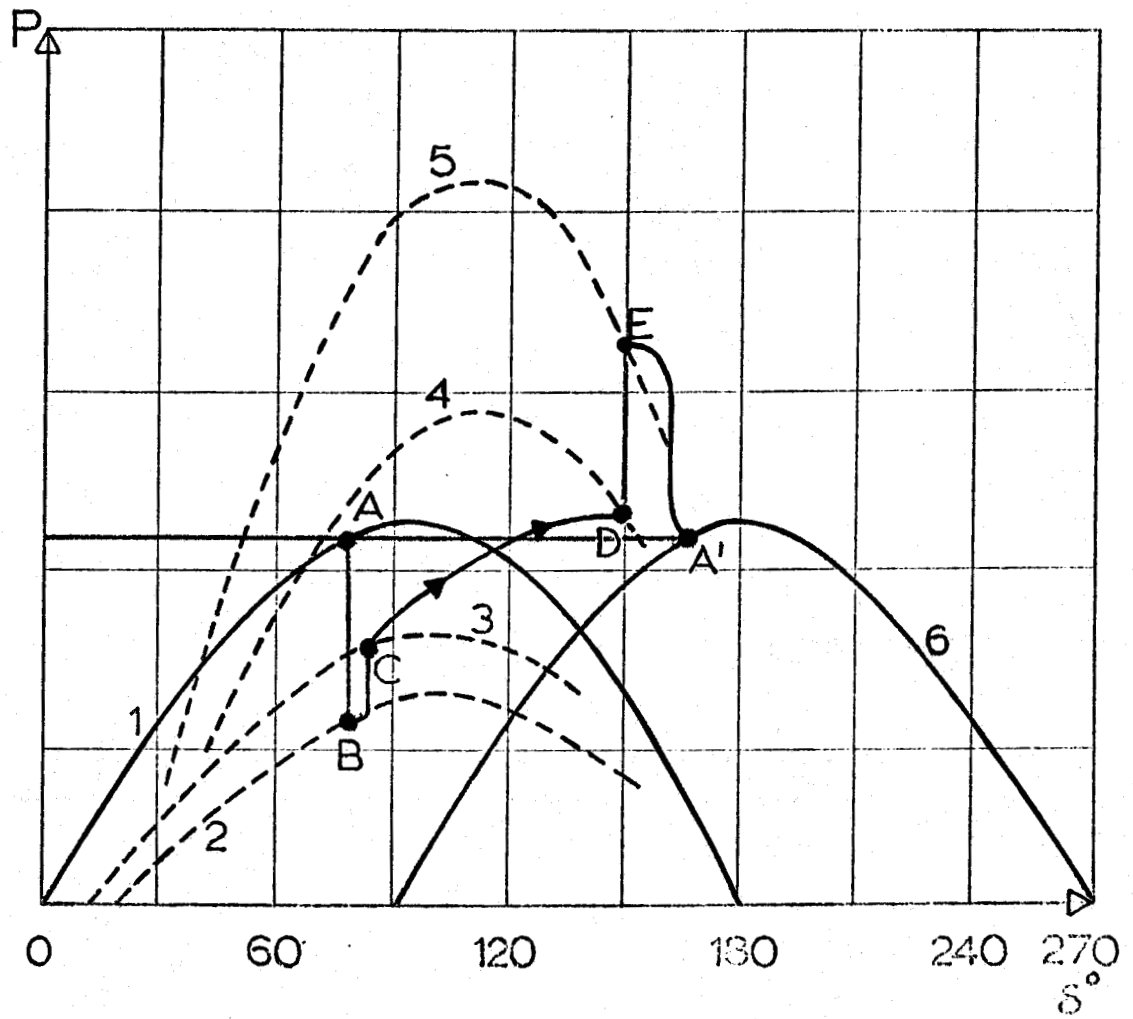
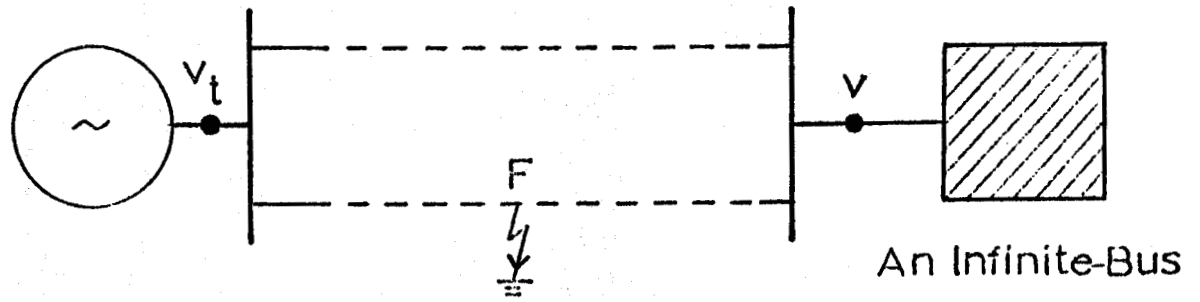


Fig. 2.4 Power/Angle Characteristics of a d-q Synchronous Generator

Point B is the operating point just after the occurrence of the short circuit, and at the same instant the quadrature-axis field winding begins to be excited.

Point C represents the situation after isolating the faulted line.

The path from C to D depends on the response of the exciters of both field windings as well as the inertia of the machine.

Points D and E are the operating points before and after reclosing respectively. At point E, it is no more necessary to keep on the excitation of the direct-axis field winding, and so it can be gradually reduced. The machine can, then, run steadily with only its quadrature-axis field winding excited. To resume normal operation, with the direct-axis field winding only excited, it is sufficient to energize the direct-axis field winding under the control of its voltage regulator, while reducing at the same time the excitation current of the quadrature-axis field winding gradually to zero. It may be expected that the increase of the cost of d-q synchronous generators will be only a fraction of the economical advantages gained by their use in power systems²⁶. It must, however, be noted that this cost increase may be counterbalanced by the possibility of using machines without damping windings, since the two field windings do its function in this case.

2.3 Steady-State Stability^{1,3,4}

While the transient stability of synchronous machines is the measure of their ability to remain in synchronism after a specific sudden, severe disturbance, the steady-state stability is the measure of their ability to remain in synchronism for small disturbances. Small disturbances, such as those produced by small changes of load, irregularities in prime-movers and manual or automatic control of excitation, are always

present in power systems. A synchronous machine does not go out of step because of such minute disturbances unless it is operating at or near its steady-state stability limit.

Steady-state stability can be classified into two categories:

a) Static stability: It denotes the stability of the machine when the disturbance is slow compared with the natural frequency of the mechanical oscillations and also with the rate of change of the field flux linkage. Thus, it is not necessary in this case to consider the transient behaviour of the machine, its regulators and the system to which it is connected.

b) Dynamic stability: It refers to the stability of the synchronous machines for relatively fast, small disturbances. In this case, the transient behaviour of the machine, its regulators and the system to which it is connected must be taken into consideration.

The steady-state stability problem of synchronous generators has become more acute in recent years as a consequence of the new developments in electric power systems. Such developments, as the establishment of more long high voltage transmission lines and the widespread use of underground cables, have brought about a change in the conditions under which synchronous generators operate. Because of the large capacitive power needed by the power network, synchronous generators often operate at leading power factors and may have to work beyond their normal static stability limit.

It is clear from the power diagrams shown in Figures 2.5 and 2.6 that the maximum capacitive power, which a synchronous generator with fixed excitation can supply for stable operation (static stability

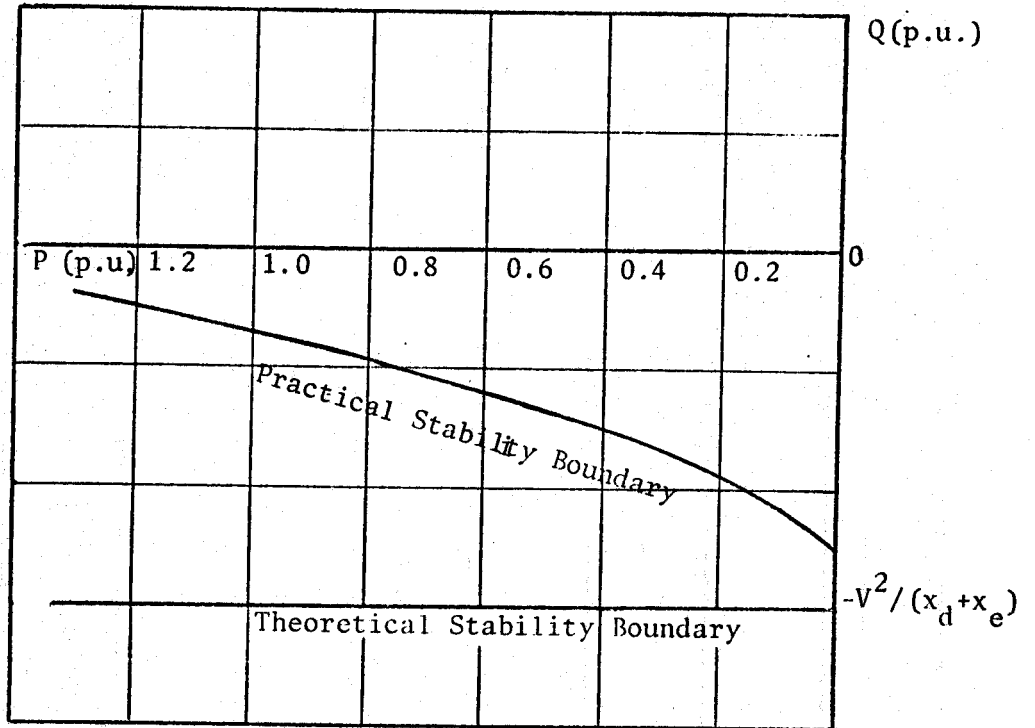


Fig. 2.5 Static Stability Boundaries of a Nonsalient-Pole Conventional Synchronous Generator

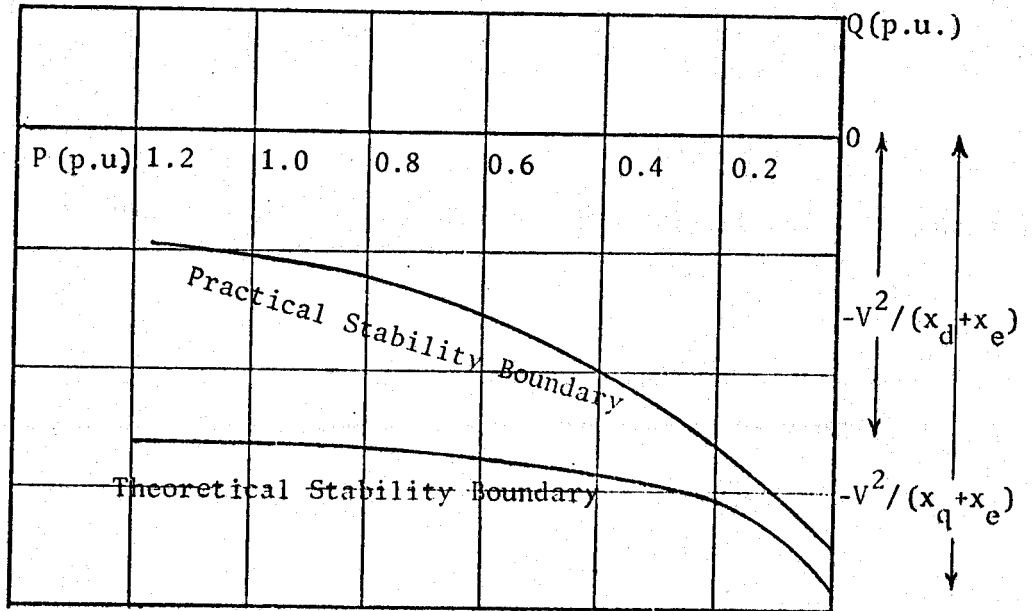


Fig. 2.6 Static Stability Boundaries of a Salient-Pole Conventional Synchronous Generator

limit), is determined by the magnitudes of their synchronous reactances.⁷ This maximum has the value $V^2/(x_d + x_e)$ for nonsalient-pole generators and ranges from $V^2/(x_d + x_e)$ at full load to $V^2/(x_q + x_e)$ at no load for salient-pole generators. The limits mentioned above are the theoretical and will be reduced if a reasonable margin is chosen.

2.3.1 Methods for improving the steady-state stability

It follows from the preceding discussion, that the extension of the steady-state stable region calls for the design of synchronous generators having low values of synchronous reactances. Synchronous generators with low synchronous reactances are expensive. The cost of increased short circuit ratio for waterwheel generators increases in general as shown in Fig. 2.7¹. On the other hand, as the production of electrical energy continues its steady rate of increase, it has become economically desirable to use larger synchronous generators. The use of efficient methods for cooling makes it also possible to obtain more K.V.A. from a given frame size of a generator. This in turn has resulted in higher per-unit reactances and as a result lower steady-state stability limits.

However, the steady-state stability region of a conventional synchronous generator can be extended very considerably by the proper control of its excitation⁸⁻²⁴. The machine can then operate dynamically stable beyond its static stability limits as shown in Fig. 2.8. The improvement achieved at full load may be very nearly equal to doubling the short circuit ratio of the generator. Unfortunately, this method is less effective at low power loading and useless at no load (Appendix A).

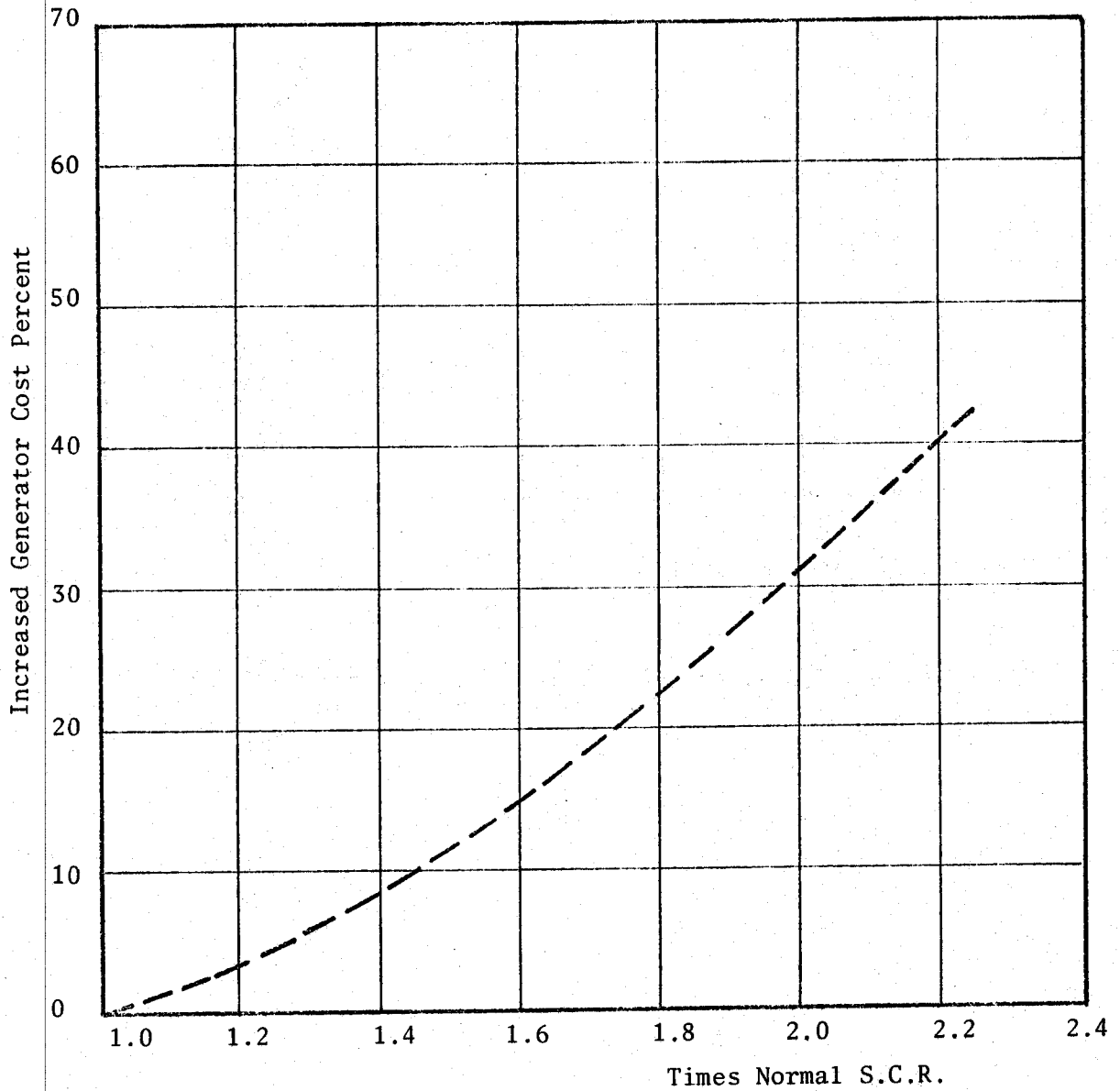


Fig. 2.7 Approximate Cost of Increasing Short Circuit Ratio (S.C.R.) of Typical Large Waterwheel Generators

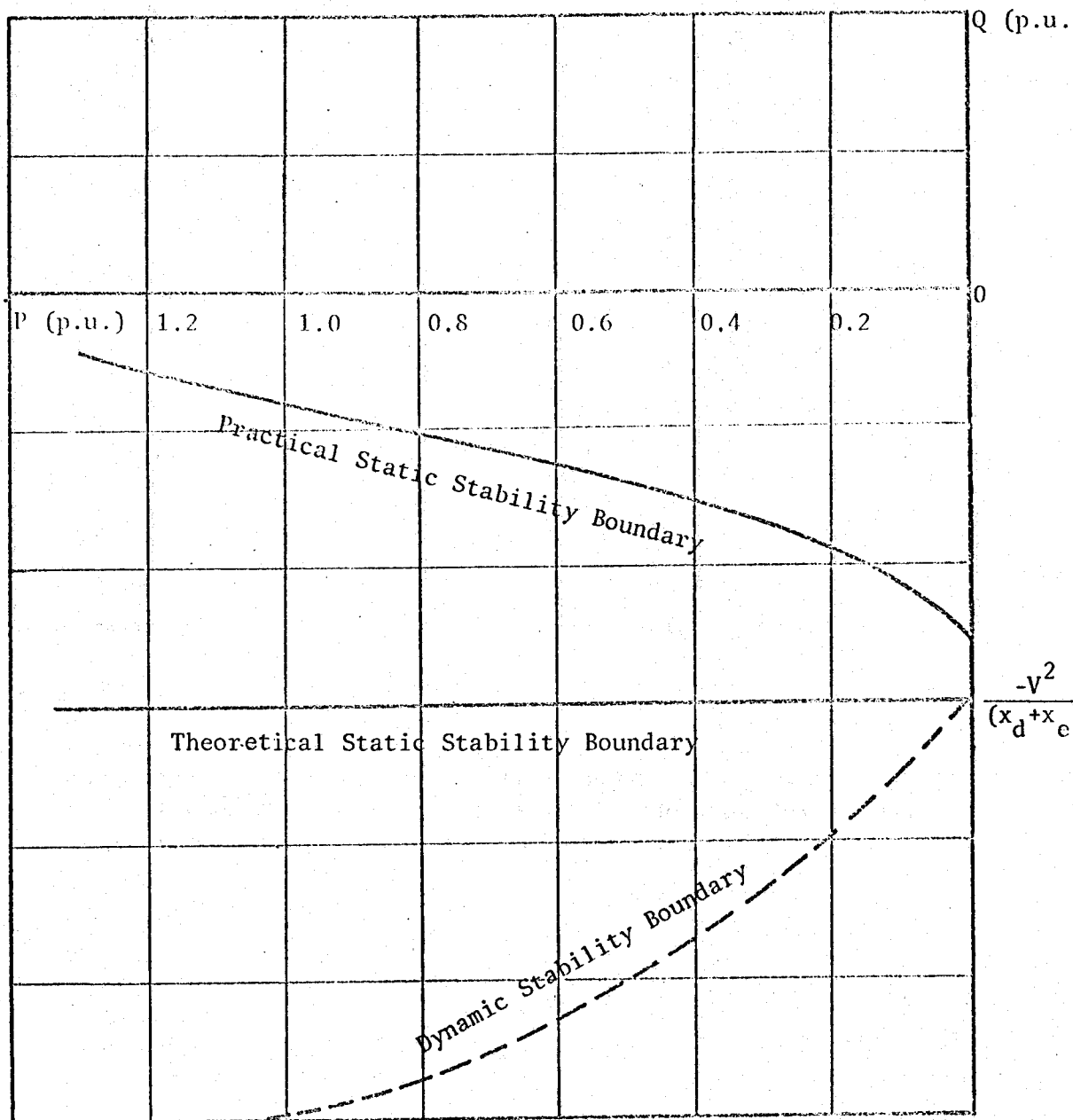


Fig. 2.8 Effect of Excitation Control on the Steady-State Stability Boundary of a Nonsalient-Pole Conventional Synchronous Generator

2.3.2 Improvement of dynamic stability by the dual-excitation of synchronous generators

To extend the dynamic stability region also at no load, it was suggested^{28,30} to provide the synchronous generator with an additional field winding on the quadrature-axis of the rotor. By controlling the excitation of this winding with a rotor-angle regulator, the stable underexcited region can be appreciably extended all over the whole active loading range. The suggested scheme for operation is to keep the rotor-angle fixed at zero value. Since the direct-axis field winding in this case coincides with the magnetic-axis of the resultant air-gap flux, a change in its current will vary the reactive power without changing the rotor position. This can be explained by considering the vector diagram of Fig. 2.9, from which the following relations can be obtained:

$$E_d = I_{q0} \cdot x_q \quad 2.1$$

$$E_q = V + I_{d0} \cdot x_d \quad 2.2$$

$$I_p = I_{q0} \quad 2.3$$

$$I_v = I_{d0} \quad 2.4$$

Where I_p and I_v are the active and reactive components of the armature current respectively.

E_q and E_d depend on the field currents as follows:

$$E_q = x_{ad} \cdot i_{fd} \quad 2.5$$

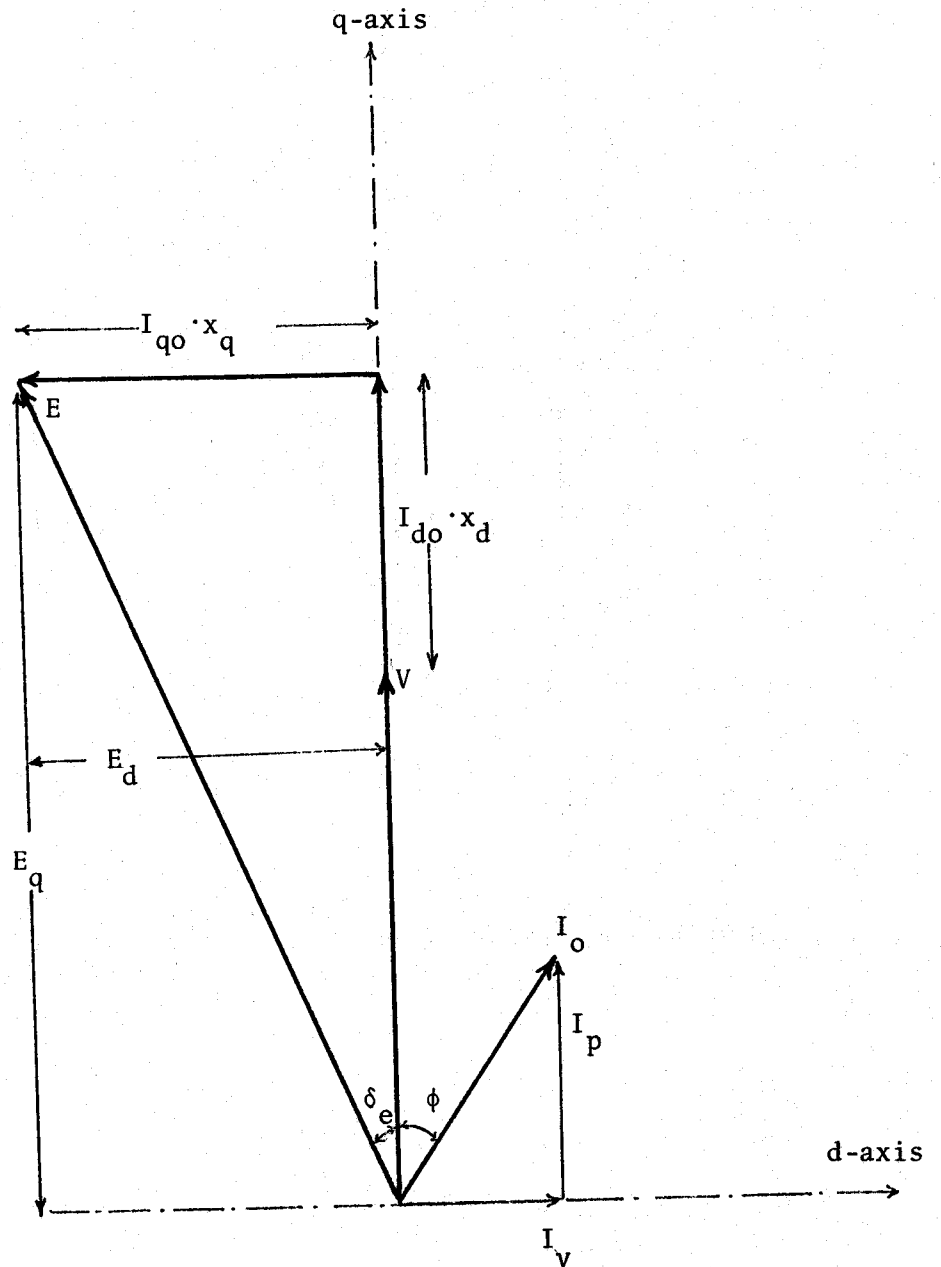


Fig. 2.9 Vector Diagram of a d-q Synchronous Generator Directly Connected to an Infinite-Bus ($\delta=0$)

$$E_d = x_{aq} \cdot i_{fq} \quad 2.6$$

Where i_{fd} and i_{fq} are the currents in the direct and quadrature-axis field windings respectively.

Hence

$$I_p = \frac{x_{aq}}{x_q} \cdot i_{fq} \quad 2.7$$

$$I_v = \frac{x_{ad}}{x_d} \cdot i_{fd} - \frac{V}{x_d} \quad 2.8$$

As a result, the direct-axis field winding can be negatively excited so that the machine can provide the required capacitive loading without resulting in a change of the rotor-angle. *definition*

2.4 Application of the Dual-Excitation to Turbo-generators

A quadrature-axis field winding on the rotor of a turbo-generator would be uneconomical because of the increase in the reluctance of the generator magnetic circuit. This will require larger excitation currents and a larger machine to prevent excessive saturation of the rotor. This has suggested the development of the divided-winding rotor (d.w.r.) construction^{27,29}. The particular feature of the d.w.r. is that the conductors are located in slots distributed as in the rotor of a conventional synchronous machine and are divided into two parts, whose axes are displaced from each other (Fig. 2.10). This arrangement makes it possible to change a conventional turbo-generator to a dual-excited one by just rewinding its rotor or changing its field end connections. Sopper and Fagg²⁷ studied through analogue computer simulation a synchronous

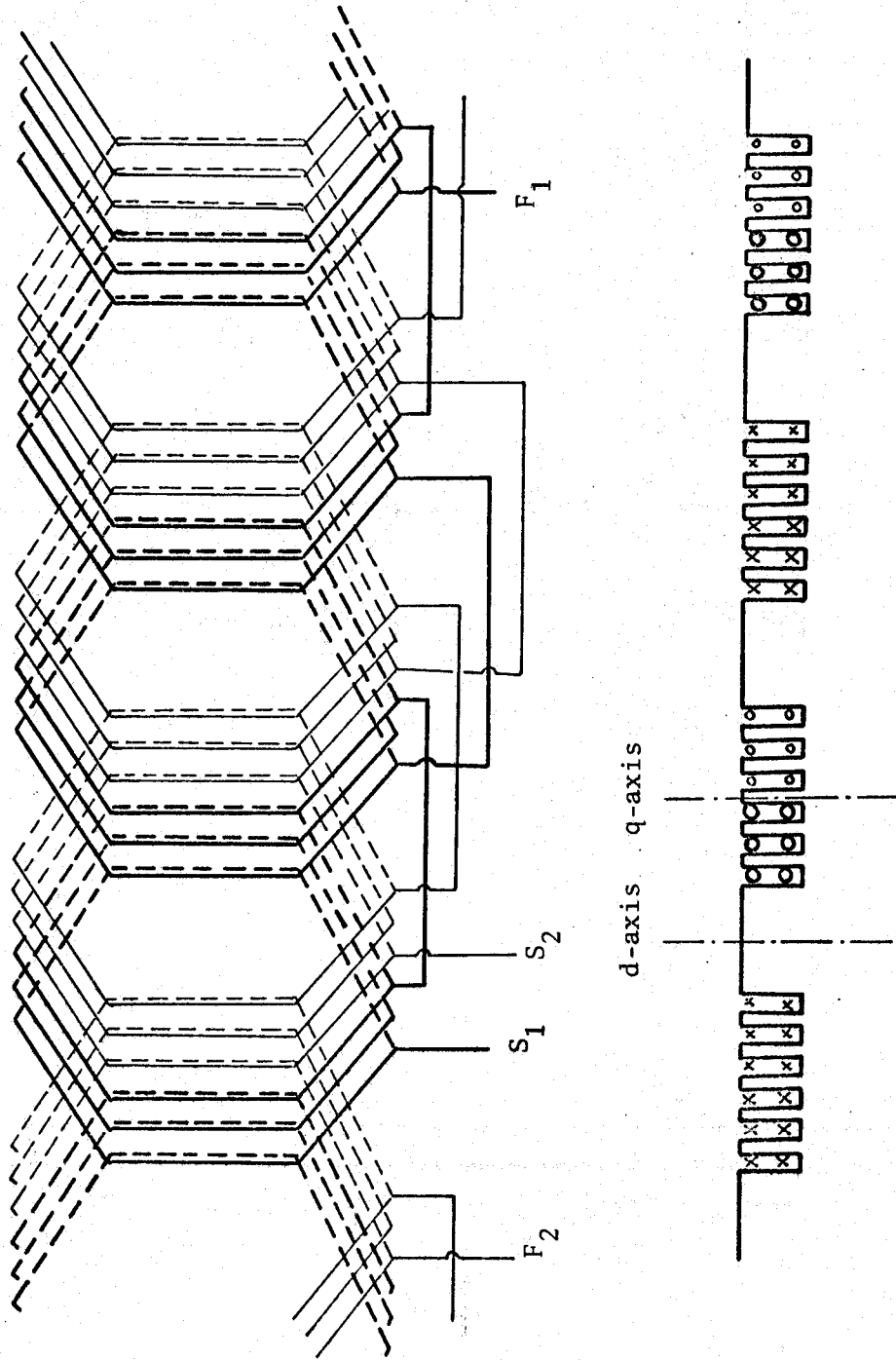


Fig. 2.10 Divided-Winding Rotor of a Turbo-Alternator

machine with rotor construction using two identical field windings arranged in X-form. Harely and Adkins²⁹ tried to simplify the analysis of the d.w.r. synchronous machine by replacing it with a d-q machine. As will be seen in this thesis, such simplification is not valid except when both field windings are identical and have the same inclination angle to the direct-axis of the rotor.

2.5 Purpose of the Thesis

Although some effort has been directed to solve the stability problem of synchronous machines by dual-exciting their rotors, all studies done till now deal with special rotor construction^{25-28,30} and some of them rely on simplifying assumptions^{28,29}.

It is the purpose of this thesis to present a generalized analysis for the dual-excited synchronous generator, in which the two field windings are not necessarily located on the rotor-axes, and may not have equal number of turns or equal inclination angles to the direct-axis of the pole structure (Fig. 2.11). To make the analysis complete, the effect of a general transmission system is taken into consideration.

Special attention is directed towards formalizing the small displacement equations, which are essential for performing dynamic stability studies. The equations readily take into consideration the effect of alternator and transmission system resistances, speed variations and the effect of the voltages induced in the armature by the rate of change of its flux linkage.

A digital computer program is established to formalize the characteristic equation of this machine, and then to check its dynamic stability by applying the well-known Routh's criterion to the equation.

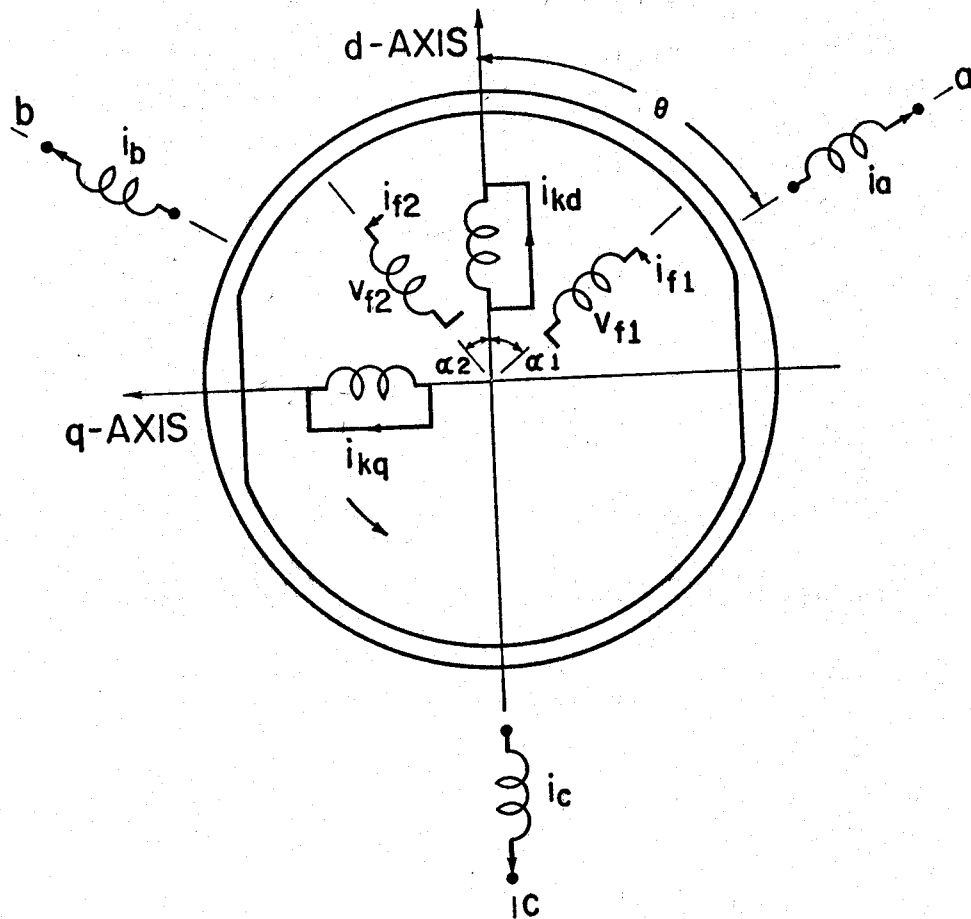


Fig. 2.11 Schematic Layout of a Dual-Excited Synchronous Machine

The program provides the possibility of investigating the effect of numerous schemes of excitation regulation on the dynamic stability boundaries. The improved dynamic stability limits of this type of synchronous generators at different operating conditions are demonstrated by studying a simple power system. The system consists of a dual-excited synchronous generator provided with an adequate control arrangement and connected to an infinite-bus through a simple tie-line.

3. ANALYSIS OF THE DUAL-EXCITED SYNCHRONOUS MACHINE

3.1 Introduction

As in the conventional synchronous machine, all mutual inductances between stator and rotor circuits of a dual-excited one are periodic functions of the rotor angular position. In addition, because of the rotor saliency, the self inductances of the stator phases and the mutual inductance between any two of them are also periodic functions of the rotor angular position. It follows that the characteristics of the dual-excited synchronous machine are expressed by a set of differential equations, most of whose coefficients are periodic functions of the rotor-angle. Such equations, even in the case of synchronous operation, are awkward to handle and difficult to solve. The two-reaction theory³³⁻³⁵, as in the case of conventional machines, can also be introduced here to overcome this difficulty. This is done by replacing the three phases of the armature winding by two fictitious stationary windings to which they are equivalent (stationary with respect to the rotor): one on the pole-axis (direct-axis) and the other on the interpole-axis (quadrature-axis), which are denoted respectively by 'd' and 'q' in Fig. 3.1.

Ideal synchronous machines are usually assumed and may be defined as follows³³⁻³⁵ :

1. Saturation, hysteresis and eddy currents in all magnetic circuits are neglected.
2. Each machine winding produces a sinusoidally space distributed magneto-motive force.

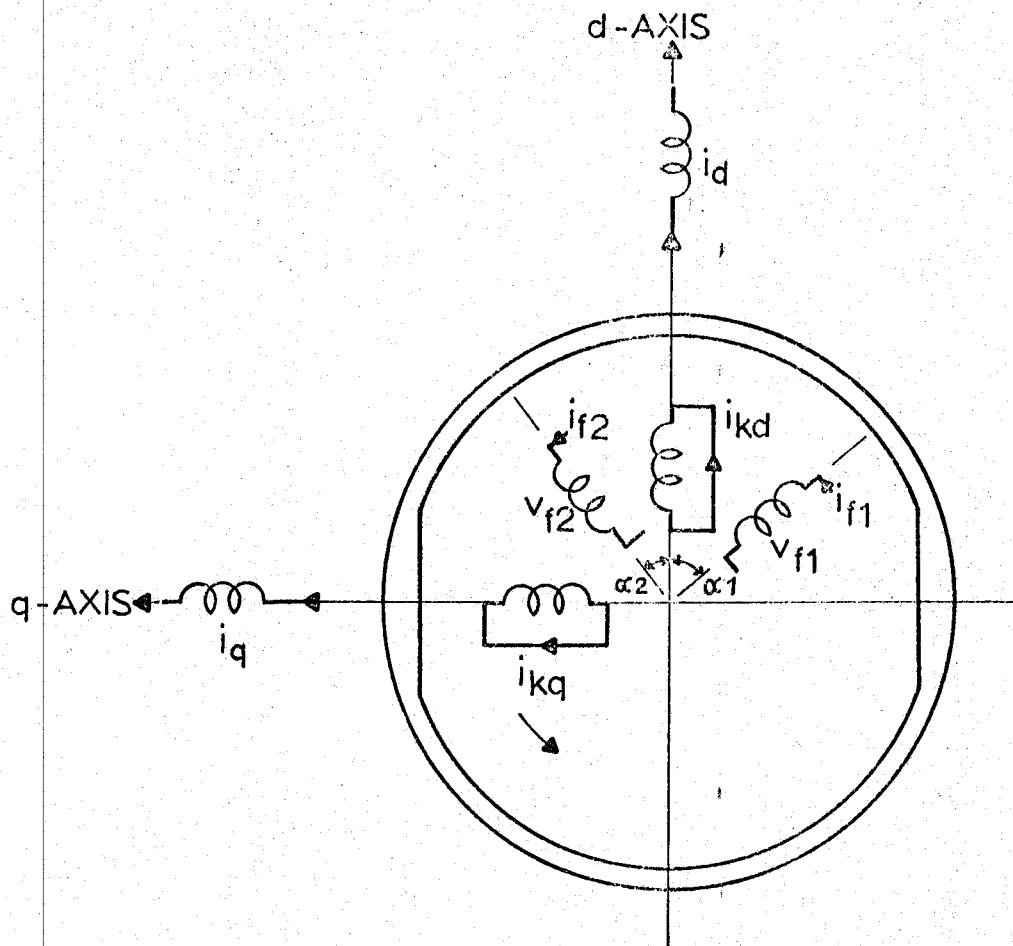


Fig. 3.1 Schematic Layout of an Idealized Dual-Excited Synchronous Machine

3. The pole structure is symmetrical about the axis of the pole. A symmetric three phase armature is also considered.
4. The self and mutual inductances of all rotor circuits are independent of rotor position. Thus, the effect of stator slots is neglected.
5. The damper winding, if it exists, is replaced by two equivalent damper circuits: one on the direct-axis and the other on the quadrature-axis.

3.2 Mathematical Representation³³⁻³⁵

Based on the preceding assumptions, the performance of the dual-excited synchronous machine may now be described by the following equations. In them, the convention adopted for the signs of voltages and currents are that v is the impressed voltage at the terminals and that the direction of positive current i corresponds to generation. The sign of the current in the damper winding is taken positive when it flows in a direction similar to that of a positive field current.

3.2.1. Inductance equations

a) Stator self-inductances

The reluctance of the magnetic circuit of a synchronous machine at any section in the air-gap depends on the position of the pole structure. As iron has a very high permeability compared with air, the permeance of the magnetic circuit of any stator phase varies from a maximum (when its axis coincides with the direct-axis of the rotor) to a minimum (when its axis coincides with the quadrature-axis). This variation can be represented by a Fourier series expansion which contains even harmonics. Considering only the zero and second harmonic terms of this series,

the self-inductances of the stator phases can then be expressed as follows:

$$L_{aa} = L_{aao} + L_{aa2} \cdot \cos 2\theta \quad 3.1$$

$$L_{bb} = L_{aao} + L_{aa2} \cdot \cos(2\theta + 120) \quad 3.2$$

$$L_{cc} = L_{aao} + L_{aa2} \cdot \cos(2\theta - 120) \quad 3.3$$

in which L_{aao} is the average value of the self-inductance and L_{aa2} is the difference between maximum and average values. As the leakage flux of any stator phase is independent of the rotor position, it is usually included in the constant term L_{aao} .

b) Stator mutual-inductances

It can also be shown that the mutual-inductance between any two stator phases varies periodically from a maximum (when the quadrature-axis is midway between the axes of the two phases) to a minimum (when the quadrature-axis is 90° electrical from the maximum position). Following the method adopted for self-inductances representation, the mutual-inductances between the stator phases can be expressed by:

$$L_{ab} = L_{ba} = -[L_{abo} + L_{bb2} \cdot \cos(2\theta + 60)] \quad 3.4$$

$$L_{bc} = L_{cb} = -[L_{abo} + L_{bb2} \cdot \cos(2\theta - 180)] \quad 3.5$$

$$L_{ca} = L_{ac} = -[L_{abo} + L_{bb2} \cdot \cos(2\theta + 300)] \quad 3.6$$

where L_{abo} is the average value of the mutual-inductance between phases and L_{bb2} is the difference between maximum and average values. Theoretical analysis shows that the difference between the maximum and minimum values of the self-inductance is the same as the difference

between the maximum and minimum values of the mutual-inductance, i.e.:

$$L_{bb2} = L_{aa2} \quad 3.7$$

It has also been found that, apart from the leakage inductance, the average value of the self-inductance of a stator phase is double the average value of the mutual-inductance between any two stator phases.

This can be expressed as follows:

$$L_{aao} - L_{\sigma} = 2L_{abo} \quad 3.8$$

c) Mutual-inductances between stator and rotor circuits

The mutual-inductances between the stator phases and the direct- and quadrature-axis damper circuits vary sinusoidally with rotor angle and are maximum when the two coils in questions are in line. Thus:

$$L_{akd} = L_{kda} = L_{akdo} \cdot \cos\theta \quad 3.9$$

$$L_{bkd} = L_{kdb} = L_{akdo} \cdot \cos(\theta - 120) \quad 3.10$$

$$L_{ckd} = L_{kdc} = L_{akdo} \cdot \cos(\theta + 120) \quad 3.11$$

$$L_{akq} = L_{kqa} = -L_{akqo} \cdot \sin\theta \quad 3.12$$

$$L_{bkq} = L_{kqb} = -L_{akqo} \cdot \sin(\theta - 120) \quad 3.13$$

$$L_{ckq} = L_{kqc} = -L_{akqo} \cdot \sin(\theta + 120) \quad 3.14$$

On the other hand, the mutual-inductances between the stator phases and any field winding depend on the permeance of the magnetic circuit in both the direct- and quadrature-axis of the rotor. The derivation of the expressions for these inductances can be done as follows.

Considering phase a, its magneto-motive force (M.M.F.)_a can be resolved into two components equal to (M.M.F.)_a · Cosθ and -(M.M.F.)_a · Sinθ acting in the direct- and quadrature-axis respectively (Fig.2.11). These components of M.M.F. produce corresponding components of flux in the direct- and quadrature-axis of magnitudes equal to λ_d · (M.M.F.)_a · Cosθ and -λ_q · (M.M.F.)_a · Sinθ respectively. The linkage of field winding 1 caused by this flux is then proportional to (M.M.F.)_a · (λ_d · Cosα₁ · Cosθ + λ_q · Sinα₁ · Sinθ). Similarly, the linkage of field winding 2 is proportional to (M.M.F.)_a · (λ_d · Cosα₂ · Cosθ - λ_q · Sinα₂ · Sinθ). It follows that the expressions for the mutual-inductances between phase a and the field windings 1 and 2 respectively can be written as:

$$L_{af1} = L_{f1a} = L_{af1d} \cdot \text{Cos}\theta + L_{af1q} \cdot \text{Sin}\theta \quad 3.15$$

$$L_{af2} = L_{f2a} = L_{af2d} \cdot \text{Cos}\theta - L_{af2q} \cdot \text{Sin}\theta \quad 3.16$$

where

L_{af1d} can be defined as the mutual-inductance between field winding 1 and phase a when the axis of the latter coincides with the direct-axis of the rotor.

L_{af1q} can be defined as the mutual-inductance between field winding 1 and phase a when the axis of the latter coincides with the quadrature-axis of the rotor.

L_{af2d} and L_{af2q} have similar corresponding definitions for field winding 2.

Following the same procedure used for deriving L_{af1} and L_{af2} , L_{bf1} , L_{bf2} , L_{cf1} and L_{cf2} are found to be:

$$L_{bf1} = L_{f1b} = L_{af1d} \cdot \cos(\theta - 120) + L_{af1q} \cdot \sin(\theta - 120) \quad 3.17$$

$$L_{bf2} = L_{f2b} = L_{af2d} \cdot \cos(\theta - 120) - L_{af2q} \cdot \sin(\theta - 120) \quad 3.18$$

$$L_{cf1} = L_{f1c} = L_{af1d} \cdot \cos(\theta + 120) + L_{af1q} \cdot \sin(\theta + 120) \quad 3.19$$

$$L_{cf2} = L_{f2c} = L_{af2d} \cdot \cos(\theta + 120) - L_{af2q} \cdot \sin(\theta + 120) \quad 3.20$$

d) Rotor self-and mutual-inductances

All inductances of the rotor circuits do not depend on the rotor position and so they are considered constant. Because of the symmetry of the damper winding, there is no mutual-inductance between the equivalent damper circuits on both the direct and quadrature-axis.

3.2.2 Flux linkage equations

Utilizing the inductance relations given before, the flux linkage equations of the dual-excited synchronous machine can be written as follows:

y_a	$-L_{aao} \cdot \cos 2\theta$ $-L_{aa2} \cdot \cos 2\theta$	L_{abo} $+L_{aa2} \cdot \cos(2\theta+60)$	L_{abo} $+L_{aa2} \cdot \cos(2\theta+300)$	$L_{afid} \cdot \cos \theta$ $+L_{afiq} \cdot \sin \theta$	$L_{af2d} \cdot \cos \theta$ $-L_{af2q} \cdot \sin \theta$	$L_{akdo} \cdot \cos \theta$	$-L_{akqo} \cdot \sin \theta$	i_{ta}
y_b	L_{abo} $+L_{aa2} \cdot \cos(2\theta+60)$	$-L_{aao}$ $-L_{aa2} \cdot \cos(2\theta+120)$	L_{abo} $-L_{aa2} \cdot \cos(2\theta-180)$	$L_{afid} \cdot \cos(\theta-120)$ $+L_{afiq} \cdot \sin(\theta-120)$	$L_{af2d} \cdot \cos(\theta-120)$ $-L_{af2q} \cdot \sin(\theta-120)$	$L_{akdo} \cdot \cos(\theta-120)$	$-L_{akqo} \cdot \sin(\theta-120)$	i_{tb}
y_c	L_{abo} $+L_{aa2} \cdot \cos(2\theta+300)$	L_{abo} $+L_{aa2} \cdot \cos(2\theta-180)$	$-L_{aao}$ $-L_{aa2} \cdot \cos(2\theta-120)$	$L_{afid} \cdot \cos(\theta+120)$ $+L_{afiq} \cdot \sin(\theta+120)$	$L_{af2d} \cdot \cos(\theta+120)$ $-L_{af2q} \cdot \sin(\theta+120)$	$L_{akdo} \cdot \cos(\theta+120)$	$-L_{akqo} \cdot \sin(\theta+120)$	i_{tc}
y_{f1}	$-L_{afid} \cdot \cos \theta$ $-L_{afiq} \cdot \sin \theta$	$-L_{afid} \cdot \cos(\theta-120)$ $-L_{afiq} \cdot \sin(\theta-120)$	$-L_{afid} \cdot \cos(\theta+120)$ $-L_{afiq} \cdot \sin(\theta+120)$	L_{ff1}	L_{ff2}	L_{kdf1}	L_{kqf1}	i_{f1}
y_{f2}	$-L_{af2d} \cdot \cos \theta$ $+L_{af2q} \cdot \sin \theta$	$-L_{af2d} \cdot \cos(\theta-120)$ $+L_{af2q} \cdot \sin(\theta-120)$	$-L_{af2d} \cdot \cos(\theta+120)$ $+L_{af2q} \cdot \sin(\theta+120)$	L_{ff1}	L_{ff2}	L_{kdf2}	L_{kqf2}	i_{f2}
y_{kd}	$-L_{akdo} \cdot \cos \theta$	$-L_{akdo} \cdot \cos(\theta-120)$	$-L_{akdo} \cdot \cos(\theta+120)$	L_{kdf1}	L_{kdf2}	L_{kkd}		i_{kd}
y_{kq}	$L_{akqo} \cdot \sin \theta$	$L_{akqo} \cdot \sin(\theta-120)$	$L_{akqo} \cdot \sin(\theta+120)$	L_{kqf1}	L_{kqf2}		L_{kkq}	i_{kq}

a b c

a b c =

3.2.3 Park's transformation

Applying the two-reaction theory, equation 3.21 can be extremely simplified by replacing the variables of the armature windings by new fictitious variables, which differ from but are related to the actual ones. For example, the transformation of the currents is expressed by the following equation:

$$\begin{bmatrix} i_{td} \\ i_{tq} \end{bmatrix} = \frac{2}{3} \cdot \begin{bmatrix} \cos\theta & \cos(\theta-120) & \cos(\theta+120) \\ -\sin\theta & -\sin(\theta-120) & -\sin(\theta+120) \end{bmatrix} \begin{bmatrix} i_{ta} \\ i_{tb} \\ i_{tc} \end{bmatrix} \quad 3.22$$

Similar transformations are used for armature voltages and flux linkages.

Equation 3.21 can then be obtained in the following two-axis frame:

$$\begin{bmatrix} \Psi_d \\ \Psi_q \\ \Psi_{f1} \\ \Psi_{f2} \\ \Psi_{k_d} \\ \Psi_{k_q} \end{bmatrix} = \begin{bmatrix} -L_d & & L_{af1d} & L_{af2d} & L_{akdo} & & \\ & -L_q & -L_{af1q} & L_{af2q} & & L_{akqo} & \\ \frac{3}{2} \cdot L_{af1d} & \frac{3}{2} \cdot L_{af1q} & L_{ff1} & L_{f1f2} & L_{kdf1} & L_{kqf1} & \\ \frac{3}{2} \cdot L_{af2d} & \frac{3}{2} \cdot L_{af2q} & L_{f1f2} & L_{ff2} & L_{kdf2} & L_{kqf2} & \\ \frac{3}{2} \cdot L_{akdo} & & L_{kdf1} & L_{kdf2} & L_{kkd} & & \\ & \frac{3}{2} \cdot L_{akqo} & L_{kqf1} & L_{kqf2} & & L_{kkq} & \end{bmatrix} \begin{bmatrix} i_{td} \\ i_{tq} \\ i_{f1} \\ i_{f2} \\ i_{kd} \\ i_{kq} \end{bmatrix} \quad 3.23$$

where

$$L_d = L_{aao} + L_{abo} + \frac{3}{2} \cdot L_{aa2}$$

$$L_q = L_{aao} + L_{abo} - \frac{3}{2} \cdot L_{aa2}$$

3.2.4 Voltage equations

While the voltage equations of the rotor circuits can be simply obtained by the direct application of Kirchoff's law, the derivation of those for the two-axis armature voltages v_{td} and v_{tq} needs a more or less lengthy analysis. This is usually done by finding firstly the expressions for v_{ta} , v_{tb} and v_{tc} and then transforming them in the two-axis frame. As a result, the machine voltage equations will be:

$$\begin{array}{|c|} \hline v_{td} + r \cdot i_{td} \\ \hline v_{tq} + r \cdot i_{tq} \\ \hline v_{f1} - r_{f1} \cdot i_{f1} \\ \hline v_{f2} - r_{f2} \cdot i_{f2} \\ \hline 0 - r_{kd} \cdot i_{kd} \\ \hline 0 - r_{kq} \cdot i_{kq} \\ \hline \end{array} = \begin{array}{|c|c|c|c|c|c|} \hline p & -p\theta & & & & \\ \hline p\theta & p & & & & \\ \hline & & p & & & \\ \hline & & & p & & \\ \hline & & & & p & \\ \hline & & & & & p \\ \hline \end{array} \begin{array}{|c|} \hline \psi_d \\ \hline \psi_q \\ \hline \psi_{f1} \\ \hline \psi_{f2} \\ \hline \psi_{kd} \\ \hline \psi_{kq} \\ \hline \end{array} \quad 3.24$$

3.2.5 Torque equations

A general expression for the torque may be derived by using the expression for the instantaneous power output:

$$\text{Power} = v_{ta} \cdot i_{ta} + v_{tb} \cdot i_{tb} + v_{tc} \cdot i_{tc} \quad 3.25$$

This equation can be rewritten in terms of the two-axis quantities as follows:

$$\text{Power} = \frac{3}{2} \cdot (v_{td} \cdot i_{td} + v_{tq} \cdot i_{tq}) \quad 3.26$$

Substituting from equation 3.24, v_{td} and v_{tq} can be eliminated to give:

$$\begin{aligned}
 \text{Power} &= \frac{3}{2} \cdot \{i_{td} \cdot (p\psi_d - p\theta \cdot \psi_q - r \cdot i_{td}) + \\
 &\quad i_{tq} \cdot (p\psi_q + p\theta \cdot \psi_d - r \cdot i_{tq})\} \\
 &= \frac{3}{2} \{(i_{td} \cdot p\psi_d + i_{tq} \cdot p\psi_q) - r(i_{td}^2 + i_{tq}^2) \\
 &\quad + p\theta \cdot (i_{tq} \cdot \psi_d - i_{td} \cdot \psi_q)\} \qquad \qquad \qquad 3.27
 \end{aligned}$$

Equation 3.27 may be interpreted as:

$$\begin{aligned}
 (\text{net power output}) &= (\text{rate of change of armature magnetic energy}) \\
 &\quad - (\text{armature copper loss}) + (\text{power transferred} \\
 &\quad \text{across the air-gap}).
 \end{aligned}$$

From this, it is evident that by dividing the air-gap power term by the rotor speed, we obtain the developed torque T_e as:

$$T_e = \frac{3}{2} \cdot n_p \cdot (i_{tq} \cdot \psi_d - i_{td} \cdot \psi_q) \qquad \qquad \qquad 3.28$$

The relation between the mechanical shaft torque and the electrical developed torque is given by:

$$T_i = T_e + J \cdot p^2\theta_m + G_D(p) \cdot p\theta_m \qquad \qquad \qquad 3.29$$

3.3 Per-Unit System for the Dual-Excited Synchronous Machine

Per-unit systems have been extensively used to simplify phenomena over a wide range of different physical problems. The advantages, which arise from the application of a well-designed per-unit system to electrical power problems, are numerous. Among of which are the following:

1. A direct comparison between machines of widely varying power ratings is straight forward.

2. In the two-axis theory of synchronous machines, a per-unit system is useful in removing those arbitrary numerical factors which can appear in the original equations and have values dependant on the transformation used.
3. In single and polyphase studies, the turns ratios of transformers (and the manner of internal connections in the polyphase case) are removed from the analysis.
4. Simplification occurs in the analysis of polyphase circuits under balanced conditions. By defining appropriate per-unit line quantities to correspond with chosen per-unit phase quantities, both line and phase parameters can be represented in one per-unit analysis.
5. A basic set of dimensionless parameters can help to prevent errors in converting performance characteristics between different systems of units.
6. The numerical range of per-unit parameters is small. This is valuable for solution by analogue or digital computers, since the variables are of convenient order. Manual calculations are also simplified.

The derivation of the per-unit system for the dual-excited synchronous machine is given as follows.

3.3.1 Stator base values

It is a common practise to choose the rated armature current and the rated phase voltage to be the stator current and voltage base values respectively. As the components of the armature current and phase voltage

in both the d- and q-axis are instantaneous values, it is rather preferred to use the maximum value of the rated armature current and terminal voltage than the root mean square values as stator bases.

$$\text{Hence: } I_{sB} = \sqrt{2} I_n \quad 3.30$$

$$V_{sB} = \sqrt{2} V_n \quad 3.31$$

where I_n and V_n are the rated armature current and the rated phase voltage respectively.

From equations 3.30 and 3.31 it follows that

$$P_{sB} = 3V_n \cdot I_n = \frac{3}{2} V_{sB} \cdot I_{sB} \quad 3.32$$

$$Z_{sB} = V_n / I_n \quad 3.33$$

$$L_{sB} = V_n / (I_n \cdot p\theta_o) \quad 3.34$$

$$\Psi_{sB} = L_{sB} \cdot I_{sB} \quad 3.35$$

where P_{sB} , Z_{sB} , L_{sB} and Ψ_{sB} are the base values for stator power, impedance, inductance and flux linkage respectively.

3.3.2 Rotor base values

a) Power equality constraint

As seen from equation 3.23, the inductance matrix is not symmetric.

From the mathematical point of view, the per-unit system can be chosen without removing this property. However, for the sake of obtaining a simple representation of the machine which facilitates the formation of its equivalent circuit, it is preferable to make this matrix reciprocal. To fulfill this requirement in a per-unit system, the following constraint should be imposed.

$$\frac{3}{2} L_{sB} \cdot I_{sB}^2 = L_{f1B} \cdot I_{f1B}^2 = L_{f2B} \cdot I_{f2B}^2 = L_{kdB} \cdot I_{kdB}^2 = L_{kqB} \cdot I_{kqB}^2 \quad 3.36$$

which implies that:

$$\frac{3}{2} V_{sB} \cdot I_{sB} = V_{f1B} \cdot I_{f1B} = V_{f2B} \cdot I_{f2B} = V_{kdB} \cdot I_{kdB} = V_{kqB} \cdot I_{kqB} \quad 3.37$$

In other words, the base power of the stator is equal to the base power of any rotor circuit.

b) Inductance relations

Before going to choose the base current for each rotor circuit of the dual-excited synchronous machine, it would be helpful to put the M.K.S. expressions of all machine mutual-inductances in terms of the permeance and the number of turns. It will be assumed that the mutual flux produced in one axis by any machine circuit links equally all the other circuits on this axis. This assumption will be referred to as perfect mutual coupling. The following relations can then be written:

$$L_{ad} = \frac{3}{2} \cdot \lambda_d \cdot N_s^2 \quad 3.38$$

$$L_{aq} = \frac{3}{2} \cdot \lambda_q \cdot N_s^2 \quad 3.39$$

$$L_{af1d} = \lambda_d \cdot \cos \alpha_1 \cdot N_s \cdot N_{f1} \quad 3.40$$

$$L_{af1q} = \lambda_q \cdot \sin \alpha_1 \cdot N_s \cdot N_{f1} \quad 3.41$$

$$L_{af2d} = \lambda_d \cdot \cos \alpha_2 \cdot N_s \cdot N_{f2} \quad 3.42$$

$$L_{af2q} = \lambda_q \cdot \sin \alpha_2 \cdot N_s \cdot N_{f2} \quad 3.43$$

$$L_{akdo} = \lambda_d \cdot N_s \cdot N_{kd} \quad 3.44$$

$$L_{akqo} = \lambda_q \cdot N_s \cdot N_{kq} \quad 3.45$$

$$L_{f1f2} = (\lambda_d \cdot \cos \alpha_1 \cdot \cos \alpha_2 - \lambda_q \cdot \sin \alpha_1 \cdot \sin \alpha_2) \cdot N_{f1} \cdot N_{f2} \quad 3.46$$

$$L_{f1kd} = \lambda_d \cdot \cos \alpha_1 \cdot N_{f1} \cdot N_{kd} \quad 3.47$$

$$L_{f1kq} = -\lambda_q \cdot \sin \alpha_1 \cdot N_{f1} \cdot N_{kq} \quad 3.48$$

$$L_{f2kd} = \lambda_d \cdot \cos \alpha_2 \cdot N_{f2} \cdot N_{kd} \quad 3.49$$

$$L_{f2kq} = \lambda_q \cdot \sin \alpha_2 \cdot N_{f2} \cdot N_{kq} \quad 3.50$$

c) Rotor base currents

The choice of the base current for any rotor circuit, even for a conventional synchronous machine, is a problem which has been subject to several discussions. In general, such a choice can be made in an infinite number of ways. For the conventional synchronous machine, it has been found more convenient to choose certain base values rather than others. The chosen values were preferred on the basis of providing a representation which displays the physical picture of the machine and results in simplified equivalent circuits. Two of the most convenient choices have resulted in the following per-unit systems:^{31,32}

a - x_{ad} base system

b - Equal mutuals base system

It is worthwhile to mention that both systems are identical for the case in which the coupling between the machine circuits on each axis is perfect.

For the dual-excited synchronous machine, suitable rotor base quantities can be obtained by choosing the ideal turns ratio* between two windings to be the ratio between their base currents. Hence, the base rotor currents can be expressed as follows:

$$\begin{array}{|c|} \hline I_{f1B} \\ \hline I_{f2B} \\ \hline I_{kdB} \\ \hline I_{kqB} \\ \hline \end{array} = \frac{3}{2} N_s \cdot \begin{array}{|c|} \hline 1/N_{f1} \\ \hline 1/N_{f2} \\ \hline 1/N_{kd} \\ \hline 1/N_{kq} \\ \hline \end{array} \cdot \boxed{I_{sB}} \quad 3.51$$

Substituting from equations 3.38 - 3.45 in 3.51, it follows that the base rotor currents in terms of the machine inductances can be written as follows:

$$\begin{array}{|c|} \hline I_{f1B} \\ \hline I_{f2B} \\ \hline I_{kdB} \\ \hline I_{kqB} \\ \hline \end{array} = \begin{array}{|c|} \hline \frac{L_{ad} \cdot \cos\alpha_1}{L_{af1d}} \text{ (or } \frac{L_{aq} \cdot \sin\alpha_1}{L_{af1q}} \text{)} \\ \hline \frac{L_{ad} \cdot \cos\alpha_2}{L_{af2d}} \text{ (or } \frac{L_{aq} \cdot \sin\alpha_2}{L_{af2q}} \text{)} \\ \hline \frac{L_{ad}}{L_{akdo}} \\ \hline \frac{L_{aq}}{L_{aqko}} \\ \hline \end{array} \cdot \boxed{I_{sB}} \quad 3.52$$

3.3.3. Per-unit time, speed and torque

The normalized equations of the dual-excited synchronous machine are further simplified if the electrical angular velocity $p\theta$ is also normalized. The synchronous electrical angular velocity $p\theta_0$ is con-

* An ideal turns ratio between two windings is defined as follows:

Ideal turns ratio = $\frac{\text{Total flux linkages of mutual flux with one winding}}{\text{Total flux linkages of mutual flux with the other winding}}$

veniently chosen as the base value. Since $p\theta \cdot t$ is a dimensionless quantity, the selection of $p\theta_0$ as the base of $p\theta$ is equivalent to selecting $1/p\theta_0$ as a base of time.

It may be noted that, as reactance is the product of the inductance and the electrical angular velocity, the per-unit inductance and per-unit rated frequency reactance will be equal. It is therefore common to find no distinction between these quantities where time is normalized.

Having normalized time, it is now possible to see the definition of the differential operator p in the per-unit system. In nonnormalized form:

$$p = \frac{d}{dt}$$

but $t(p \cdot u) = t/p\theta_0$; so it follows that

$$p(p \cdot u) = p/p\theta_0 \tag{3.53}$$

When writing the torque equations in M.K.S. system, it is inevitable that the number of pole pairs n_p appears. It is desirable in forming the per-unit equations of the machine to remove this parameter because it is not fundamental to the performance of the machine. As a consequence, the form of the per-unit rotor angular velocity is simplified becoming the same whether expressed in mechanical or electrical form. This is done by defining the base mechanical angular velocity $p\theta_{mB}$ as that corresponding to the base electrical velocity

Thus:

$$p\theta_{mB} = p\theta_0/n_p \tag{3.54}$$

Using the expressions for the base power and base mechanical speed given by equations 3.32 and 3.54 respectively, the base torque will be:

$$T_{eB} = \frac{3}{2} \cdot \frac{V_{sB} \cdot I_{sB}}{p\theta_o} \cdot n_p$$

$$= \frac{3}{2} \cdot \Psi_{sB} \cdot I_{sB} \cdot n_p \quad 3.55$$

3.4 The Normalized Equations

Having established the per-unit system, the normalized equations of the dual-excited synchronous machine can be derived. In the following equations and here after, all the parameters are in per-unit values.

3.4.1. Flux linkage equations

The normalized flux linkage equations can be arranged as follows:

ψ_d	$-x_d$		$x_{ad} \cdot \cos\alpha_1$	$x_{ad} \cdot \cos\alpha_2$	x_{ad}		i_{td}
ψ_q		$-x_q$	$-x_{aq} \cdot \sin\alpha_1$	$x_{aq} \cdot \sin\alpha_2$		x_{aq}	i_{tq}
ψ_{f1}	$-x_{ad} \cdot \cos\alpha_1$	$x_{aq} \cdot \sin\alpha_1$	x_{ff1}	x_{f12}	$x_{ad} \cdot \cos\alpha_1$	$-x_{aq} \cdot \sin\alpha_1$	i_{f1}
ψ_{f2}	$-x_{ad} \cdot \cos\alpha_2$	$-x_{aq} \cdot \sin\alpha_2$	x_{f12}	x_{ff2}	$x_{ad} \cdot \cos\alpha_2$	$x_{aq} \cdot \sin\alpha_2$	i_{f2}
ψ_{kd}	$-x_{ad}$		$x_{ad} \cdot \cos\alpha_1$	$x_{ad} \cdot \cos\alpha_2$	x_{kkd}		i_{kd}
ψ_{kq}		$-x_{aq}$	$-x_{aq} \cdot \sin\alpha_1$	$x_{aq} \cdot \sin\alpha_2$		x_{kkq}	i_{kq}

3.56

where:

$$x_d = x_{a\sigma} + x_{ad}$$

$$x_q = x_{a\sigma} + x_{aq}$$

$$x_{f12} = x_{ad} \cdot \cos\alpha_1 \cdot \cos\alpha_2 - x_{aq} \cdot \sin\alpha_1 \cdot \sin\alpha_2$$

$$x_{ff1} = x_{f1\sigma} + x_{ad} \cdot \cos^2\alpha_1 + x_{aq} \cdot \sin^2\alpha_1$$

$$x_{ff2} = x_{f2\sigma} + x_{ad} \cdot \cos^2\alpha_2 + x_{aq} \cdot \sin^2\alpha_2$$

$$x_{kkd} = x_{kd\sigma} + x_{ad}$$

$$x_{kkq} = x_{kq\sigma} + x_{aq}$$

3.4.2 Voltage equations

The normalized voltage equations in matrix form can be written as:

$v_{td} + r \cdot i_{td}$	p	-pθ					Ψ_d	3.57
$v_{tq} + r \cdot i_{tq}$	pθ	p					Ψ_q	
$v_{f1} - r_{f1} \cdot i_{f1}$			p				Ψ_{f1}	
$v_{f2} - r_{f2} \cdot i_{f2}$				p			Ψ_{f2}	
$0 - r_{kd} \cdot i_{kd}$					p		Ψ_{kd}	
$0 - r_{kq} \cdot i_{kq}$						p	Ψ_{kq}	

3.4.3 Torque equations

The developed electrical torque in per-unit values can be written in the following form:

$$T_e = i_{tq} \cdot \Psi_d - i_{td} \cdot \Psi_q \quad 3.58$$

Normalizing equation 3.29, which relates the developed electrical torque of the dual-excited synchronous machine to both the shaft and inertial torques, gives the following:

$$T_i = i_{tq} \cdot \psi_d - i_{td} \cdot \psi_q + \textcircled{H}^* \cdot p^2 \theta + g_{D(p)} \cdot p \theta \quad 3.59$$

3.4.4 The operational equations

For the study of the performance of synchronous machines, especially from the power system analysis point of view, one is only interested in the variables at the terminal, namely: voltage, current and power. So, the rotor currents can be eliminated from equation 3.56 to give the following flux linkage equations:

* The inertial torque = $J \cdot p^2 \theta_m$

In normalized form, it will be equal to:

$$= J \cdot p \theta_o \cdot \frac{p}{p \theta_o} \cdot \frac{p \theta_m}{p \theta_{mB}} \cdot \frac{(p \theta_{mB})^2}{\frac{3}{2} \cdot V_{sB} \cdot I_{sB}}$$

but from the definition of the inertia constant H:

$$H = \frac{1}{2} \frac{J \cdot (p \theta_{mB})^2}{\frac{3}{2} \cdot V_{sB} \cdot I_{sB}},$$

it follows that the per-unit expression for the inertial torque is given by:

$$\text{Inertial torque} = 2 \cdot H \cdot p \theta_o \cdot p^2 \theta$$

from which it appears that the normalized value of the inertia constant

\textcircled{H} is $2 \cdot p \theta_o \cdot H$

$$\psi_d = -x_d(p) \cdot i_{td} + G_{f1d}(p) \cdot v_{f1} + G_{f2d}(p) \cdot v_{f2} + M(p) \cdot i_{tq} \quad 3.60$$

$$\psi_q = M(p) \cdot i_{td} + G_{f1q}(p) \cdot v_{f1} + G_{f2q}(p) \cdot v_{f2} - x_q(p) \cdot i_{tq} \quad 3.61$$

where $x_d(p)$, $x_q(p)$, $G_{f1d}(p)$, $G_{f2d}(p)$, $G_{f1q}(p)$, $G_{f2q}(p)$ and $M(p)$ are the operational functions of the dual-excited synchronous machine and can be put in polynomial forms (Appendix C).

Equations 3.60 and 3.61 show that both the direct- and quadrature-axis circuits are no longer independent of each other as in the conventional synchronous machine. However, for the special case in which both field windings are identical and have the same inclination angles to the physical axis of the rotor, the cross coupling term $M(p)$ vanishes. This proves that the technique suggested in reference 29 for simplifying the analysis by replacing the dual-excited synchronous machine by an equivalent conventional machine having an additional field winding on the quadrature axis cannot be applied except to this special case.

By substituting equations 3.60 and 3.61 in 3.57 and 3.59, the following operational form of the normalized equations is derived:

$$\begin{aligned}
 v_{td} &= (G_{f1d}(p) \cdot p - p\theta \cdot G_{f1q}(p)) \cdot v_{f1} \\
 &\quad - (G_{f2d}(p) \cdot p - p\theta \cdot G_{f2q}(p)) \cdot v_{f2} \\
 v_{tq} &= (p\theta \cdot G_{f1d}(p) + G_{f1q}(p) \cdot p) \cdot v_{f1} \\
 &\quad - (p\theta \cdot G_{f2d}(p) + G_{f2q}(p) \cdot p) \cdot v_{f2} \\
 T_i &= (i_{tq} \cdot G_{f1d}(p) - i_{td} \cdot G_{f1q}(p)) \cdot v_{f1} \\
 &\quad - (i_{tq} \cdot G_{f2d}(p) - i_{td} \cdot G_{f2q}(p)) \cdot v_{f2} \\
 &\quad - g_D(p) \cdot p\theta
 \end{aligned}$$

$$= \begin{array}{|c|c|c|c|}
 \hline
 -r-x_d(p) \cdot p - p\theta \cdot M(p) & p\theta \cdot x_q(p) + M(p) \cdot p & & i_{td} \\
 \hline
 -p\theta \cdot x_d(p) + M(p) \cdot p & -r-x_q(p) \cdot p + p\theta \cdot M(p) & & i_{tq} \\
 \hline
 -i_{tq} \cdot x_d(p) - i_{td} \cdot M(p) & i_{td} \cdot x_q(p) + i_{tq} \cdot M(p) & \textcircled{H} \cdot p & p\theta \\
 \hline
 \end{array} \quad 3.62$$

3.5 Dual-Excited Synchronous Machine Connected to an Infinite-Bus Through a General Transmission System

3.5.1 Analysis of the transmission system

No complete analysis for the dual-excited synchronous machine can be claimed without taking into consideration the effect of its external connection with the power network. Equation 3.62 describes

the relations among the components of the terminal voltage of the machine and the components of its armature current as a function of its excitation voltages and speed. If the machine is connected to an infinite-bus via a transmission system having driving point impedances Z_{11} , Z_{22} and transfer impedance Z_{12} , then the relations between the voltages at both sides of the transmission system can be written as follows:

$$\begin{bmatrix} v_{ta} \\ v_{tb} \\ v_{tc} \end{bmatrix} = \begin{bmatrix} Z_{11}(p) \\ Z_{12}(p) \\ Z_{11}(p) \end{bmatrix} \begin{bmatrix} v_a & v_b & v_c \\ i_{ta} & i_{tb} & i_{tc} \end{bmatrix} \quad 3.63$$

The analysis is based on replacing the unknown terminal voltage of the machine v_t with the known bus-voltage v . Park's transformation helps again to formalize equation 3.63 in the two-axis frame. For example, the relations between the variables for phase a and its two-axis components are:

$$\begin{bmatrix} v_{ta} \\ v_a \\ i_{ta} \end{bmatrix} = \begin{bmatrix} v_{td} & v_{tq} \\ v_d & v_q \\ i_{td} & i_{tq} \end{bmatrix} \cdot \begin{bmatrix} \frac{e^{j\theta} + e^{-j\theta}}{2} \\ \frac{e^{j\theta} - e^{-j\theta}}{-2j} \end{bmatrix} \quad 3.64$$

Substituting equation 3.64 in 3.63, the following equation is obtained:

$$\begin{aligned} [v_{td} + jv_{tq}] \cdot e^{j\theta} + [v_{td} - jv_{tq}] \cdot e^{-j\theta} &= \frac{Z_{11}(p)}{Z_{12}(p)} [(v_d + jv_q) \cdot e^{j\theta} + \\ &+ (v_d - jv_q) \cdot e^{-j\theta}] + Z_{11}(p) [(i_{td} + ji_{tq}) \cdot e^{j\theta} + (i_{td} - ji_{tq}) \cdot e^{-j\theta}] \end{aligned} \quad 3.65$$

Putting $\theta = \delta_o + \Delta\delta + p\theta_o \cdot t$ and applying the Laplace transform theorem³⁶ $F(p) \cdot e^{at} f(t) = e^{at} \cdot F(p+a) \cdot f(t)$, equation 3.65 becomes:

$$\begin{aligned}
 & [v_{td} + jv_{tq}] \cdot e^{j(\delta_o + \Delta\delta + p\theta_o \cdot t)} + [v_{td} - jv_{tq}] \cdot e^{-j(\delta_o + \Delta\delta + p\theta_o \cdot t)} \\
 &= e^{j(\delta_o + p\theta_o \cdot t)} \cdot \frac{Z_{11}(p + jp\theta_o)}{Z_{12}(p + jp\theta_o)} [v_d + jv_q] \cdot e^{j\Delta\delta} + e^{-j(\delta_o + p\theta_o \cdot t)} \cdot \\
 & \frac{Z_{11}(p - jp\theta_o)}{Z_{12}(p - jp\theta_o)} [v_d - jv_q] \cdot e^{-j\Delta\delta} + e^{j(\delta_o + p\theta_o \cdot t)} \cdot Z_{11}(p + jp\theta_o) \\
 & [i_{td} + ji_{tq}] \cdot e^{j\Delta\delta} + e^{-j(\delta_o + p\theta_o \cdot t)} \cdot Z_{11}(p - jp\theta_o) \\
 & [i_{td} - ji_{tq}] \cdot e^{-j\Delta\delta}
 \end{aligned} \tag{3.66}$$

By equating the coefficients of $e^{j(\delta_o + p\theta_o \cdot t)}$ and $e^{-j(\delta_o + p\theta_o \cdot t)}$ in both the right and the left hand side, the following equation can be written:

$(v_{td} + jv_{tq}) \cdot e^{j\Delta\delta}$	$=$	$\frac{Z_{11}(p + jp\theta_o)}{Z_{12}(p + jp\theta_o)} \cdot e^{j\Delta\delta}$	$\frac{Z_{11}(p + jp\theta_o)}{Z_{12}(p + jp\theta_o)} \cdot je^{j\Delta\delta}$	
$(v_{td} - jv_{tq}) \cdot e^{-j\Delta\delta}$		$\frac{Z_{11}(p - jp\theta_o)}{Z_{12}(p - jp\theta_o)} \cdot e^{-j\Delta\delta}$	$\frac{Z_{11}(p - jp\theta_o)}{Z_{12}(p - jp\theta_o)} \cdot je^{-j\Delta\delta}$	

$Z_{11}(p + jp\theta_o) \cdot e^{j\Delta\delta}$	$Z_{11}(p + jp\theta_o) \cdot je^{j\Delta\delta}$	v_d
$Z_{11}(p - jp\theta_o) \cdot e^{-j\Delta\delta}$	$-Z_{11}(p - jp\theta_o) \cdot je^{-j\Delta\delta}$	v_q
		i_{td}
		i_{tq}

3.67

Considering equation 3.67, the axis components of the machine voltage can be given by:

v_{td}	Cos $\Delta\delta$	Sin $\Delta\delta$	$\text{Re} \left[\frac{Z_{11}(p+jp\theta_o)}{Z_{12}(p+jp\theta_o)} \right]$ $\text{Cos}\Delta\delta$ $-\text{Im} \left[\frac{Z_{11}(p+jp\theta_o)}{Z_{12}(p+jp\theta_o)} \right]$ $\text{Sin}\Delta\delta$	$-\text{Re} \left[\frac{Z_{11}(p+jp\theta_o)}{Z_{12}(p+jp\theta_o)} \right]$ $\text{Sin}\Delta\delta$ $-\text{Im} \left[\frac{Z_{11}(p+jp\theta_o)}{Z_{12}(p+jp\theta_o)} \right]$ $\text{Cos}\Delta\delta$
	=			
v_{tq}	-Sin $\Delta\delta$	Cos $\Delta\delta$	$\text{Re} \left[\frac{Z_{11}(p+jp\theta_o)}{Z_{12}(p+jp\theta_o)} \right]$ $\text{Sin}\Delta\delta$ $+\text{Im} \left[\frac{Z_{11}(p+jp\theta_o)}{Z_{12}(p+jp\theta_o)} \right]$ $\text{Cos}\Delta\delta$	$\text{Re} \left[\frac{Z_{11}(p+jp\theta_o)}{Z_{12}(p+jp\theta_o)} \right]$ $\text{Cos}\Delta\delta$ $-\text{Im} \left[\frac{Z_{11}(p+jp\theta_o)}{Z_{12}(p+jp\theta_o)} \right]$ $\text{Sin}\Delta\delta$

$\text{Re} [Z_{11}(p+jp\theta_o)]$ $\text{Cos}\Delta\delta$ $-\text{Im} [Z_{11}(p+jp\theta_o)]$ $\text{Sin}\Delta\delta$	$-\text{Re} [Z_{11}(p+jp\theta_o)]$ $\text{Sin}\Delta\delta$ $-\text{Im} [Z_{11}(p+jp\theta_o)]$ $\text{Cos}\Delta\delta$	v_d
$\text{Re} [Z_{11}(p+jp\theta_o)]$ $\text{Sin}\Delta\delta$ $+\text{Im} [Z_{11}(p+jp\theta_o)]$ $\text{Cos}\Delta\delta$	$\text{Re} [Z_{11}(p+jp\theta_o)]$ $\text{Cos}\Delta\delta$ $-\text{Im} [Z_{11}(p+jp\theta_o)]$ $\text{Sin}\Delta\delta$	v_q
		i_{td}
		i_{tq}

3.68

3.5.2 Equations of the machine in connection with the system

The general equation is obtained by replacing v_{td} and v_{tq} in equation 3.62 by the expressions of equation 3.68. After rearranging its terms, the equation takes the following form:

$$\begin{aligned}
 & \left(\text{Cos}\Delta\delta \cdot \text{Re} \left[\frac{Z_{11}(p+jp\theta_0)}{Z_{12}(p+jp\theta_0)} \right] \text{Cos}\Delta\delta - \text{Cos}\Delta\delta \cdot \text{Im} \left[\frac{Z_{11}(p+jp\theta_0)}{Z_{12}(p+jp\theta_0)} \right] \text{Sin}\Delta\delta \right. \\
 & + \text{Sin}\Delta\delta \cdot \text{Re} \left[\frac{Z_{11}(p+jp\theta_0)}{Z_{12}(p+jp\theta_0)} \right] \text{Sin}\Delta\delta + \text{Sin}\Delta\delta \cdot \text{Im} \left[\frac{Z_{11}(p+jp\theta_0)}{Z_{12}(p+jp\theta_0)} \right] \text{Cos}\Delta\delta \left. \right) v_d \\
 & + \left(-\text{Cos}\Delta\delta \cdot \text{Re} \left[\frac{Z_{11}(p+jp\theta_0)}{Z_{12}(p+jp\theta_0)} \right] \text{Sin}\Delta\delta - \text{Cos}\Delta\delta \cdot \text{Im} \left[\frac{Z_{11}(p+jp\theta_0)}{Z_{12}(p+jp\theta_0)} \right] \text{Cos}\Delta\delta \right. \\
 & + \text{Sin}\Delta\delta \cdot \text{Re} \left[\frac{Z_{11}(p+jp\theta_0)}{Z_{12}(p+jp\theta_0)} \right] \text{Cos}\Delta\delta - \text{Sin}\Delta\delta \cdot \text{Im} \left[\frac{Z_{11}(p+jp\theta_0)}{Z_{12}(p+jp\theta_0)} \right] \text{Sin}\Delta\delta \left. \right) v_q \\
 & - (G_{f1d}(p) \cdot p - (p\theta_0 + p\Delta\delta) \cdot G_{f1q}(p)) v_{f1} - (G_{f2d}(p) \cdot p - (p\theta_0 + p\Delta\delta) \cdot G_{f2q}(p)) v_{f2} \\
 & = \\
 & \left(-\text{Sin}\Delta\delta \cdot \text{Re} \left[\frac{Z_{11}(p+jp\theta_0)}{Z_{12}(p+jp\theta_0)} \right] \text{Cos}\Delta\delta + \text{Sin}\Delta\delta \cdot \text{Im} \left[\frac{Z_{11}(p+jp\theta_0)}{Z_{12}(p+jp\theta_0)} \right] \text{Sin}\Delta\delta \right. \\
 & + \text{Cos}\Delta\delta \cdot \text{Re} \left[\frac{Z_{11}(p+jp\theta_0)}{Z_{12}(p+jp\theta_0)} \right] \text{Sin}\Delta\delta + \text{Cos}\Delta\delta \cdot \text{Im} \left[\frac{Z_{11}(p+jp\theta_0)}{Z_{12}(p+jp\theta_0)} \right] \text{Cos}\Delta\delta \left. \right) v_d \\
 & + \left(\text{Sin}\Delta\delta \cdot \text{Re} \left[\frac{Z_{11}(p+jp\theta_0)}{Z_{12}(p+jp\theta_0)} \right] \text{Sin}\Delta\delta + \text{Sin}\Delta\delta \cdot \text{Im} \left[\frac{Z_{11}(p+jp\theta_0)}{Z_{12}(p+jp\theta_0)} \right] \text{Cos}\Delta\delta \right. \\
 & + \text{Cos}\Delta\delta \cdot \text{Re} \left[\frac{Z_{11}(p+jp\theta_0)}{Z_{12}(p+jp\theta_0)} \right] \text{Cos}\Delta\delta - \text{Cos}\Delta\delta \cdot \text{Im} \left[\frac{Z_{11}(p+jp\theta_0)}{Z_{12}(p+jp\theta_0)} \right] \text{Sin}\Delta\delta \left. \right) v_q \\
 & - ((p\theta_0 + p\Delta\delta) \cdot G_{f1d}(p) + G_{f1q}(p) \cdot p) v_{f1} - ((p\theta_0 + p\Delta\delta) \cdot G_{f2d}(p) + G_{f2q}(p) \cdot p) v_{f2} \\
 & T_i - \varepsilon_D(p) \cdot p\Delta\delta - (i_{tq} \cdot G_{f1d}(p) - i_{td} \cdot G_{f1q}(p)) v_{f1} - (i_{tq} \cdot G_{f2d}(p) - i_{td} \cdot G_{f2q}(p)) v_{f2}
 \end{aligned}$$

$ \begin{aligned} & -r \cdot x_d(p) \cdot p - (p\theta_0 + p\Delta\delta) \cdot M(p) \\ & - (\text{Cos}\Delta\delta \cdot \text{Re} [Z_{11}(p+jp\theta_0)] \text{Cos}\Delta\delta \\ & - \text{Cos}\Delta\delta \cdot \text{Im} [Z_{11}(p+jp\theta_0)] \text{Sin}\Delta\delta \\ & + \text{Sin}\Delta\delta \cdot \text{Re} [Z_{11}(p+jp\theta_0)] \text{Sin}\Delta\delta \\ & + \text{Sin}\Delta\delta \cdot \text{Im} [Z_{11}(p+jp\theta_0)] \text{Cos}\Delta\delta) \end{aligned} $	$ \begin{aligned} & (p\theta_0 + p\Delta\delta) \cdot x_q(p) + M(p) \cdot p \\ & + (\text{Cos}\Delta\delta \cdot \text{Re} [Z_{11}(p+jp\theta_0)] \text{Sin}\Delta\delta \\ & + \text{Cos}\Delta\delta \cdot \text{Im} [Z_{11}(p+jp\theta_0)] \text{Cos}\Delta\delta \\ & - \text{Sin}\Delta\delta \cdot \text{Re} [Z_{11}(p+jp\theta_0)] \text{Cos}\Delta\delta \\ & + \text{Sin}\Delta\delta \cdot \text{Im} [Z_{11}(p+jp\theta_0)] \text{Sin}\Delta\delta) \end{aligned} $
$ \begin{aligned} & - (p\theta_0 + p\Delta\delta) \cdot x_d(p) + M(p) \cdot p \\ & - (\text{Sin}\Delta\delta \cdot \text{Re} [Z_{11}(p+jp\theta_0)] \text{Cos}\Delta\delta \\ & + \text{Sin}\Delta\delta \cdot \text{Im} [Z_{11}(p+jp\theta_0)] \text{Sin}\Delta\delta \\ & + \text{Cos}\Delta\delta \cdot \text{Re} [Z_{11}(p+jp\theta_0)] \text{Sin}\Delta\delta \\ & + \text{Cos}\Delta\delta \cdot \text{Im} [Z_{11}(p+jp\theta_0)] \text{Cos}\Delta\delta) \end{aligned} $	$ \begin{aligned} & -r \cdot x_q(p) \cdot p + (p\theta_0 + p\Delta\delta) \cdot M(p) \\ & - (\text{Sin}\Delta\delta \cdot \text{Re} [Z_{11}(p+jp\theta_0)] \text{Sin}\Delta\delta \\ & + \text{Sin}\Delta\delta \cdot \text{Im} [Z_{11}(p+jp\theta_0)] \text{Cos}\Delta\delta \\ & + \text{Cos}\Delta\delta \cdot \text{Re} [Z_{11}(p+jp\theta_0)] \text{Cos}\Delta\delta \\ & - \text{Cos}\Delta\delta \cdot \text{Im} [Z_{11}(p+jp\theta_0)] \text{Sin}\Delta\delta) \end{aligned} $
$ -i_{tq} \cdot x_d(p) - i_{td} \cdot M(p) $	$ i_{td} \cdot x_q(p) + i_{tq} \cdot M(p) $

=

i_{td}	
i_{tq}	
$\Delta\delta$	

3.69

(H) · p²

3.5.3 Steady-state equations

At steady state operation, it can be shown that the axis currents and voltages corresponding to the time varying quantities are constant values independent of time (Appendix D). Hence, the general equations of the synchronous generator at this mode of operation can be derived by putting $p=0$ in equation 3.69. This, in addition to the fact that there are no variations in speed or rotor angle, would result in the following simplified equation:

$\operatorname{Re} \left[\frac{Z_{11}(jp\theta_o)}{Z_{12}(jp\theta_o)} \right] \cdot v_{do} - \operatorname{Im} \left[\frac{Z_{11}(jp\theta_o)}{Z_{12}(jp\theta_o)} \right] \cdot v_{qo} + p\theta_o \cdot e_d$	=
$\operatorname{Im} \left[\frac{Z_{11}(jp\theta_o)}{Z_{12}(jp\theta_o)} \right] \cdot v_{do} + \operatorname{Re} \left[\frac{Z_{11}(jp\theta_o)}{Z_{12}(jp\theta_o)} \right] \cdot v_{qo} - p\theta_o \cdot e_q$	
T_i	

$-r - \operatorname{Re}[Z_{11}(jp\theta_o)]$	$p\theta_o \cdot x_q + \operatorname{Im}[Z_{11}(jp\theta_o)]$	<table border="1" style="border-collapse: collapse;"> <tr> <td style="padding: 5px;">i_{tdo}</td> </tr> <tr> <td style="padding: 5px;">i_{tqo}</td> </tr> </table>	i_{tdo}	i_{tqo}
i_{tdo}				
i_{tqo}				
$-p\theta_o \cdot x_d - \operatorname{Im}[Z_{11}(jp\theta_o)]$	$-r - \operatorname{Re}[Z_{11}(jp\theta_o)]$			
$-e_d + i_{tqo} \cdot x_q$	$e_q - i_{tdo} \cdot x_d$	3.70		

where

$$e_d = -\frac{v_{f1o}}{r_{f1}} \cdot x_{aq} \cdot \sin\alpha_1 + \frac{v_{f2o}}{r_{f2}} \cdot x_{aq} \cdot \sin\alpha_2$$

$$e_q = \frac{v_{f1}}{r_{f1}} \cdot x_{ad} \cdot \cos\alpha_1 + \frac{v_{f2o}}{r_{f2}} \cdot x_{ad} \cdot \cos\alpha_2$$

3.5.4. Simplified transient equations

Since the speed of a synchronous machine cannot deviate appreciably from its steady synchronous value, it is justified to neglect its change on the machine electrical transients. As a result, the general equation 3.69 can be reduced to:

$$\begin{aligned}
 & \operatorname{Re} \left[\frac{Z_{11}(p+jp\theta_o)}{Z_{12}(p+jp\theta_o)} \right] v_d - \operatorname{Im} \left[\frac{Z_{11}(p+jp\theta_o)}{Z_{12}(p+jp\theta_o)} \right] v_q \\
 & - (G_{f1d}(p) \cdot p - p\theta_o \cdot G_{f1q}(p)) v_{f1} - (G_{f2d}(p) \cdot p - p\theta_o \cdot G_{f2q}(p)) v_{f2} \\
 & \operatorname{Im} \left[\frac{Z_{11}(p+jp\theta_o)}{Z_{12}(p+jp\theta_o)} \right] v_d + \operatorname{Re} \left[\frac{Z_{11}(p+jp\theta_o)}{Z_{12}(p+jp\theta_o)} \right] v_q \\
 & - (p\theta_o \cdot G_{f1d}(p) + G_{f1q}(p) \cdot p) v_{f1} - (p\theta_o \cdot G_{f2d}(p) + G_{f2q}(p) \cdot p) v_{f2} \\
 & T_i - (i_{tq} \cdot G_{f1d}(p) - i_{td} \cdot G_{f1q}(p)) v_{f1} - (i_{tq} \cdot G_{f2d}(p) - i_{td} \cdot G_{f2q}(p)) v_{f2} \\
 & \quad - g_D(p) \cdot p \Delta\delta
 \end{aligned}$$

$-r - x_d(p) \cdot p - p\theta_o \cdot M(p)$ $-\operatorname{Re} [Z_{11}(p+jp\theta_o)]$	$p\theta_o \cdot x_q(p) + M(p) \cdot p$ $+\operatorname{Im} [Z_{11}(p+jp\theta_o)]$		i_{td}
$-p\theta_o \cdot x_d(p) + M(p) \cdot p$ $-\operatorname{Im} [Z_{11}(p+jp\theta_o)]$	$-r - x_q(p) \cdot p + p\theta_o \cdot M(p)$ $-\operatorname{Re} [Z_{11}(p+jp\theta_o)]$		i_{tq}
$-i_{tq} \cdot x_d(p) - i_{td} \cdot M(p)$	$i_{td} \cdot x_q(p) + i_{tq} \cdot M(p)$	$\oplus \cdot p^2$	$\Delta\delta$

3.71

3.5.5 Application to a simple power system

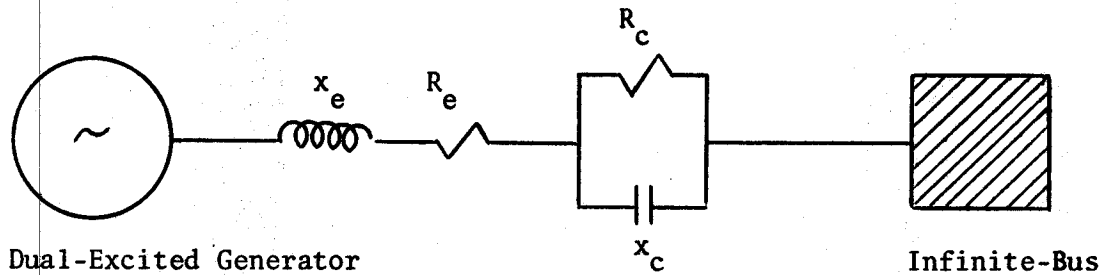


Fig. 3.2 A Simple Power System

For the system shown in Fig. 3.2, the following equations can be written:

$$Z_{11}(p) = Z_{12}(p) = R_e + x_e \cdot p + \frac{x_c}{p + \alpha} \quad 3.72$$

where $\alpha = X_c / R_c$

$$\operatorname{Re}[Z_{11}(p+jp\theta_o)] = R_e + x_e \cdot p + \frac{x_c \cdot (p+\alpha)}{(p+\alpha)^2 + (p\theta_o)^2} \quad 3.73$$

$$\operatorname{Im}[Z_{11}(p+jp\theta_o)] = x_e \cdot p\theta_o - \frac{p\theta_o \cdot x_c}{(p+\alpha)^2 + (p\theta_o)^2} \quad 3.74$$

$$\operatorname{Re}\left[\frac{Z_{11}(p+jp\theta_o)}{Z_{12}(p+jp\theta_o)}\right] = 1 \quad 3.75$$

$$\operatorname{Im}\left[\frac{Z_{11}(p+jp\theta_o)}{Z_{12}(p+jp\theta_o)}\right] = 0 \quad 3.76$$

$$i_{td} = i_d \quad 3.77$$

$$i_{tq} = i_q \quad 3.78$$

Substituting from equations 3.72 - 3.78 in equations 3.70 and 3.71, the system during steady state and transient conditions may be represented as follows:

a) Steady-state equations

$v_{do} + p\theta_o \cdot e_d$	$-(r+R_e) \cdot \frac{\alpha \cdot x_c}{\alpha^2 + (p\theta_o)^2}$	$p\theta_o \cdot (x_e + x_q) - \frac{p\theta_o \cdot x_c}{\alpha^2 + (p\theta_o)^2}$	i_{do}	3.79	
$v_{qo} - p \cdot e_q$	$-p\theta_o \cdot (x_e + x_d) + \frac{p\theta_o \cdot x_c}{\alpha^2 + (p\theta_o)^2}$	$-(r+R_e) \cdot \frac{\alpha \cdot x_c}{\alpha^2 + (p\theta_o)^2}$			i_{qo}
T_i	$e_d + i_{qo} \cdot x_q$	$e_q - i_{do} \cdot x_d$			

b) Simplified transient equations

$v_d - (G_{f1d}(p) \cdot p - p\theta_o \cdot G_{f1q}(p)) v_{f1}$	=
$- (G_{f2d}(p) \cdot p - p\theta_o \cdot G_{f2q}(p)) v_{f2}$	
$v_q - (p\theta_o \cdot G_{f1d}(p) + G_{f1q}(p) \cdot p) v_{f1}$	
$- (p\theta_o \cdot G_{f2d}(p) + G_{f2q}(p) \cdot p) v_{f2}$	
$T_i - (i_{tq} \cdot G_{f1d}(p) - i_{td} \cdot G_{f1q}(p)) v_{f1}$	
$- (i_{tq} \cdot G_{f2d}(p) - i_{td} \cdot G_{f2q}(p)) v_{f2}$	

$-(r+R_e) \cdot \frac{x_c \cdot (p+\alpha)}{(p+\alpha)^2 + (p\theta_o)^2}$	$p\theta_o \cdot (x_e + x_q(p)) - \frac{x_c \cdot p\theta_o}{(p+\alpha)^2 + (p\theta_o)^2}$	i_d	3.80
$-p\theta_o \cdot (x_e + x_d(p)) + \frac{x_c \cdot p\theta_o}{(p+\alpha)^2 + (p\theta_o)^2}$	$-(r+R_e) \cdot \frac{x_c \cdot (p+\alpha)}{(p+\alpha)^2 + (p\theta_o)^2}$		
$-i_q \cdot x_d(p) - i_d \cdot M(p)$	$i_d \cdot x_q(p) + i_q \cdot M(p)$	Δs	

4. SMALL DISPLACEMENT EQUATIONS OF THE DUAL-EXCITED SYNCHRONOUS MACHINE

4.1 Introduction

Since the static stability is concerned with a very slow variation, the determination of its limit is based on representing the synchronous machines simply by their synchronous reactances. In this case, a mathematical expression can be deduced from the steady-state vector diagram. When there is no saliency, the expression for the static stability boundary of the dual-excited synchronous machine is quite simple and is the same as that of a nonsalient conventional one. If saliency is considered, the expressions obtained will be very complicated and no physical interpretations can be understood from it.

On the other hand, the instability of the regulated synchronous machines in the neighbourhood of the dynamic stability boundary shows up in the form of self-excited oscillations and not, as normally happens at the static limit, by slow falling out of synchronism with continuously and monotonically increasing rotor angle. The period of these oscillations ranges from 0.5 to 10 seconds or more for large machines. Thus, a determination of the dynamic stability limit through representing the machine by its synchronous reactance cannot be justified, as this does not allow for the changes in the variables. Going to the other extreme and using the transient reactances of the machine cannot be justified either, since the transient reactances apply only to sudden changes which take place within a fraction of a second. A more accurate representation of the machine allowing for field time constants, inertia and other transient quantities is therefore necessary for investigating

its dynamic stability.

4.2 Possible Techniques for Dynamic Stability Studies

An accurate dynamic stability analysis should be based on the generalized machine representation in the two-axis frame given by equation 3.69. The differential equations involved are non-linear and, with the inclusion of regulating devices in the representation, the number of variables to be handled becomes excessively large. Consequently, it is necessary to rely on some simplifications, or some computing devices to perform the calculations, or upon a combination of both. The methods, which have been used in the past, may be broadly grouped into two categories:

a) Methods relying upon a full solution of the general equation:

In these methods, the solution of the general equation is obtained by numerical methods or by analogue computer simulation. The latter is not generally preferred due to the limited capacity of most analogue computers, its relative inaccuracy and the long time required for setting such problems. On the other hand, solving the general equation of the machine using a digital computer would be uneconomical especially if many operating conditions are to be studied.

b) Methods using a linearizing approach:

This is the usual approach to dynamic stability studies. It is mathematically valid if only very small changes around the operating point are postulated. The assumption of a linear system makes it possible to apply a range of techniques which have been used in control system applications. The solution in this case may be accomplished by a digital computer. The computing time will be far shorter than in the case of the complete solution of the general equation by numerical means. Among the methods

that have been used are the following:

1. Nyquist Criterion

This is one of the oldest of the control systems techniques. Nyquist diagrams have been used by Messerle and Bruck¹¹, Jacovides and Adkins²² and others^{28,29}. Apart from the indirect approach to the stability limit, it suffers from the disadvantages of extensive computation and poor presentation of results but is able to show the degree of stability and to indicate the possible procedure for improvement.

2. Root Locus

In this method, the system characteristic equation is formed and the eigenvalues are calculated. It has been used by Stapleton²³. It suffers from the extensive effort consumed in finding the characteristic roots.

3. Domain Separation

The Russians make use of this method to show the stability limit in the plane of two parameters of interest. The method is fast and appears to have considerable application to problems involving the setting of regulator parameters for optimum results. It has been used by Yu¹⁹.

4. Routh's Criterion

This is perhaps the best method available for general problems. It allows a direct approach to the stability limit using a set of criteria which can be easily programmed on a digital computer. This method has been extensively used^{8,9,19,30}. It is utilized herein for

investigating the dynamic stability limits of the dual-excited synchronous machine.

4.3 Small Displacement Equations

As explained before, it is quite sufficient for studying the dynamic stability of the dual-excited synchronous machine to use a linearized small displacement representation. Such a representation can be obtained by considering deviations in the time dependant variables from their steady-state values. Thus

$$v = v_o + \Delta v \quad 4.1$$

$$i = i_o + \Delta i \quad 4.2$$

$$\delta = \delta_o + \Delta \delta \quad 4.3$$

Substituting equations 4.1 - 4.3 in the general equation of the dual-excited synchronous machine (equation 3.69) and subtracting the terms corresponding to the initial steady-state operating point, the equations of the machine will be given in terms of the time dependant deviations. If these deviations are very small, the terms of power 2 and more can be neglected and the following approximations can also be applied:

$$\text{Cos} \Delta \delta \approx 1 \quad 4.4$$

$$\text{Sin} \Delta \delta \approx \Delta \delta \quad 4.5$$

Hence, the following small displacement equations result:

Δi_{td}		
Δi_{tdq}		
$\Delta \delta$		

$-r \cdot x_d(p) \cdot p$	$p \theta_0 \cdot x_q(p)$	$(-i_{tdq} \cdot x_d + e_q) \cdot p$ $+ i_{tdo} \cdot \text{Im}[Z_{11}(p+jp\theta_0)]$
$-p \theta_0 \cdot M(p)$	$+M(p) \cdot p$	$-i_{tdo} \cdot \text{Im}[Z_{11}(p)]$ $+ i_{tdq} \cdot \text{Re}[Z_{11}(p+jp\theta_0)]$
$-\text{Re}[Z_{11}(p+jp\theta_0)]$	$+ \text{Im}[Z_{11}(p+jp\theta_0)]$	$-i_{tdq} \cdot \text{Re}[Z_{11}(p)]$ $+ i_{tdo} \cdot \text{Im}[Z_{11}(p)]$
$-p \theta_0 \cdot x_d(p)$	$-r \cdot x_q(p) \cdot p$	$(-i_{tdo} \cdot x_d + e_q) \cdot p$ $- i_{tdo} \cdot \text{Re}[Z_{11}(p+jp\theta_0)]$
$+M(p) \cdot p$	$p \theta_0 \cdot M(p)$	$+ i_{tdo} \cdot \text{Re}[Z_{11}(p)]$ $+ i_{tdq} \cdot \text{Im}[Z_{11}(p+jp\theta_0)]$
$-\text{Im}[Z_{11}(p+jp\theta_0)]$	$-\text{Re}[Z_{11}(p+jp\theta_0)]$	$- i_{tdq} \cdot \text{Im}[Z_{11}(p)]$ $- i_{tdo} \cdot \text{Re}[Z_{11}(p)]$
$-i_{tdq} \cdot x_d(p)$ $-i_{tdo} \cdot M(p)$ $-e_d + i_{tdq} \cdot x_q$	$i_{tdo} \cdot x_q(p)$ $+ i_{tdq} \cdot M(p)$ $e_q - i_{tdo} \cdot x_d$	$(H) \cdot p^2$ $+ g_D(p) \cdot p$

$\text{Re} \left[\frac{Z_{11}(p+jp\theta_0)}{Z_{12}(p+jp\theta_0)} \right] (\Delta v_d - v_{qo} \cdot \Delta \delta) - \text{Im} \left[\frac{Z_{11}(p+jp\theta_0)}{Z_{12}(p+jp\theta_0)} \right] (\Delta v_q + v_{do} \cdot \Delta \delta)$ $+ \left(\text{Re} \left[\frac{Z_{11}(p\theta_0)}{Z_{12}(p\theta_0)} \right] \cdot v_{qo} + \text{Im} \left[\frac{Z_{11}(p\theta_0)}{Z_{12}(p\theta_0)} \right] \cdot v_{do} \right) \cdot \Delta \delta$	$-\text{Im} \left[\frac{Z_{11}(p+jp\theta_0)}{Z_{12}(p+jp\theta_0)} \right] (\Delta v_d - v_{qo} \cdot \Delta \delta) + \text{Re} \left[\frac{Z_{11}(p+jp\theta_0)}{Z_{12}(p+jp\theta_0)} \right] (\Delta v_q + v_{do} \cdot \Delta \delta)$ $- \left(\text{Re} \left[\frac{Z_{11}(p\theta_0)}{Z_{12}(p\theta_0)} \right] \cdot v_{do} - \text{Im} \left[\frac{Z_{11}(p\theta_0)}{Z_{12}(p\theta_0)} \right] \cdot v_{qo} \right) \cdot \Delta \delta$	$-\text{Re} \left[\frac{Z_{11}(p+jp\theta_0)}{Z_{12}(p+jp\theta_0)} \right] (\Delta v_d - v_{qo} \cdot \Delta \delta) + \text{Im} \left[\frac{Z_{11}(p+jp\theta_0)}{Z_{12}(p+jp\theta_0)} \right] (\Delta v_q + v_{do} \cdot \Delta \delta)$ $- \left(\text{Re} \left[\frac{Z_{11}(p\theta_0)}{Z_{12}(p\theta_0)} \right] \cdot v_{do} - \text{Im} \left[\frac{Z_{11}(p\theta_0)}{Z_{12}(p\theta_0)} \right] \cdot v_{qo} \right) \cdot \Delta \delta$
$-\text{Im} \left[\frac{Z_{11}(p+jp\theta_0)}{Z_{12}(p+jp\theta_0)} \right] (\Delta v_d - v_{qo} \cdot \Delta \delta) + \text{Re} \left[\frac{Z_{11}(p+jp\theta_0)}{Z_{12}(p+jp\theta_0)} \right] (\Delta v_q + v_{do} \cdot \Delta \delta)$ $- \left(\text{Re} \left[\frac{Z_{11}(p\theta_0)}{Z_{12}(p\theta_0)} \right] \cdot v_{do} - \text{Im} \left[\frac{Z_{11}(p\theta_0)}{Z_{12}(p\theta_0)} \right] \cdot v_{qo} \right) \cdot \Delta \delta$	$-\text{Re} \left[\frac{Z_{11}(p+jp\theta_0)}{Z_{12}(p+jp\theta_0)} \right] (\Delta v_d - v_{qo} \cdot \Delta \delta) + \text{Im} \left[\frac{Z_{11}(p+jp\theta_0)}{Z_{12}(p+jp\theta_0)} \right] (\Delta v_q + v_{do} \cdot \Delta \delta)$ $- \left(\text{Re} \left[\frac{Z_{11}(p\theta_0)}{Z_{12}(p\theta_0)} \right] \cdot v_{do} - \text{Im} \left[\frac{Z_{11}(p\theta_0)}{Z_{12}(p\theta_0)} \right] \cdot v_{qo} \right) \cdot \Delta \delta$	$-\text{Im} \left[\frac{Z_{11}(p+jp\theta_0)}{Z_{12}(p+jp\theta_0)} \right] (\Delta v_d - v_{qo} \cdot \Delta \delta) + \text{Re} \left[\frac{Z_{11}(p+jp\theta_0)}{Z_{12}(p+jp\theta_0)} \right] (\Delta v_q + v_{do} \cdot \Delta \delta)$ $- \left(\text{Re} \left[\frac{Z_{11}(p\theta_0)}{Z_{12}(p\theta_0)} \right] \cdot v_{do} - \text{Im} \left[\frac{Z_{11}(p\theta_0)}{Z_{12}(p\theta_0)} \right] \cdot v_{qo} \right) \cdot \Delta \delta$
$-(i_{tdq} \cdot G_{f1d}(p) - i_{tdo} \cdot G_{f1q}(p)) \Delta v_{f1}$ $-(i_{tdq} \cdot G_{f2d}(p) - i_{tdo} \cdot G_{f2q}(p)) \Delta v_{f2}$	$-(i_{tdq} \cdot G_{f1d}(p) - i_{tdo} \cdot G_{f1q}(p)) \Delta v_{f1}$ $-(i_{tdq} \cdot G_{f2d}(p) - i_{tdo} \cdot G_{f2q}(p)) \Delta v_{f2}$	$-(i_{tdq} \cdot G_{f1d}(p) - i_{tdo} \cdot G_{f1q}(p)) \Delta v_{f1}$ $-(i_{tdq} \cdot G_{f2d}(p) - i_{tdo} \cdot G_{f2q}(p)) \Delta v_{f2}$

From equation 3.70, the following relations are obtained:

$$\begin{aligned} & \left\{ \operatorname{Re} \left[\frac{Z_{11}(jp\theta_o)}{Z_{12}(jp\theta_o)} \right] \cdot v_{qo} + \operatorname{Im} \left[\frac{Z_{11}(jp\theta_o)}{Z_{12}(jp\theta_o)} \right] \cdot v_{do} \right\} \Delta\delta \\ & = \{ v_{tqo} - i_{tdo} \cdot \operatorname{Im}[Z_{11}(jp\theta_o)] - i_{tqo} \cdot \operatorname{Re}[Z_{11}(jp\theta_o)] \} \cdot \Delta\delta \end{aligned} \quad 4.7$$

$$\begin{aligned} & \left\{ \operatorname{Re} \left[\frac{Z_{11}(jp\theta_o)}{Z_{12}(jp\theta_o)} \right] \cdot v_{do} - \operatorname{Im} \left[\frac{Z_{11}(jp\theta_o)}{Z_{12}(jp\theta_o)} \right] \cdot v_{qo} \right\} \Delta\delta \\ & = \{ v_{tdo} - i_{tdo} \cdot \operatorname{Re}[Z_{11}(jp\theta_o)] + i_{tqo} \cdot \operatorname{Im}[Z_{11}(jp\theta_o)] \} \cdot \Delta\delta \end{aligned} \quad 4.8$$

Also for a constant bus voltage, the following relations are valid:

$$\Delta v_d = v \cdot \sin(\delta_o + \Delta\delta) - v \sin \delta_o \approx v_{qo} \cdot \Delta\delta \quad 4.9$$

$$\Delta v_q = v \cdot \cos(\delta_o + \Delta\delta) - v \cos \delta_o \approx -v_{do} \cdot \Delta\delta \quad 4.10$$

Substituting equations 4.7 - 4.10 in 4.6, the small displacement equations can be written as follows:

4.4 Machine Regulation

The superior dynamic and transient performance of the dual-excited synchronous machine is mainly due to the availability of two separate field circuits with the possibility of controlling each in a different way. One of the suggested regulation schemes is to provide one of the two field windings (winding 1) with a voltage regulator while the other is provided with a rotor angle regulator^{27,29,30}. However, it would be interesting to study the performance of this machine for various other schemes of excitation regulation. Fig.4.1 shows a single-line block diagram for dual-excited synchronous machine excitation control, in which any possible feed-back signal combination can be chosen by using a group of arbitrary constants C_{1v} , C_{2v} , $C_{1\delta}$, $C_{2\delta}$, $C_{1p\delta}$, $C_{2p\delta}$, $C_{1p2\delta}$, $C_{2p2\delta}$, C_{1p} , C_{2p} , C_{1q} , C_{2q} , C_{1I} , C_{2I} .

In general, the expressions of the excitation controlling signals for both field windings may be given as follows:

$$\begin{aligned} \Delta v_{f1} = g_{R1}(p) [& C_{1v} \cdot \Delta v + C_{1p} \cdot \Delta P + C_{1q} \cdot \Delta Q + C_{1I} \cdot \Delta i + C_{1\delta} \cdot \Delta \delta \\ & + C_{1p\delta} \cdot p \Delta \delta + C_{1p2\delta} \cdot p^2 \Delta \delta] \end{aligned} \quad 4.12$$

$$\begin{aligned} \Delta v_{f2} = g_{R2}(p) [& C_{2v} \cdot \Delta v + C_{2p} \cdot \Delta P + C_{2q} \cdot \Delta Q + C_{2I} \cdot \Delta i + C_{2\delta} \cdot \Delta \delta \\ & + C_{2p\delta} \cdot p \Delta \delta + C_{2p2\delta} \cdot p^2 \Delta \delta] \end{aligned} \quad 4.13$$

The equations giving the terminal voltage, power, reactive power and current deviations in terms of Δi_{td} , Δi_{tq} and $\Delta \delta$ can be derived by expanding these variables in the neighbourhood of the operating point. This will result in the following equations:

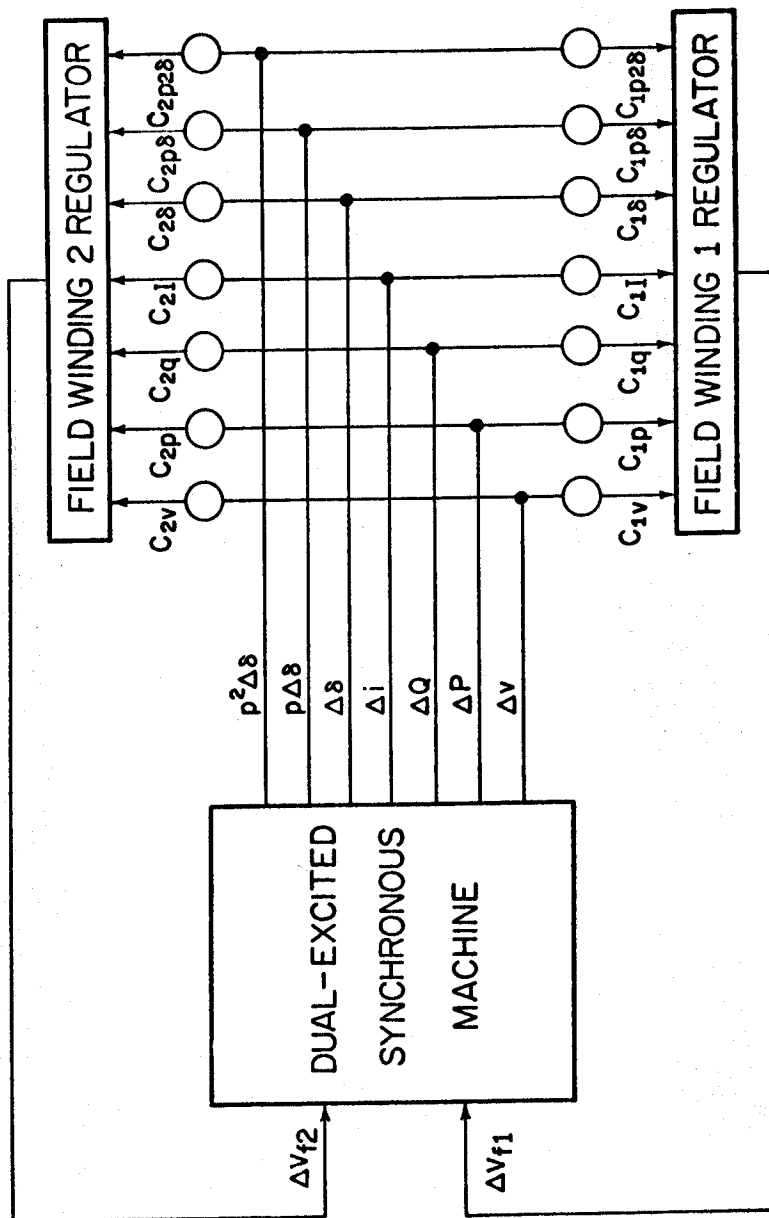


Fig. 4.1 Single Line Block Diagram for the Excitation Control of a Dual-Excited Synchronous Machine

$$\Delta v_t = \frac{v_{tdo}}{v_{to}} \cdot \Delta v_{td} + \frac{v_{tqo}}{v_{to}} \cdot \Delta v_{tq} \quad 4.14$$

$$\Delta i_t = \frac{i_{tdo}}{i_{to}} \cdot \Delta i_{td} + \frac{i_{tqo}}{i_{to}} \cdot \Delta i_{tq} \quad 4.15$$

$$\begin{aligned} \Delta P_t = i_{tdo} \cdot \Delta v_{td} + i_{tqo} \cdot \Delta v_{tq} + v_{tdo} \cdot \Delta i_{td} \\ + v_{tqo} \cdot \Delta i_{tq} \end{aligned} \quad 4.16$$

$$\begin{aligned} \Delta Q_t = -i_{tqo} \cdot \Delta v_{td} + i_{tdo} \cdot \Delta v_{tq} + v_{tqo} \cdot \Delta i_{td} \\ - v_{tdo} \cdot \Delta i_{tq} \end{aligned} \quad 4.17$$

The elimination of Δv_{td} and Δv_{tq} from equations 4.14, 4.16 and 4.17 in favour of Δi_{td} , Δi_{tq} and $\Delta \delta$ can be done through linearizing equation 3.68 as follows:

Δv_{td}	$\operatorname{Re} \left[\frac{Z_{11}(p+jp\theta_o)}{Z_{12}(p+jp\theta_o)} \right]$	$-\operatorname{Im} \left[\frac{Z_{11}(p+jp\theta_o)}{Z_{12}(p+jp\theta_o)} \right]$	$\operatorname{Re} [Z_{11}(p+jp\theta_o)]$
Δv_{tq}	$\operatorname{Im} \left[\frac{Z_{11}(p+jp\theta_o)}{Z_{12}(p+jp\theta_o)} \right]$	$\operatorname{Re} \left[\frac{Z_{11}(p+jp\theta_o)}{Z_{12}(p+jp\theta_o)} \right]$	$\operatorname{Im} [Z_{11}(p+jp\theta_o)]$

$-\operatorname{Im} [Z_{11}(p+jp\theta_o)]$	$-v_{do} \cdot \operatorname{Im} \left[\frac{Z_{11}(p+jp\theta_o)}{Z_{12}(p+jp\theta_o)} \right] + v_{do} \cdot \operatorname{Im} \left[\frac{Z_{11}(jp\theta_o)}{Z_{12}(jp\theta_o)} \right]$ $-v_{qo} \cdot \operatorname{Re} \left[\frac{Z_{11}(p+jp\theta_o)}{Z_{12}(p+jp\theta_o)} \right] + v_{qo} \cdot \operatorname{Re} \left[\frac{Z_{11}(jp\theta_o)}{Z_{12}(jp\theta_o)} \right]$ $-i_{tdo} \cdot \operatorname{Im} [Z_{11}(p+jp\theta_o)] + i_{tdo} \cdot \operatorname{Im} [Z_{11}(jp\theta_o)]$ $-i_{tqo} \cdot \operatorname{Re} [Z_{11}(p+jp\theta_o)] + i_{tqo} \cdot \operatorname{Re} [Z_{11}(jp\theta_o)]$	Δv_d
$\operatorname{Re} [Z_{11}(p+jp\theta_o)]$	$v_{do} \cdot \operatorname{Re} \left[\frac{Z_{11}(p+jp\theta_o)}{Z_{12}(p+jp\theta_o)} \right] - v_{do} \cdot \operatorname{Re} \left[\frac{Z_{11}(jp\theta_o)}{Z_{12}(jp\theta_o)} \right]$ $-v_{qo} \cdot \operatorname{Im} \left[\frac{Z_{11}(p+jp\theta_o)}{Z_{12}(p+jp\theta_o)} \right] + v_{qo} \cdot \operatorname{Im} \left[\frac{Z_{11}(jp\theta_o)}{Z_{12}(jp\theta_o)} \right]$ $+i_{tdo} \cdot \operatorname{Re} [Z_{11}(p+jp\theta_o)] - i_{tdo} \cdot \operatorname{Re} [Z_{11}(jp\theta_o)]$ $-i_{tqo} \cdot \operatorname{Im} [Z_{11}(p+jp\theta_o)] + i_{tqo} \cdot \operatorname{Im} [Z_{11}(jp\theta_o)]$	Δv_q
		Δi_{td}
		Δi_{tq}
		$\Delta \delta$

4.18

But:

v_{tdo}	$\text{Re} \left[\frac{Z_{11}(jp\theta_o)}{Z_{12}(jp\theta_o)} \right]$	$-\text{Im} \left[\frac{Z_{11}(jp\theta_o)}{Z_{12}(jp\theta_o)} \right]$	$\text{Re}[Z_{11}(jp\theta_o)]$	$-\text{Im}[Z_{11}(jp\theta_o)]$	v_{do}
v_{tqo}	$\text{Im} \left[\frac{Z_{11}(jp\theta_o)}{Z_{12}(jp\theta_o)} \right]$	$\text{Re} \left[\frac{Z_{11}(jp\theta_o)}{Z_{12}(jp\theta_o)} \right]$	$\text{Im}[Z_{11}(jp\theta_o)]$	$\text{Re}[Z_{11}(jp\theta_o)]$	i_{tdo}
					i_{tqo}

4.19

Using equations 4.9, 4.10 and 4.19, equation 4.18 can be reduced to:

Δv_{td}	$\text{Re}[Z_{11}(p+jp\theta_o)]$	$-\text{Im}[Z_{11}(p+jp\theta_o)]$	
Δv_{tq}	$\text{Im}[Z_{11}(p+jp\theta_o)]$	$\text{Re}[Z_{11}(p+jp\theta_o)]$	

v_{tqo}	$-\dot{i}_{tdo} \cdot \text{Im}[Z_{11}(p + jp\theta_o)]$	Δi_{td}
v_{tdo}	$-\dot{i}_{tqo} \cdot \text{Re}[Z_{11}(p + jp\theta_o)]$	Δi_{tq}
$-v_{tqo}$	$+\dot{i}_{tdo} \cdot \text{Re}[Z_{11}(p + jp\theta_o)]$	$\Delta \delta$
$-v_{tdo}$	$-\dot{i}_{tqo} \cdot \text{Im}[Z_{11}(p + jp\theta_o)]$	

4.20

Substituting equations 4.12 - 4.17 and 4.20 in 4.11, the following general form of the small displacement equations results:

$GRG1(p) \cdot B_1 + GRG2(p) \cdot B_2$	$GRG1(p) \cdot C_1 + GRG2(p) \cdot C_2$	$GRG1(p) \cdot (C_{1\delta} + C_{1p\delta} \cdot p + C_{1p2\delta} \cdot p^2) +$ $GRG2(p) \cdot (C_{2\delta} + C_{2p\delta} \cdot p + C_{2p2\delta} \cdot p^2)$ $GRG1(p) \cdot D_1 + GRG2(p) \cdot D_2$	Δi_{td}
$GRG3(p) \cdot B_1 + GRG4(p) \cdot B_2$	$GRG3(p) \cdot C_1 + GRG4(p) \cdot C_2$	$GRG3(p) \cdot (C_{1\delta} + C_{1p\delta} \cdot p + C_{1p2\delta} \cdot p^2) +$ $GRG4(p) \cdot (C_{2\delta} + C_{2p\delta} \cdot p + C_{2p2\delta} \cdot p^2)$ $GRG3(p) \cdot D_1 + GRG4(p) \cdot D_2$	Δi_{tq}
$GRG5(p) \cdot B_1 + GRG6(p) \cdot B_2$	$GRG5(p) \cdot C_1 + GRG6(p) \cdot C_2$	$GRG5(p) \cdot (C_{1\delta} + C_{1p\delta} \cdot p + C_{1p2\delta} \cdot p^2) +$ $GRG6(p) \cdot (C_{2\delta} + C_{2p\delta} \cdot p + C_{2p2\delta} \cdot p^2)$ $GRG5(p) \cdot D_1 + GRG6(p) \cdot D_2$	$\Delta \delta$

$-r \cdot x_d(p) \cdot p$ $-(p\theta_o) \cdot M(p)$ $-\text{Re}[Z_{11}(p+jp\theta_o)]$	$p\theta_o \cdot x_q(p)$ $+M(p) \cdot p$ $+ \text{Im}[Z_{11}(p+jp\theta_o)]$	$(i_{tqo} \cdot x_q - e_d) \cdot p - v_{tqo}$ $+ i_{tdo} \cdot \text{Im}[Z_{11}(p+jp\theta_o)]$ $+ i_{tqo} \cdot \text{Re}[Z_{11}(p+jp\theta_o)]$	Δi_{td}
$-p\theta_o \cdot x_d(p)$ $+M(p) \cdot p$ $-\text{Im}[Z_{11}(p+jp\theta_o)]$	$-r \cdot x_q(p) \cdot p$ $+p\theta_o \cdot M(p)$ $-\text{Re}[Z_{11}(p+jp\theta_o)]$	$(-i_{tdo} \cdot x_d + c_q) \cdot p + v_{tdo}$ $-i_{tdo} \cdot \text{Re}[Z_{11}(p+jp\theta_o)]$ $+ i_{tqo} \cdot \text{Im}[Z_{11}(p+jp\theta_o)]$	Δi_{td}
$-i_{tqo} \cdot x_d(p)$ $-i_{tdo} \cdot M(p)$ $-e_d + i_{tqo} \cdot x_q$	$i_{tdo} \cdot x_q(p)$ $+i_{tqo} \cdot M(p)$ $+c_q - i_{tdo} \cdot x_d$	$\textcircled{H} \cdot p^2 + g_D(p) \cdot p$	$\Delta \delta$

4.21

where:

$$B_1 = (C_{1p} \cdot v_{tdo} + C_{1q} \cdot v_{tqo} + C_{1I} \cdot \frac{i_{tdo}}{i_{to}}) + (C_{1v} \cdot \frac{v_{tdo}}{v_{to}} + C_{1p} \cdot i_{tdo} - C_{1q} \cdot i_{tqo}) \cdot$$

$$\text{Re}[Z_{11}(p+jp\theta_o)] + (C_{1v} \cdot \frac{v_{tqo}}{v_{to}} + C_{1p} \cdot i_{tqo} + C_{1q} \cdot i_{tdo}) \cdot \text{Im}[Z_{11}(p+jp\theta_o)]$$

$$B_2 = (C_{2p} \cdot v_{tdo} + C_{2q} \cdot v_{tqo} + C_{2I} \cdot \frac{i_{tdo}}{i_{to}}) + (C_{2v} \cdot \frac{v_{tdo}}{v_{to}} + C_{2p} \cdot i_{tdo} - C_{2q} \cdot i_{tqo}) \cdot \operatorname{Re}[Z_{11}(p+jp\theta_o)] + (C_{2v} \cdot \frac{v_{tqo}}{v_{to}} + C_{2p} \cdot i_{tqo} + C_{2q} \cdot i_{tdo}) \cdot \operatorname{Im}[Z_{11}(p+jp\theta_o)]$$

$$C_1 = (C_{1p} \cdot v_{tqo} - C_{1q} \cdot v_{tdo} + C_{1I} \cdot \frac{i_{tqo}}{i_{to}}) - (C_{1v} \cdot \frac{v_{tdo}}{v_{to}} + C_{1p} \cdot i_{tdo} - C_{1q} \cdot i_{tqo}) \cdot \operatorname{Im}[Z_{11}(p+jp\theta_o)] + (C_{1v} \cdot \frac{v_{tqo}}{v_{to}} + C_{1p} \cdot i_{tqo} + C_{1q} \cdot i_{tdo}) \cdot \operatorname{Re}[Z_{11}(p+jp\theta_o)]$$

$$C_2 = (C_{2p} \cdot v_{tqo} - C_{2q} \cdot v_{tdo} + C_{2I} \cdot \frac{i_{tqo}}{i_{to}}) - (C_{2v} \cdot \frac{v_{tdo}}{v_{to}} + C_{2p} \cdot i_{tdo} - C_{2q} \cdot i_{tqo}) \cdot \operatorname{Im}[Z_{11}(p+jp\theta_o)] + (C_{2v} \cdot \frac{v_{tqo}}{v_{to}} + C_{2p} \cdot i_{tqo} + C_{2q} \cdot i_{tdo}) \cdot \operatorname{Re}[Z_{11}(p+jp\theta_o)]$$

$$D_1 = (C_{1v} \cdot \frac{v_{tdo}}{v_{to}} + C_{1p} \cdot i_{tdo} - C_{1q} \cdot i_{tqo}) \cdot [v_{tqo} - i_{tdo} \cdot \operatorname{Im}[Z_{11}(p+jp\theta_o)]] - i_{tqo} \cdot \operatorname{Re}[Z_{11}(p+jp\theta_o)] + (C_{1v} \cdot \frac{v_{tqo}}{v_{to}} + C_{1p} \cdot i_{tqo} + C_{1q} \cdot i_{tdo}) \cdot [-v_{tdo} + i_{tdo} \cdot \operatorname{Re}[Z_{11}(p+jp\theta_o)]] - i_{tqo} \cdot \operatorname{Im}[Z_{11}(p+jp\theta_o)]$$

$$D_2 = (C_{2v} \cdot \frac{v_{tdo}}{v_{to}} + C_{2p} \cdot i_{tdo} - C_{2q} \cdot i_{tqo}) \cdot [v_{tqo} - i_{tdo} \cdot \operatorname{Im}[Z_{11}(p+jp\theta_o)]] - i_{tqo} \cdot \operatorname{Re}[Z_{11}(p+jp\theta_o)] + (C_{2v} \cdot \frac{v_{tqo}}{v_{to}} + C_{2p} \cdot i_{tqo} + C_{2q} \cdot i_{tdo}) \cdot [-v_{tdo} + i_{tdo} \cdot \operatorname{Re}[Z_{11}(p+jp\theta_o)]] - i_{tqo} \cdot \operatorname{Im}[Z_{11}(p+jp\theta_o)]$$

$$\text{GRG1}(p) = [-G_{f1d}(p) \cdot p + p^{\theta_o} \cdot G_{f1q}(p)] \cdot g_{R1}(p)$$

$$\text{GRG2}(p) = [-G_{f2d}(p) \cdot p + p^{\theta_o} \cdot G_{f2q}(p)] \cdot g_{R2}(p)$$

$$\text{GRG3}(p) = [-p^{\theta_o} \cdot G_{f1d}(p) - G_{f1q}(p) \cdot p] \cdot g_{R1}(p)$$

$$\text{GRG4}(p) = [-p^{\theta_o} \cdot G_{f2d}(p) - G_{f2q}(p) \cdot p] \cdot g_{R2}(p)$$

$$\text{GRG5}(p) = [-i_{tqo} \cdot G_{f1d}(p) + i_{tdo} \cdot G_{f1q}(p)] \cdot g_{R1}(p)$$

$$\text{GRG6}(p) = [-i_{tqo} \cdot G_{f2d}(p) + i_{tdo} \cdot G_{f2q}(p)] \cdot g_{R2}(p)$$

4.5 Application to a Simple Power System

For the system shown in Fig. 3.1, the small displacement equations can be written as follows:

$GRG1(p) \cdot B_1 + GRG2(p) \cdot B_2$	$GRG1(p) \cdot C_1 + GRG2(p) \cdot C_2$	$GRG1(p) \cdot (C_{1\delta} + C_{1p\delta} \cdot p + C_{1p2\delta} \cdot p^2) +$ $GRG2(p) \cdot (C_{2\delta} + C_{2p\delta} \cdot p + C_{2p2\delta} \cdot p^2)$ $GRG1(p) \cdot D_1 + GRG2(p) \cdot D_2$
$GRG3(p) \cdot B_1 + GRG4(p) \cdot B_2$	$GRG3(p) \cdot C_1 + GRG4(p) \cdot C_2$	$GRG3(p) \cdot (C_{1\delta} + C_{1p\delta} \cdot p + C_{1p2\delta} \cdot p^2) +$ $GRG4(p) \cdot (C_{2\delta} + C_{2p\delta} \cdot p + C_{2p2\delta} \cdot p^2)$ $GRG3(p) \cdot D_1 + GRG4(p) \cdot D_2$
$GRG5(p) \cdot B_1 + GRG6(p) \cdot B_2$	$GRG5(p) \cdot C_1 + GRG6(p) \cdot C_2$	$GRG5(p) \cdot (C_{1\delta} + C_{1p\delta} \cdot p + C_{1p2\delta} \cdot p^2) +$ $GRG6(p) \cdot (C_{2\delta} + C_{2p\delta} \cdot p + C_{2p2\delta} \cdot p^2)$ $GRG5(p) \cdot D_1 + GRG6(p) \cdot D_2$

Δi_d
Δi_q
$\Delta \delta$

=

$-[r+R_e] \cdot [x_e + x_d(p)] \cdot p$ $-p\theta_o \cdot M(p)$ $\frac{x_c \cdot (p+\alpha)}{(p+\alpha)^2 + (p\theta_o)^2}$	$p\theta_o \cdot [x_e + x_q(p)]$ $+M(p) \cdot p$ $\frac{x_c \cdot p\theta_o}{(p+\alpha)^2 + (p\theta_o)^2}$	$[i_{qo} \cdot (x_e + x_q) - e_d] \cdot p - v_{tqo}$ $+Y$
$-p\theta_o \cdot [x_e + x_d(p)]$ $+M(p) \cdot p$ $\frac{x_c \cdot p\theta_o}{(p+\alpha)^2 + (p\theta_o)^2}$	$-[r+R_e] \cdot [x_e + x_q(p)] \cdot p$ $+p\theta_o \cdot M(p)$ $\frac{x_c \cdot (p+\alpha)}{(p+\alpha)^2 + (p\theta_o)^2}$	$[-i_{do} \cdot (x_e + x_d) + e_q] \cdot p + v_{tdo}$ $+Z$
$-i_{qo} \cdot x_d(p)$ $-i_{do} \cdot M(p)$ $-e_d + i_{qo} \cdot x_q$	$i_{do} \cdot x_q(p)$ $+i_{qo} \cdot M(p)$ $+e_q - i_{do} \cdot x_d$	$(H) \cdot p^2$ $+g_D(p) \cdot p$

=

Δi_d
Δi_q
$\Delta \delta$

6.22

where:

$$B_1 = (C_{1p} \cdot v_{tdo} + C_{1q} \cdot v_{tqo} + C_{1I} \cdot \frac{i_{do}}{i_o}) + (C_{1v} \cdot \frac{v_{tdo}}{v_{to}} + C_{1p} \cdot i_{do} - C_{1q} \cdot i_{qo}) \cdot$$

$$[R_e + x_e \cdot p + \frac{x_c \cdot (p+\alpha)}{(p+\alpha)^2 + (p\theta_o)^2}] + (C_{1v} \cdot \frac{v_{tqo}}{v_{to}} + C_{1p} \cdot i_{qo} + C_{1q} \cdot i_{do}) \cdot$$

$$[x_e \cdot p\theta_o - \frac{x_c \cdot p\theta_o}{(p+\alpha)^2 + (p\theta_o)^2}]$$

$$B_2 = (C_{2p} \cdot v_{tdo} + C_{2q} \cdot v_{tqo} + C_{2I} \cdot \frac{i_{do}}{i_o}) + (C_{2v} \cdot \frac{v_{tdo}}{v_{to}} + C_{2p} \cdot i_{do} - C_{2q} \cdot i_{qo}) \cdot$$

$$[R_e + x_e \cdot p + \frac{x_c \cdot (p+\alpha)}{(p+\alpha)^2 + (p\theta_o)^2}] + (C_{2v} \cdot \frac{v_{tqo}}{v_{to}} + C_{2p} \cdot i_{qo} + C_{2q} \cdot i_{do}) \cdot$$

$$[x_e \cdot p\theta_o - \frac{x_c \cdot p\theta_o}{(p+\alpha)^2 + (p\theta_o)^2}]$$

$$C_1 = (C_{1p} \cdot v_{tqo} - C_{1q} \cdot v_{tdo} + C_{1I} \cdot \frac{i_{qo}}{i_o}) - (C_{1v} \cdot \frac{v_{tdo}}{v_{to}} + C_{1p} \cdot i_{do} - C_{1q} \cdot i_{qo}) \cdot$$

$$[x_e \cdot p\theta_o - \frac{x_c \cdot p\theta_o}{(p+\alpha)^2 + (p\theta_o)^2}] + (C_{1v} \cdot \frac{v_{tqo}}{v_{to}} + C_{1p} \cdot i_{qo} + C_{1q} \cdot i_{do}) \cdot$$

$$[R_e + x_e \cdot p + \frac{x_c \cdot (p+\alpha)}{(p+\alpha)^2 + (p\theta_o)^2}]$$

$$C_2 = (C_{2p} \cdot v_{tqo} - C_{2q} \cdot v_{tdo} + C_{2I} \cdot \frac{i_{qo}}{i_o}) - (C_{2v} \cdot \frac{v_{tdo}}{v_{to}} + C_{2p} \cdot i_{do} - C_{2q} \cdot i_{qo}) \cdot$$

$$[x_e \cdot p\theta_o - \frac{x_c \cdot p\theta_o}{(p+\alpha)^2 + (p\theta_o)^2}] + (C_{2v} \cdot \frac{v_{tqo}}{v_{to}} + C_{2p} \cdot i_{qo} + C_{2q} \cdot i_{do}) \cdot$$

$$[R_e + x_e \cdot p + \frac{x_c \cdot (p+\alpha)}{(p+\alpha)^2 + (p\theta_o)^2}]$$

$$D_1 = (C_{1v} \cdot \frac{v_{tdo}}{v_{to}} + C_{1p} \cdot i_{do} - C_{1q} \cdot i_{qo}) \cdot [v_{tqo} - i_{do} \cdot [x_e \cdot p\theta_o - \frac{x_c \cdot p\theta_o}{(p+\alpha)^2 + (p\theta_o)^2}] - i_{qo} \cdot [R_e + x_e \cdot p + \frac{x_c \cdot (p+\alpha)}{(p+\alpha)^2 + (p\theta_o)^2}]] + (C_{1v} \cdot \frac{v_{tqo}}{v_{to}} + C_{1p} \cdot i_{qo} + C_{1q} \cdot i_{do}) \cdot [-v_{tdo} + i_{do} \cdot [R_e + x_e \cdot p + \frac{x_c \cdot (p+\alpha)}{(p+\alpha)^2 + (p\theta_o)^2}] - i_{qo} \cdot [x_e \cdot p\theta_o - \frac{x_c \cdot p\theta_o}{(p+\alpha)^2 + (p\theta_o)^2}]]$$

$$D_2 = (C_{2v} \cdot \frac{v_{tdo}}{v_{to}} + C_{2p} \cdot i_{do} - C_{2q} \cdot i_{qo}) \cdot [v_{tqo} - i_{do} \cdot [x_e \cdot p\theta_o - \frac{x_c \cdot p\theta_o}{(p+\alpha)^2 + (p\theta_o)^2}] - i_{qo} \cdot [R_e + x_e \cdot p + \frac{x_c \cdot (p+\alpha)}{(p+\alpha)^2 + (p\theta_o)^2}]] + (C_{2v} \cdot \frac{v_{tqo}}{v_{to}} + C_{2p} \cdot i_{qo} + C_{2q} \cdot i_{do}) \cdot [-v_{tdo} + i_{do} \cdot [R_e + x_e \cdot p + \frac{x_c \cdot (p+\alpha)}{(p+\alpha)^2 + (p\theta_o)^2}] - i_{qo} \cdot [x_e \cdot p\theta_o - \frac{x_c \cdot p\theta_o}{(p+\alpha)^2 + (p\theta_o)^2}]]$$

$$Y = i_{qo} \cdot [R_e + x_e \cdot p + \frac{x_c \cdot (p+\alpha)}{(p+\alpha)^2 + (p\theta_o)^2}] + i_{do} \cdot [x_e \cdot p\theta_o - \frac{x_c \cdot p\theta_o}{(p+\alpha)^2 + (p\theta_o)^2}]$$

$$Z = -i_{do} \cdot [R_e + x_e \cdot p + \frac{x_c \cdot (p+\alpha)}{(p+\alpha)^2 + (p\theta_o)^2}] + i_{qo} \cdot [x_e \cdot p\theta_o - \frac{x_c \cdot p\theta_o}{(p+\alpha)^2 + (p\theta_o)^2}]$$

5. EXTENSION OF THE UNDER-EXCITED STABLE REGION
OF THE DUAL-EXCITED SYNCHRONOUS GENERATOR

5.1 Introduction

It has been a common practise to conduct the dynamic stability studies of synchronous machines on a reduced power system usually consisting of a single machine connected through a transmission line to an infinite-bus ^{11,13,22,28-30}. This form of representation has the advantage that attention can be focused on the machine and its excitation system, both of which may be reasonably completely described without unnecessarily complicating the analysis.

In this chapter, the possibility of improving the dynamic stability limits of the dual-excited synchronous generator through controlling its excitation is demonstrated by considering such simple power system (Fig. 5.1). A block diagram of the regulator used for each field winding is given in Fig. 5.2. The parameters of the generator, its regulators and the tie line are as follows:

$$v = 1.0 \quad \text{p.u.}$$

$$x_e = 0.200 \quad \text{p.u.}$$

$$R_e = 0.010 \quad \text{p.u.}$$

$$r = 0.006 \quad \text{p.u.}$$

$$x_d = 2.32 \quad \text{p.u.}$$

$$x_q = 2.07 \quad \text{p.u.}$$

$$x_{ad} = 2.22 \quad \text{p.u.}$$

$$x_{aq} = 1.97 \quad \text{p.u.}$$

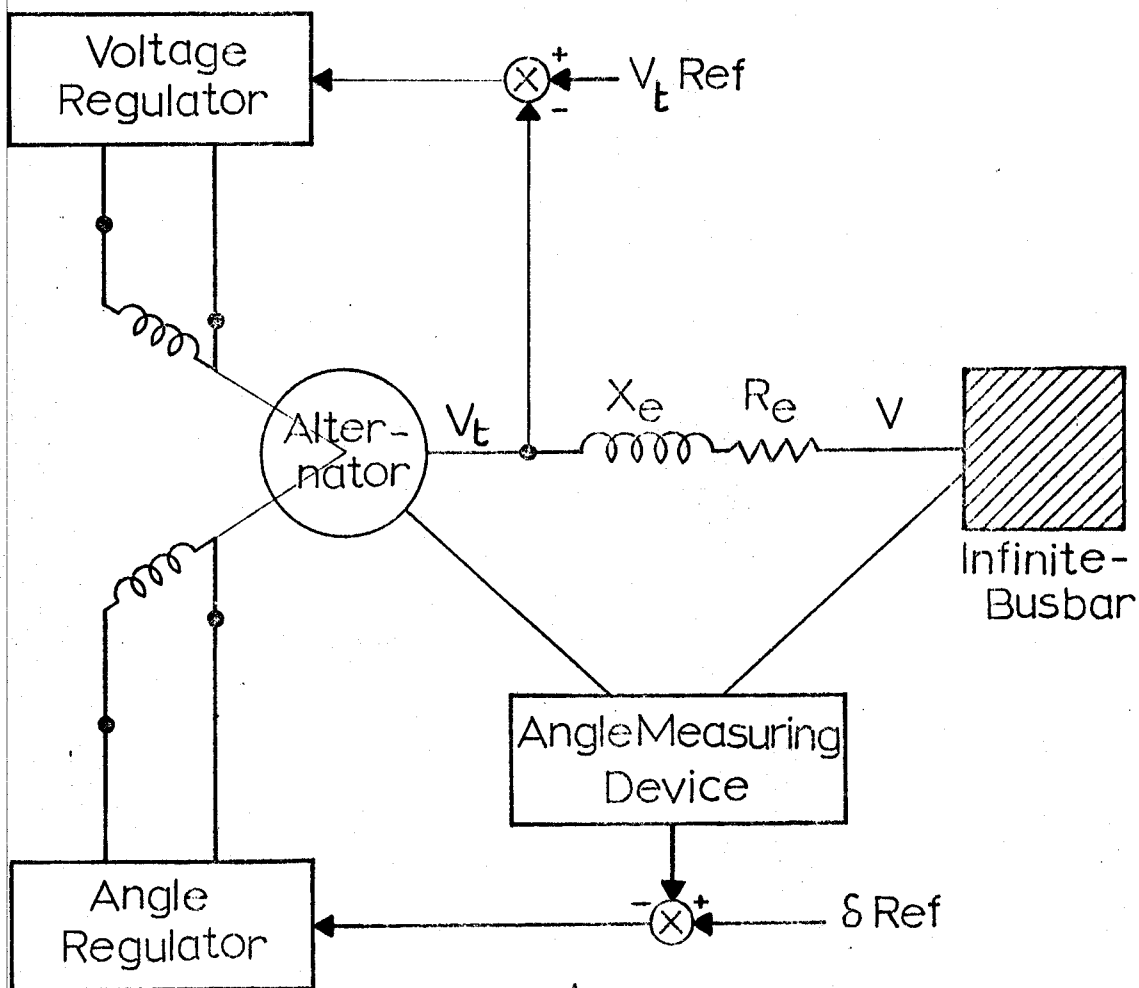


Fig. 5.1 Schematic Single Line Diagram of the Studied System

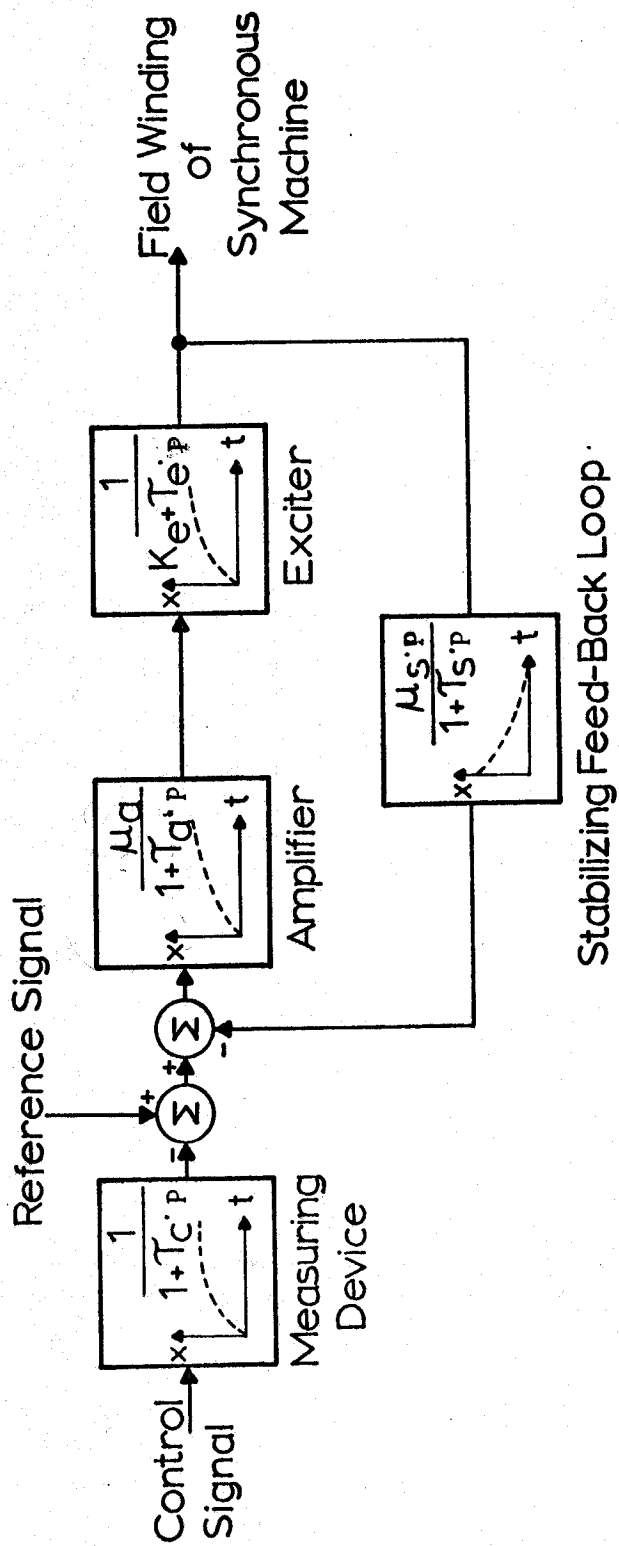


Fig. 5.2 Block Diagram of the Regulator used for each Field Winding

$$x_{ff1} = 2.442 \text{ p.u.}$$

$$r_{f1} = 0.0025 \text{ p.u.}$$

$$x_{ff2} = 2.442 \text{ p.u.}$$

$$r_{f2} = 0.0025 \text{ p.u.}$$

$$x_{kkd} = 2.33 \text{ p.u.}$$

$$r_{kd} = 0.01 \text{ p.u.}$$

$$x_{kkq} = 2.11 \text{ p.u.}$$

$$r_{kq} = 0.02 \text{ p.u.}$$

$$\alpha_1 = 33.75^\circ$$

$$\alpha_2 = 33.75^\circ$$

$$\textcircled{H} = 2185 \text{ p.u.}$$

$$T_a = 0.02 \text{ sec} = 7.54 \text{ p.u.}$$

$$T_c = 0.0 \text{ sec} = 0.0 \text{ p.u.}$$

$$T_e = 0.8 \text{ sec} = 301.6 \text{ p.u.}$$

$$T_s = 1.0 \text{ sec} = 377.0 \text{ p.u.}$$

$$K_e = 1.0$$

$$\mu_s = 0.03$$

5.2 Method of Investigation

It has been pointed out in Chapter 4 that, for studying the dynamic stability of synchronous machines, it is sufficient to apply any of the well-known control theories to its linearized small displacement equations. Such equations have been already derived in

the preceding chapter for the dual-excited synchronous machine and can be arranged in the following compact form:

$$\frac{1}{D(p)} \cdot \begin{array}{|c|c|c|} \hline A_{11}(p) & A_{12}(p) & A_{13}(p) \\ \hline A_{21}(p) & A_{22}(p) & A_{23}(p) \\ \hline A_{31}(p) & A_{32}(p) & A_{33}(p) \\ \hline \end{array} \cdot \begin{array}{|c|} \hline \Delta i_d \\ \hline \Delta i_q \\ \hline \Delta \delta \\ \hline \end{array} = 0 \quad 5.1$$

which represents a set of homogeneous algebraic equations. To get a nontrivial solution for these equations, the determinant of the coefficient matrix should be equal to zero. This implies that:

$$\begin{vmatrix} A_{11}(p) & A_{12}(p) & A_{13}(p) \\ A_{21}(p) & A_{22}(p) & A_{23}(p) \\ A_{31}(p) & A_{32}(p) & A_{33}(p) \end{vmatrix} = 0 \quad 5.2$$

Equation 5.2 is the characteristic equation of the machine and its roots are the characteristic roots. If the real part of any of them is positive, the machine will be unstable. Thus, the problem of determining the stability is one of finding the characteristic roots. However, this task is tedious and time consuming and the use of an alternative method, by which stability can be checked without actually solving for the characteristic roots, would be desirable. Routh's criterion provides a simple technique for finding out whether the characteristic equation has roots with positive real parts or not, and hence for checking the machine dynamic stability. If the characteristic equation is written in the following polynomial form:

$$a_n \cdot p^n + a_{n-1} \cdot p^{n-1} + a_{n-2} \cdot p^{n-2} + \dots + \dots + a_0 = 0 \quad 5.3$$

Routh's criterion for stability can be summarized as follows:

1. All the coefficients of the polynomial have the same sign.
2. None of the coefficients vanish.
3. The signs of the elements in the first column of the following array must be the same:

$$\begin{array}{cccccc}
 a_n & & a_{n-2} & & a_{n-4} & & \dots & & \dots \\
 a_{n-1} & & a_{n-3} & & a_{n-5} & & \dots & & \dots \\
 a_{11} & & a_{12} & & a_{13} & & \dots & & \dots \\
 a_{21} & & a_{22} & & a_{23} & & \dots & & \dots \\
 \dots & & \dots & & \dots & & \dots & & \dots \\
 \dots & & \dots & & \dots & & \dots & & \dots
 \end{array}$$

where

$$a_{11} = \frac{a_{n-1} \cdot a_{n-2} - a_{n-3} \cdot a_n}{a_{n-1}}$$

$$a_{12} = \frac{a_{n-1} \cdot a_{n-4} - a_{n-5} \cdot a_n}{a_{n-1}}$$

$$a_{21} = \frac{a_{11} \cdot a_{n-3} - a_{12} \cdot a_{n-1}}{a_{11}}$$

$$a_{22} = \frac{a_{11} \cdot a_{n-5} - a_{13} \cdot a_{n-1}}{a_{11}}$$

...

...

A digital computer program has been developed to form the characteristic equation of the system at each operating point and

then to check its stability by applying Routh's criterion to this equation. A flow chart for this program is given in Appendix F. The results obtained are in the form of curves representing the dynamic stability boundaries with the freedom of using any two system parameters under study as variables. In the present investigation, the reactive power at the infinite bus Q is chosen as the variable on one axis, while the active power P or the regulating system gain μ_a is the variable on the other axis.

5.3 Static Stability Boundaries and Capability Diagram

As shown in Fig. 5.3, the steady-state operating range of a dual-excited synchronous generator is limited by many factors, namely: the static stability boundary, the maximum prime mover power, the stator heating limit and the rotor heating limit.

For a non-salient pole dual-excited synchronous generator, the static stability limits are similar to those of a non-salient pole conventional one. This is true for any ratio between the excitation currents in the two field windings. If saliency is present, the limits will insignificantly change for different ratios between the two field currents as shown in Fig. 5.4.

The maximum prime mover power and stator heating limits are fixed for a certain machine design independent of its excitation system.

On the other hand, the rotor heating limit depends on the ratio between the two field currents. It is essential to keep always not only the total copper losses in the field winding minimum but also the copper losses of each field winding within safe limits.

Fig. 5.5 shows that, for machines whose field windings are identical

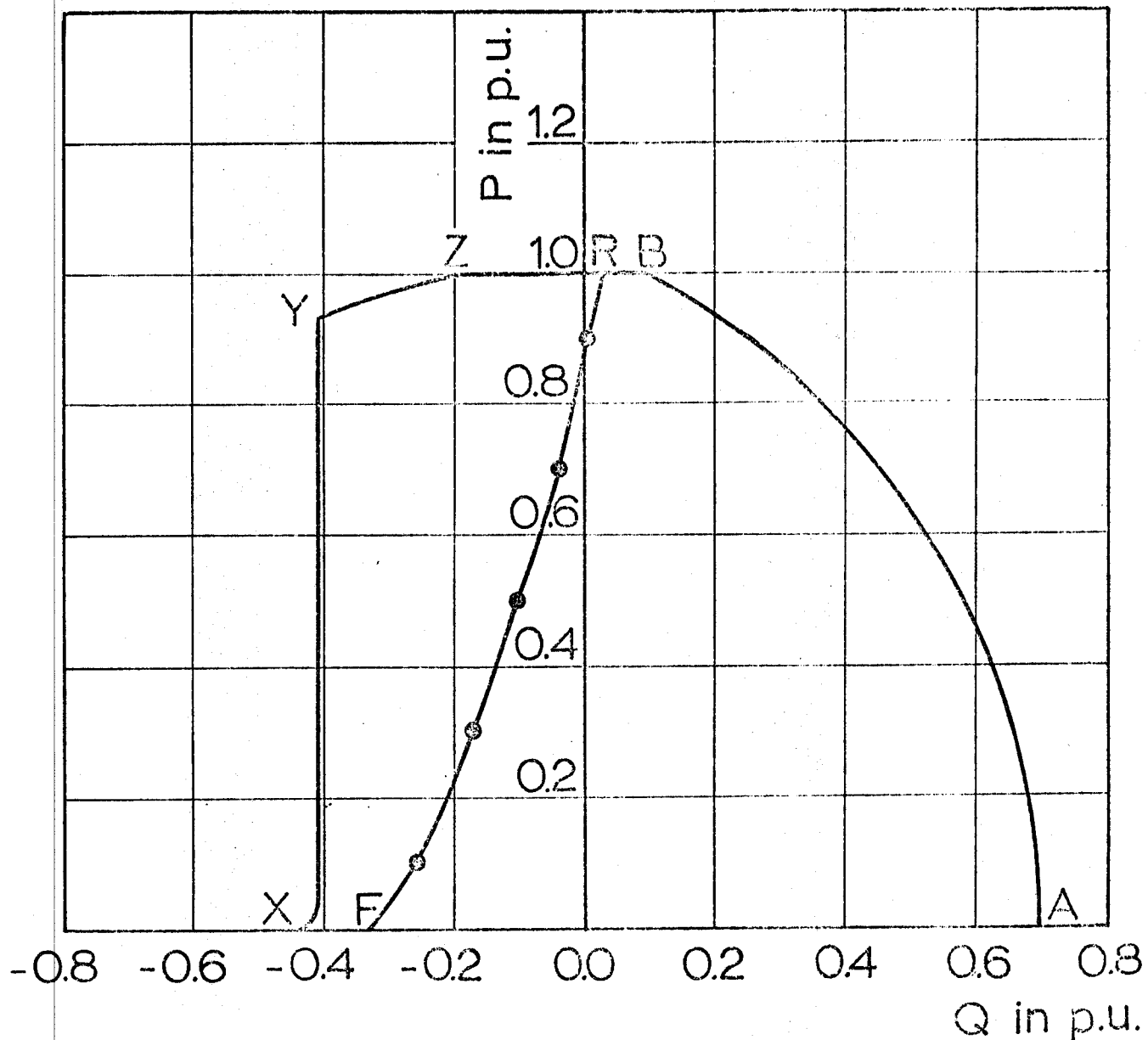


Fig. 5.3 Steady-State Capability Diagram of the Unregulated Dual-Excited Synchronous Generator

- xY Theoretical Static Stability Limit
- FR Practical Static Stability Limit
- YZ Stator Heating Limit
- ZB Maximum Prime Mover Power
- BA Rotor Heating Limit

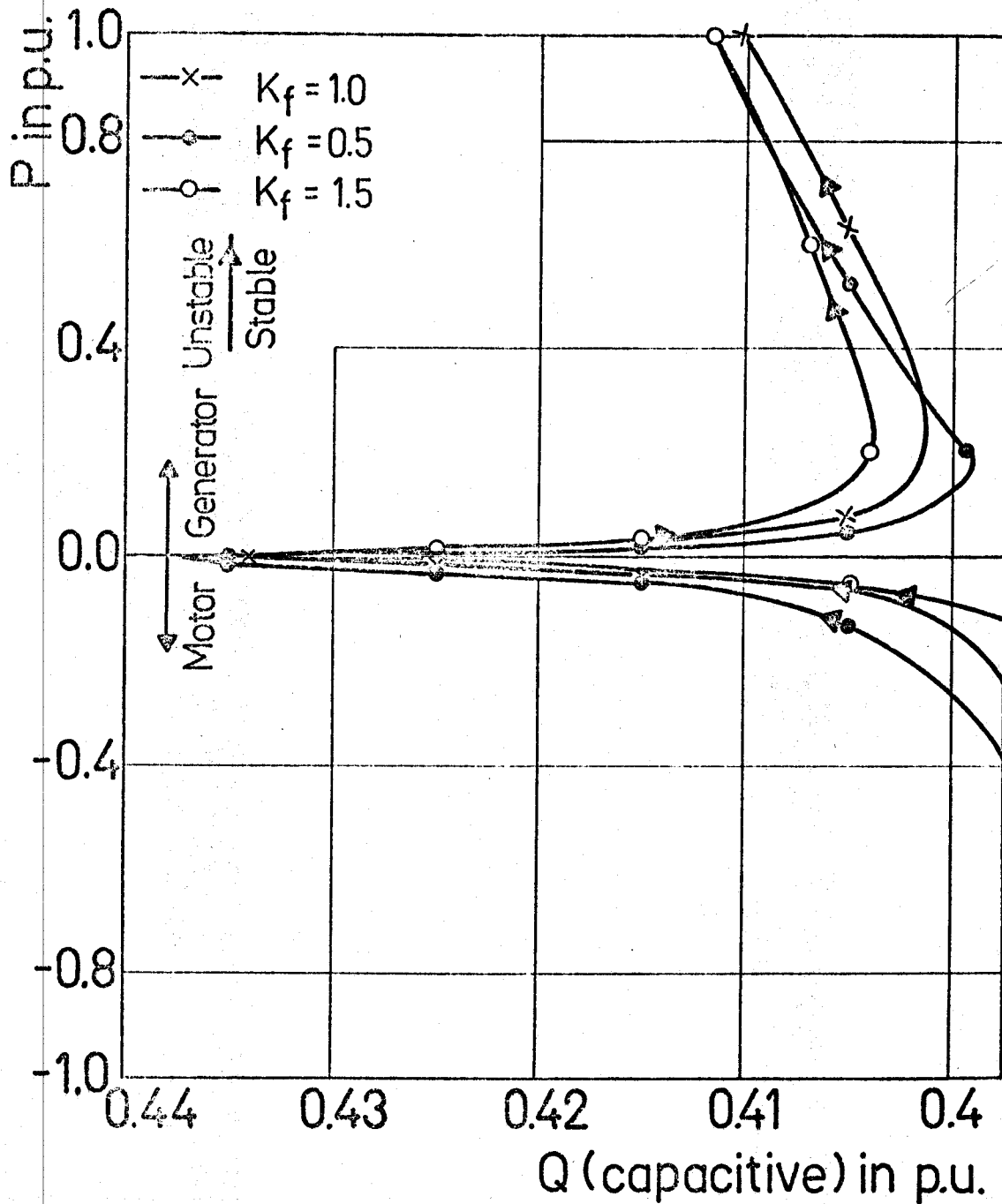


Fig. 5.4 Static Stability Boundaries of the Dual-Excited Synchronous Machine for Different Ratios of Excitation Currents

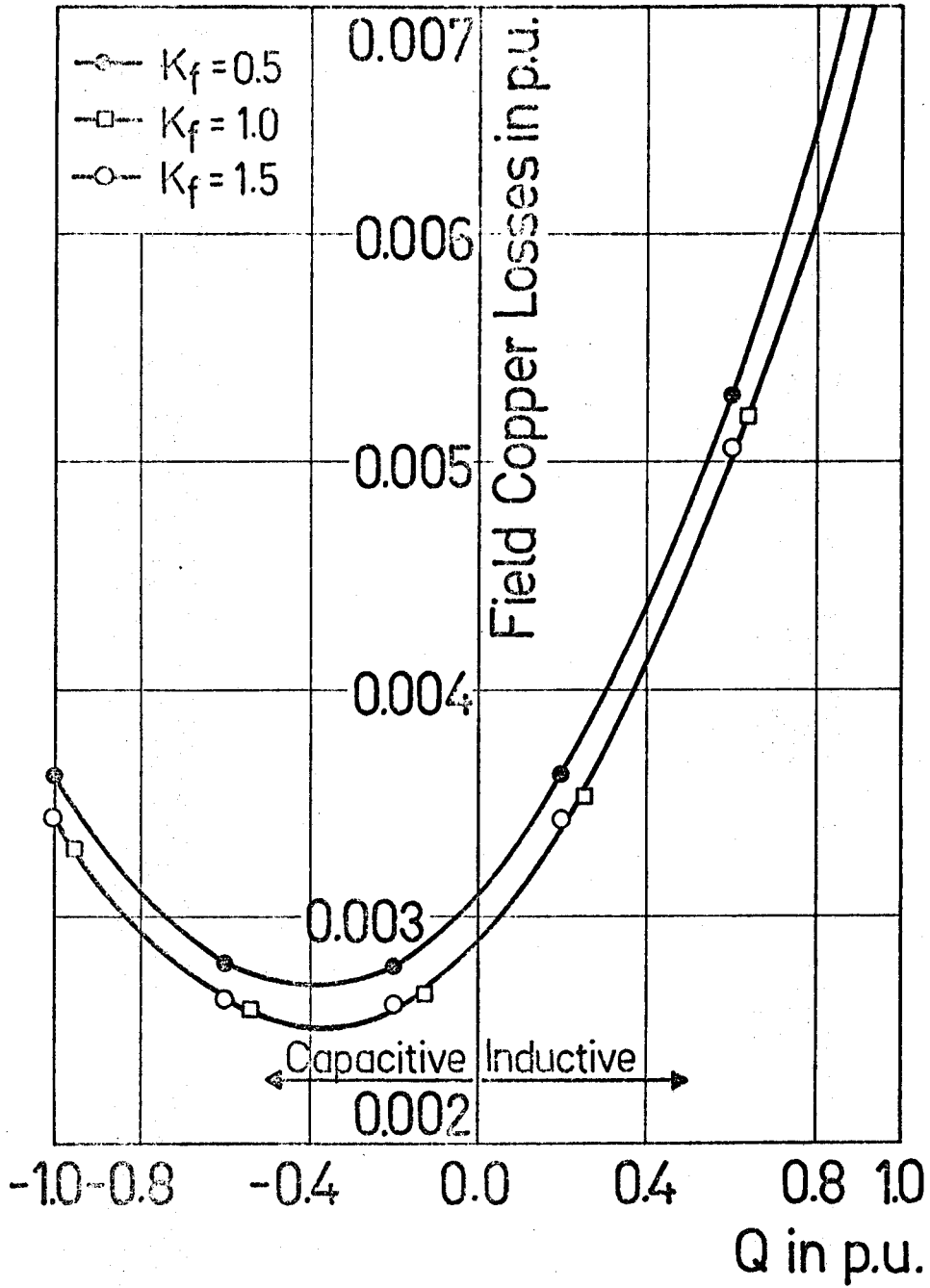


Fig. 5.5 Total Field Copper Losses of the Dual-Excited Synchronous Generator for Different Ratios of Excitation Currents ($p=1.0$ p.u.)

and have the same inclination angle to the direct-axis of the rotor, the rotor heating is minimum when both are equally excited. This has also the virtue of resulting in an even distribution of copper losses between the two field windings and so preventing the overheating of any of them as shown in Fig. 5.6.

5.4 Dynamic Stability Boundaries

As mentioned in Chapter 2, the possible capacitive power, which a conventional synchronous machine can supply at no load, cannot be changed through the application of regulating systems. This is due to the fact that the magnetic-axis of the field winding in this case is always in alignment with the resultant flux (neglecting armature and tie-line resistances). Hence, any regulating signal is unable to produce a stabilizing torque which can suppress the rotor angle oscillations. For the same reason, the improvement of the dynamic stability limit at low power consumption is also not satisfactory.

It is therefore expected that these limitations can be overcome in a dual-excited generator, since the magnetic-axis of either of the two field windings or both can be kept inclined to the resultant flux. This can be simply achieved by equally exciting the two field windings and then controlling either or both by suitable regulators.

5.4.1 Effect of voltage regulators

In the normal operation of conventional synchronous generators, it is customary and almost necessary to keep the terminal voltages at a specified value. This is usually achieved by controlling the generator excitation by voltage regulators, which has also the advantage of limiting the overvoltages that may occur on loss of load. It has

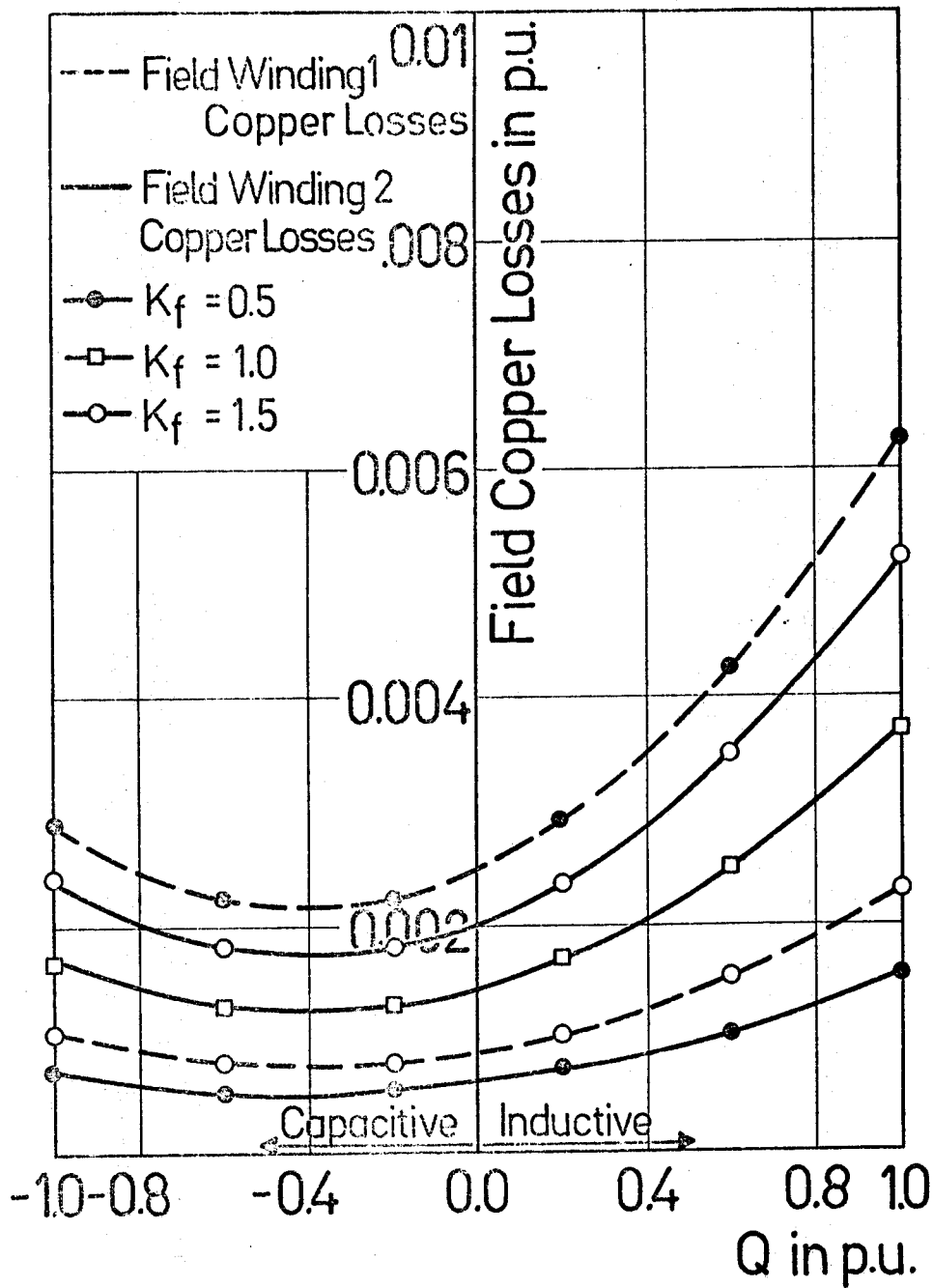


Fig. 5.6 Distribution of Copper Losses between the two Field Windings of the Dual-Excited Synchronous Generator for Different Ratios of Excitation Currents. ($p=1.0$ p.u.)

been found that continuously-acting voltage regulators extend also the stable under-excited region of these generators at loading conditions. However, it has no effect on these limits at no load.

For operation of the dual-excited synchronous generator with equally excited field windings, the dynamic stability boundaries are shown in Figs. 5.7 and 5.8 for the case of controlling any of the two field windings by a voltage regulator. The under-excited stable region is considerably extended at full load, while no improvement is achieved at no load. The ineffectiveness of this type of control at no load could be explained by the following analysis.

Neglecting the armature and transmission line resistances, the machine terminal voltage v_t in terms of the three quantities i_d , i_q and δ can be expressed as:

$$v_t^2 = (v \cdot \sin \delta - i_q \cdot x_e)^2 + (v \cdot \cos \delta + i_d \cdot x_e)^2 \quad 5.4$$

Hence:

$$\begin{aligned} (v_{to} + \Delta v_t)^2 = & (v \cdot \sin(\delta_o + \Delta \delta) - (i_{qo} + \Delta i_q) \cdot x_e)^2 + \\ & (v \cdot \cos(\delta_o + \Delta \delta) + (i_{do} + \Delta i_d) \cdot x_e)^2 \end{aligned} \quad 5.5$$

The corresponding small-displacement equation is:

$$\begin{aligned} \Delta v_t = \frac{x_e}{v_{to}} \cdot & (-(v_{do} \cdot i_{do} + v_{qo} \cdot i_{qo}) \cdot \Delta \delta + (v_{qo} + i_{do} \cdot x_e) \cdot \Delta i_d \\ & - (v_{do} - i_{qo} \cdot x_e) \cdot \Delta i_q) \end{aligned} \quad 5.6$$

This can be rewritten as:

$$\Delta v_t = \frac{x_e}{v_{to}} \cdot (-P \cdot \Delta \delta + v_{tqo} \cdot \Delta i_d - v_{tdo} \cdot \Delta i_q) \quad 5.7$$

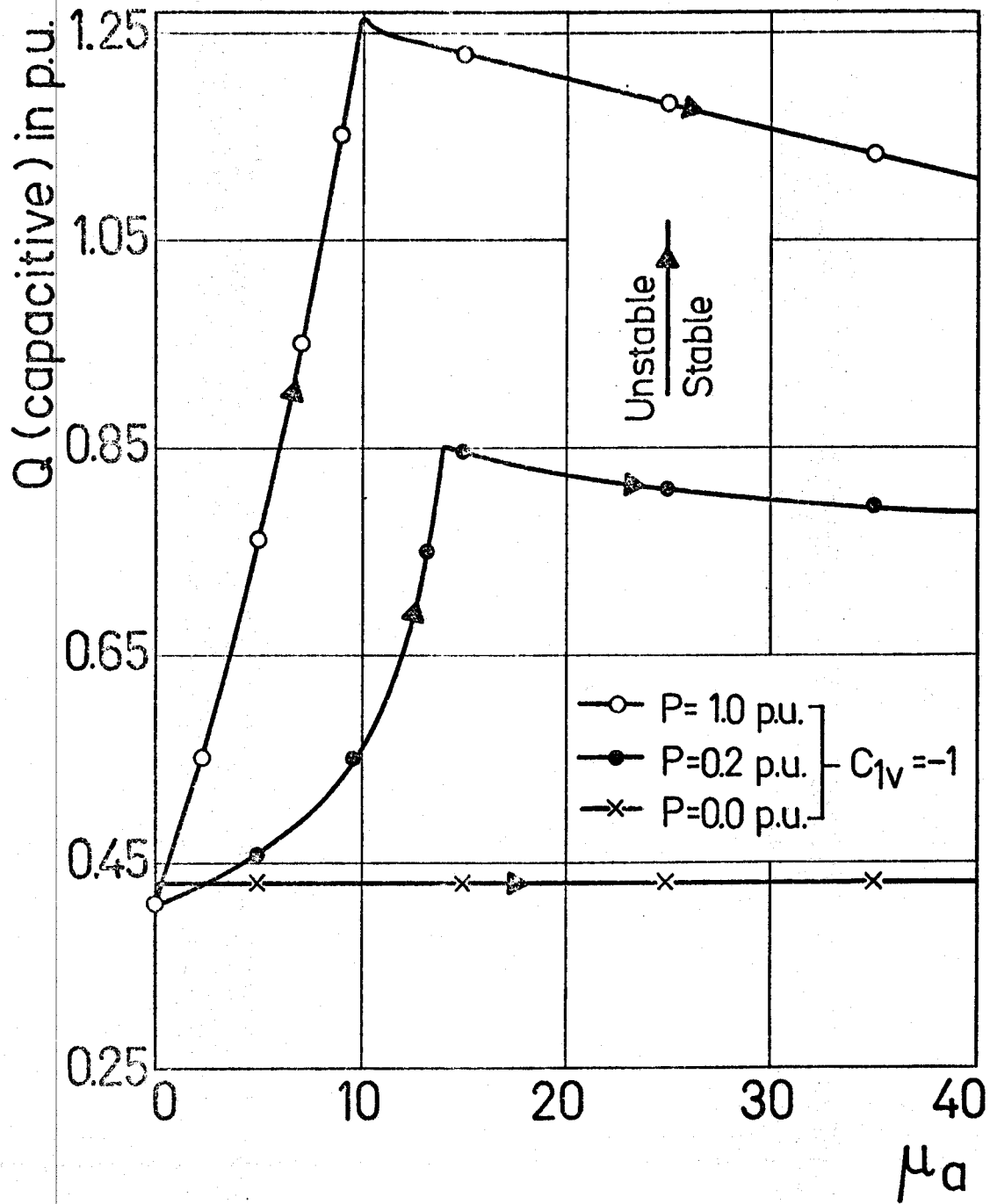


Fig. 5.7 Dynamic Stability Boundaries of the Dual-Excited Synchronous Generator for Operation with Equally Excited Field Windings (Field Winding 1 is Controlled by a Voltage Regulator)

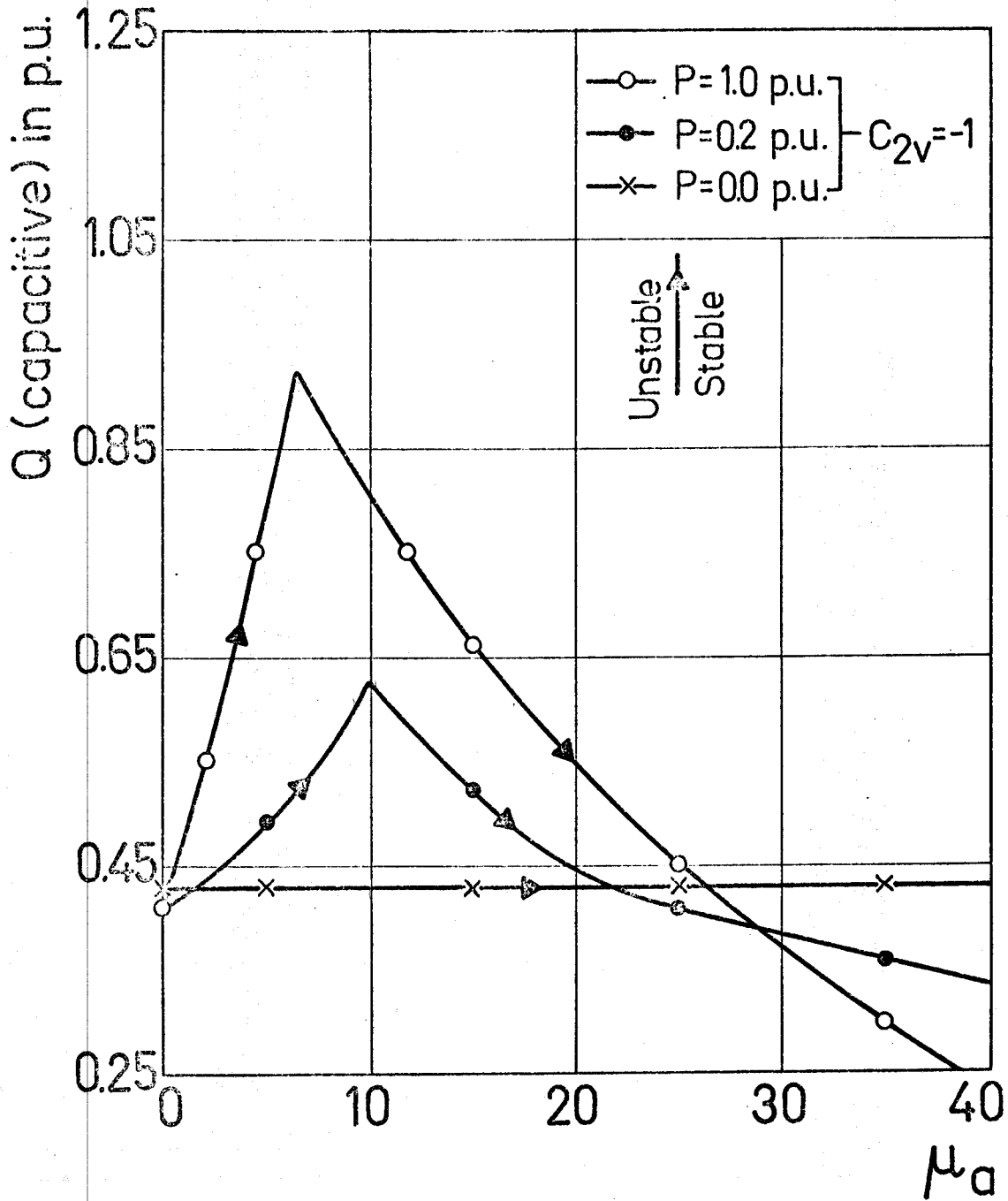


Fig. 5.8 Dynamic Stability Boundaries of the Dual-Excited Synchronous Generator for Operation with Equally Excited Field Windings (Field Winding 2 is Controlled by a Voltage Regulator)

At no load and for equally excited field windings:

$$v_{tdo} = 0 \quad 5.8$$

$$v_{tqo} = v_{to} \quad 5.9$$

Hence, equation 5.7 is reduced to:

$$\Delta v_t = x_e \cdot \Delta i_d \quad 5.10$$

This shows that a signal proportional to the change in the terminal voltage is proportional to the change in the direct-axis component of the current. In Appendix B, it has been proved that the latter cannot improve the dynamic stability of the dual-excited synchronous generator at no load. Hence, it follows that a voltage regulator used for any of the two field windings is ineffective from this point of view.

It should be noted that, when both field windings are equally excited and simultaneously controlled by identical voltage regulators, the generator becomes equivalent to a conventional one provided with a voltage regulator. Hence, the same dynamic stability limitations of the latter hold also for this case and no improvement can be achieved at no load.

5.4.2 Effect of rotor-angle regulators

In this investigation, as for the case of using voltage regulators, the steady-state excitation currents in both field windings are adjusted to be equal at every operating condition.

a) Control of field winding 1

The dynamic stability boundaries representing this case are given in Fig. 5.9. It is clear that the dynamically stable region is extended far beyond the static stability limits, even at no load. However,

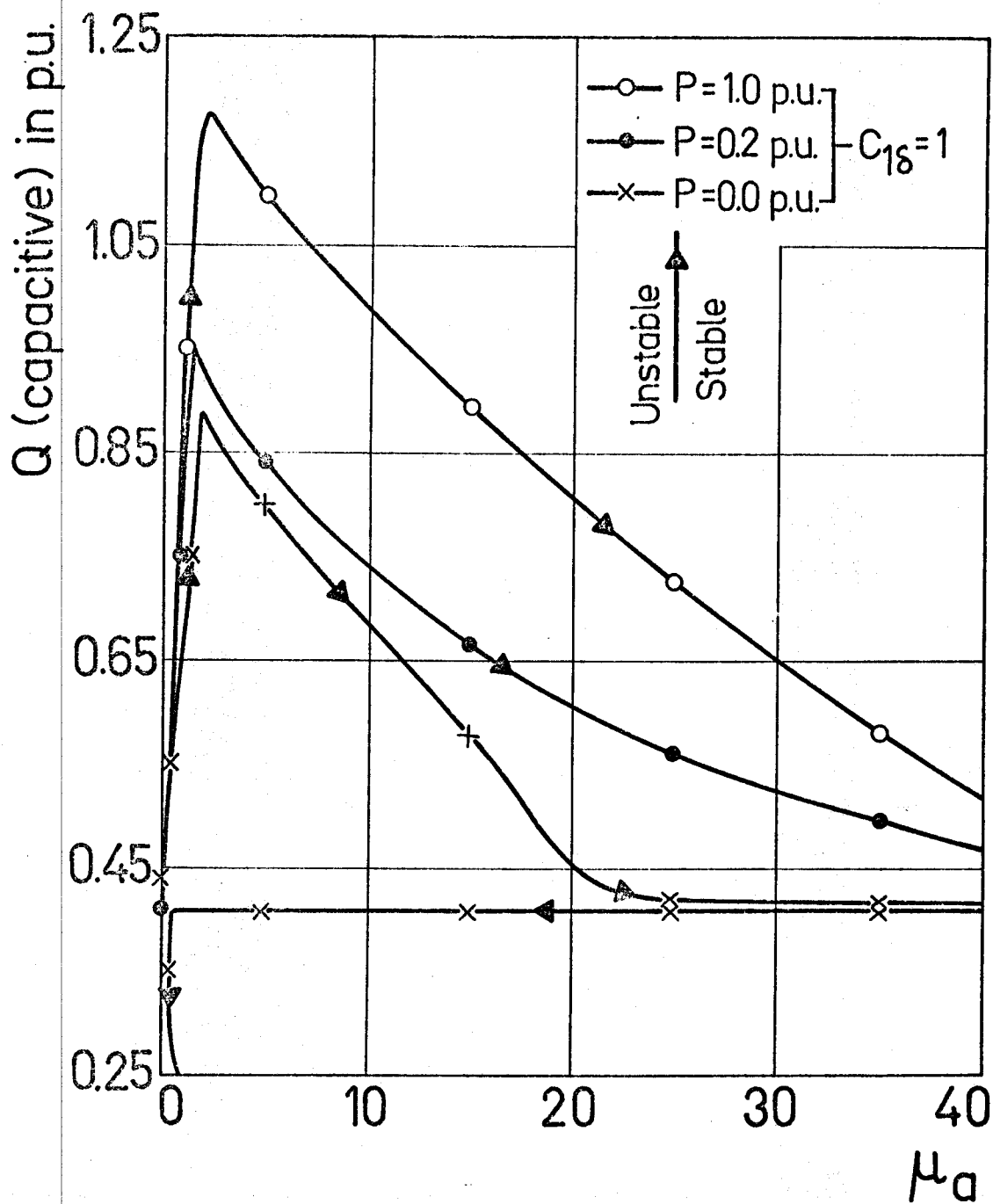


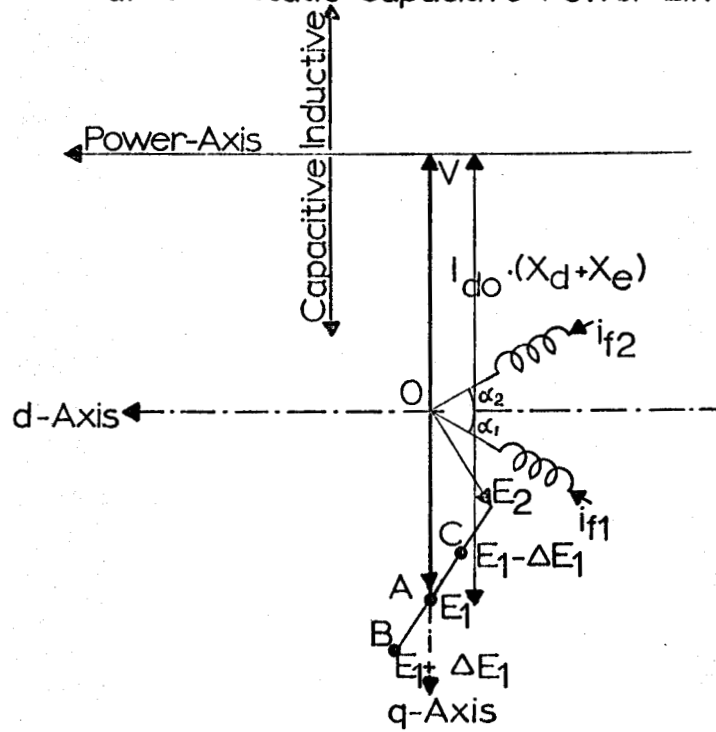
Fig. 5.9 Dynamic Stability Boundaries ($Q-\mu_a$) of the Dual-Excited Synchronous Generator for Operation with Equally Excited Field Windings (Field Winding 1 is Controlled by a Rotor-Angle Regulator)

it is noticed that instability will occur at no load when the capacitive power becomes less than its value at the static stability limit. This would restrict the use of this signal to the range of capacitive loadings beyond the static stability limit. However, if the sign of the control signal could be reversed in this region, stability will be also achieved for this loading range. This phenomenon can be explained by examining Fig. 5.10 a., which represents the vector relations of the dual-excited machine at no load when it is operating beyond its static stability boundary. Point A represents the normal operating point for this specific loading. If the rotor accelerates due to the occurrence of a disturbance, a positive control signal will result in increasing the excitation of field winding 1. Consequently, the operating point will move to point B, which means an increase of the electrical output power. This will in turn cause deceleration of the rotor and the machine at last settles in a stable position. On the other hand, when a negative control signal is used, the acceleration of the rotor will be followed by a decrease of field winding 1 excitation and the operating point moves to C. This will result in an increase of the accelerating power which makes the machine go out of step. Using the same procedure, it can be easily shown from Fig. 5.10 b. that, when the capacitive power loading is less than its value at the static stability limit, a positive control signal will lead to instability while a negative control signal will not. Fig. 5.11 shows that this instability problem is not created only at no load but over certain operating range.

b) Control of field winding 2

As shown from Fig. 5.12, the dynamic stability boundaries of the dual-excited machine at no load as well as at full load can also be

a. $Q > \text{Static Capacitive Power Limit.}$



b. $Q < \text{Static Capacitive Power Limit.}$

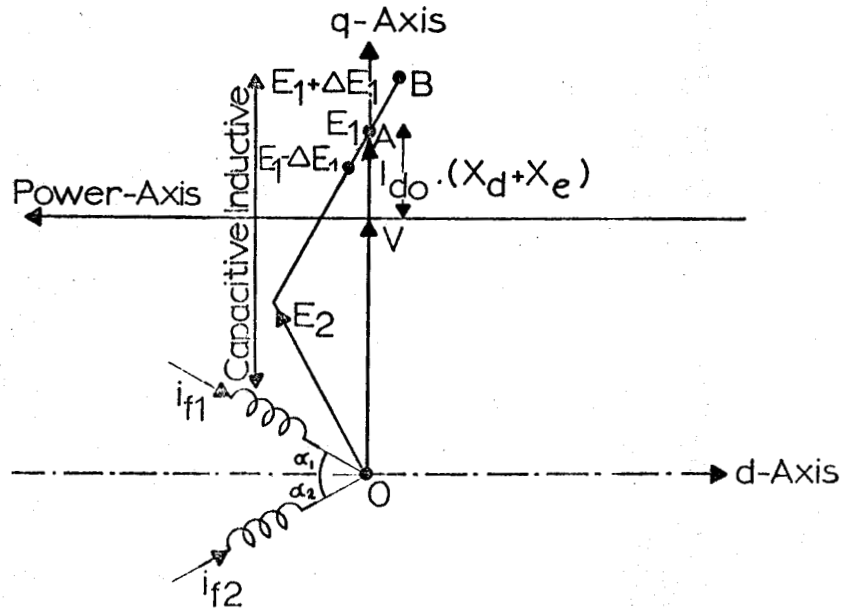


Fig. 5.10 Vector Representation of the Dual-Excited Synchronous Machine at No Load (Field Winding 1 is Controlled)

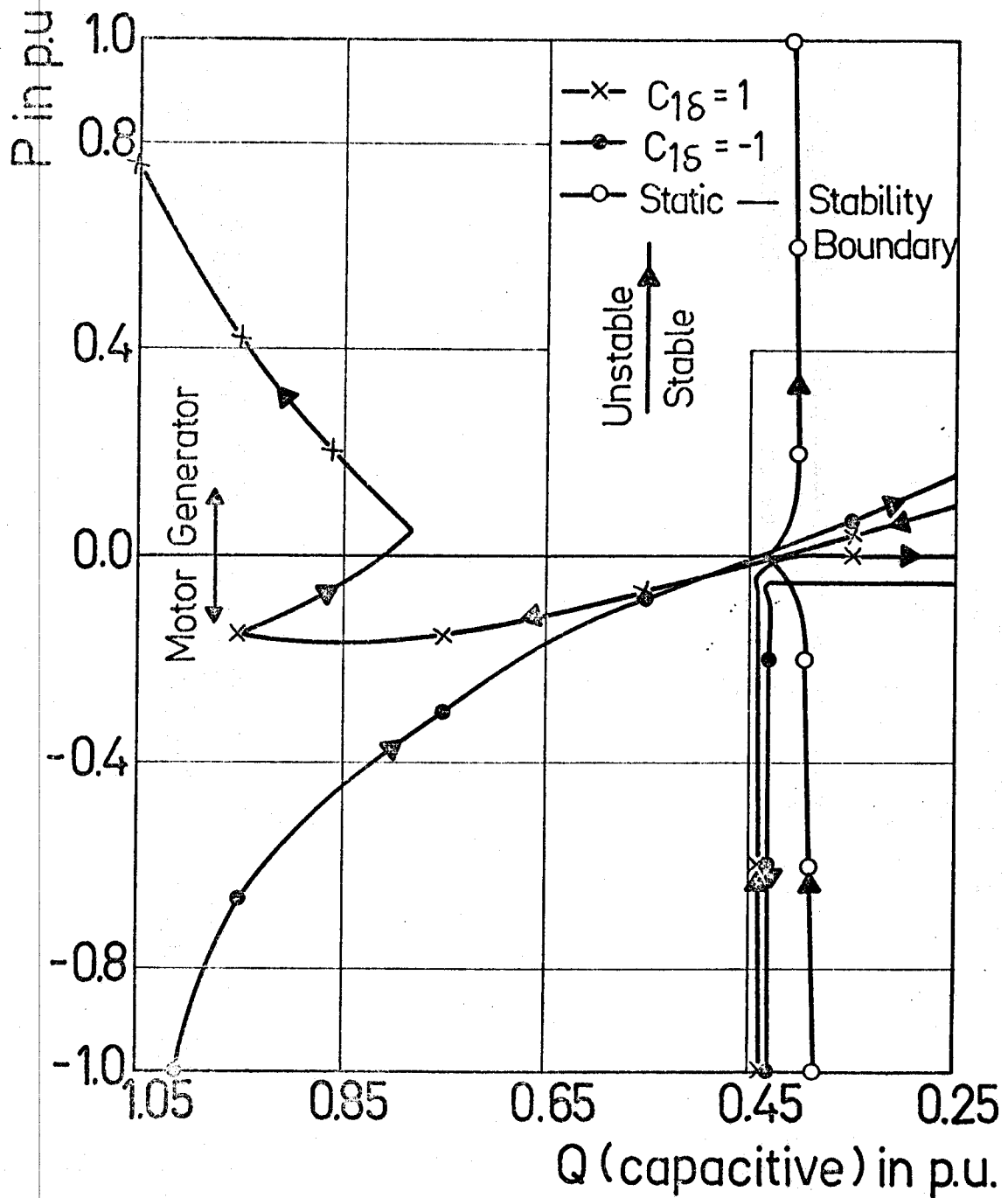


Fig. 5.11 Dynamic Stability Boundaries (P-Q) of the Dual-Excited Synchronous Generator for Operation with Equally Excited Field Windings (Field Winding 1 is Controlled by a Rotor-Angle Regulator, $\mu_a = 5$)

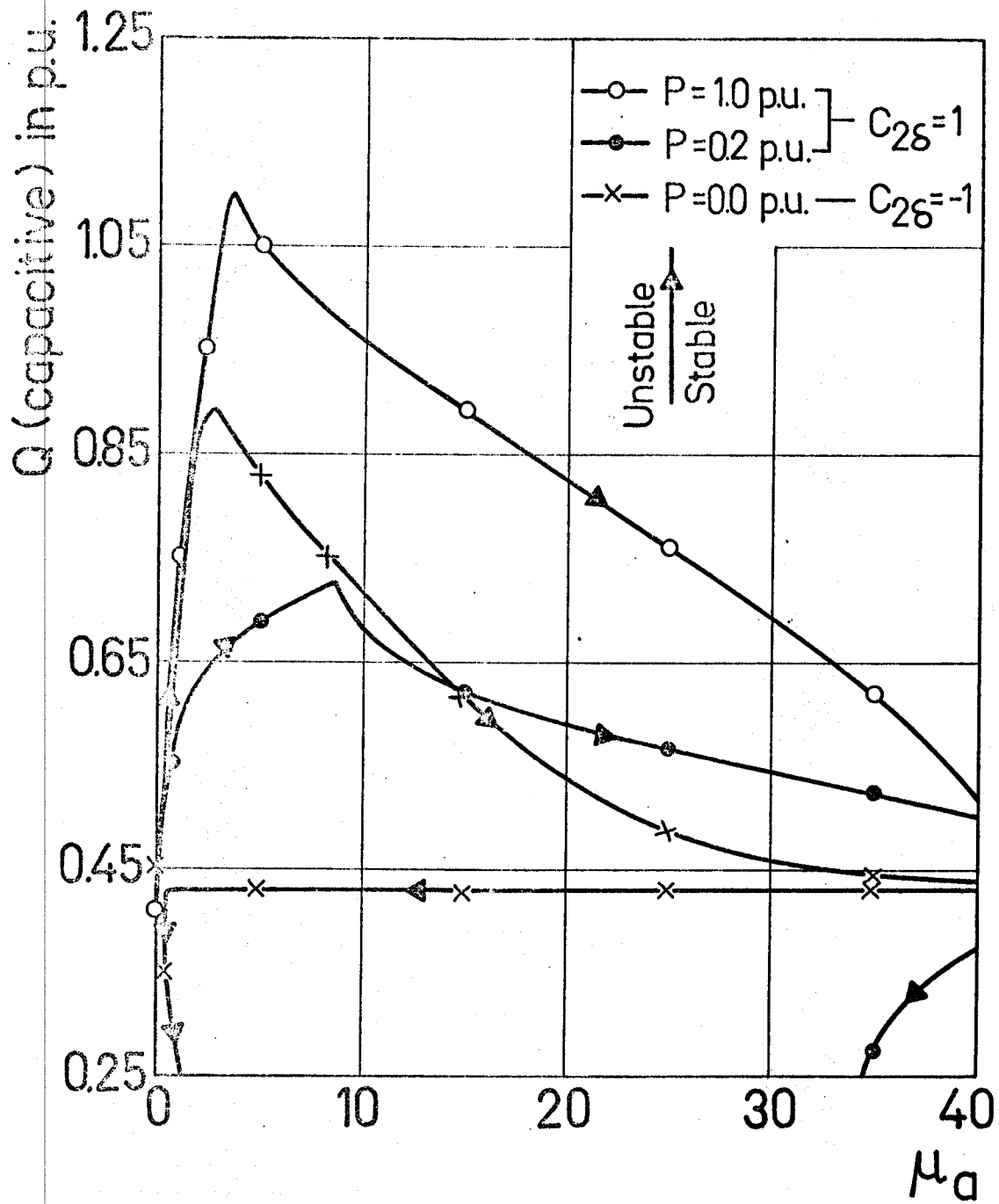


Fig. 5.12 Dynamic Stability Boundaries ($Q-\mu_a$) of the Dual-Excited Synchronous Generator for Operation with Equally Excited Field Windings (Field Winding 2 is Controlled by a Rotor-Angle Regulator)

considerably improved by this scheme of regulation, providing that the proper sign of the control signal is used. The improvement achieved at 0.2 p. unit load is not satisfactory. At full load, a positive control signal is required, while the sign of the control signal at no load depends on the operating range. It should be positive for operation within the static stable region and negative for operation beyond the static stability boundary. An explanation for this could be found by studying Fig. 5.13. Fig. 5.13 a. represents the vector relations of the dual-excited synchronous generator at no load when operating beyond its static stability boundary. Point A is the corresponding operating point. If the rotor-angle increases due to a disturbance, a positive control signal will increase the excitation of field winding 2. The operating point will then move to point B, which indicates an increase of the input electrical power. As a result, the rotor will continue to accelerate and the machine will go out of synchronism. On the other hand, when negative control signal is used, the operating point will move to C indicating that the electrical output power of the machine will increase. It follows that a case of equilibrium can be reached and the machine keeps running in synchronism. Following the same method of explanation, it is also possible to show from Fig. 5.13 b. that the opposite will occur when the machine operates within the static stable region. In this case, negative control signal will cause instability, while positive control signal will stabilize the machine. The P - Q stability boundaries given in Fig. 5.14 shows clearly the stable and unstable regions associated with each sign of control signal.

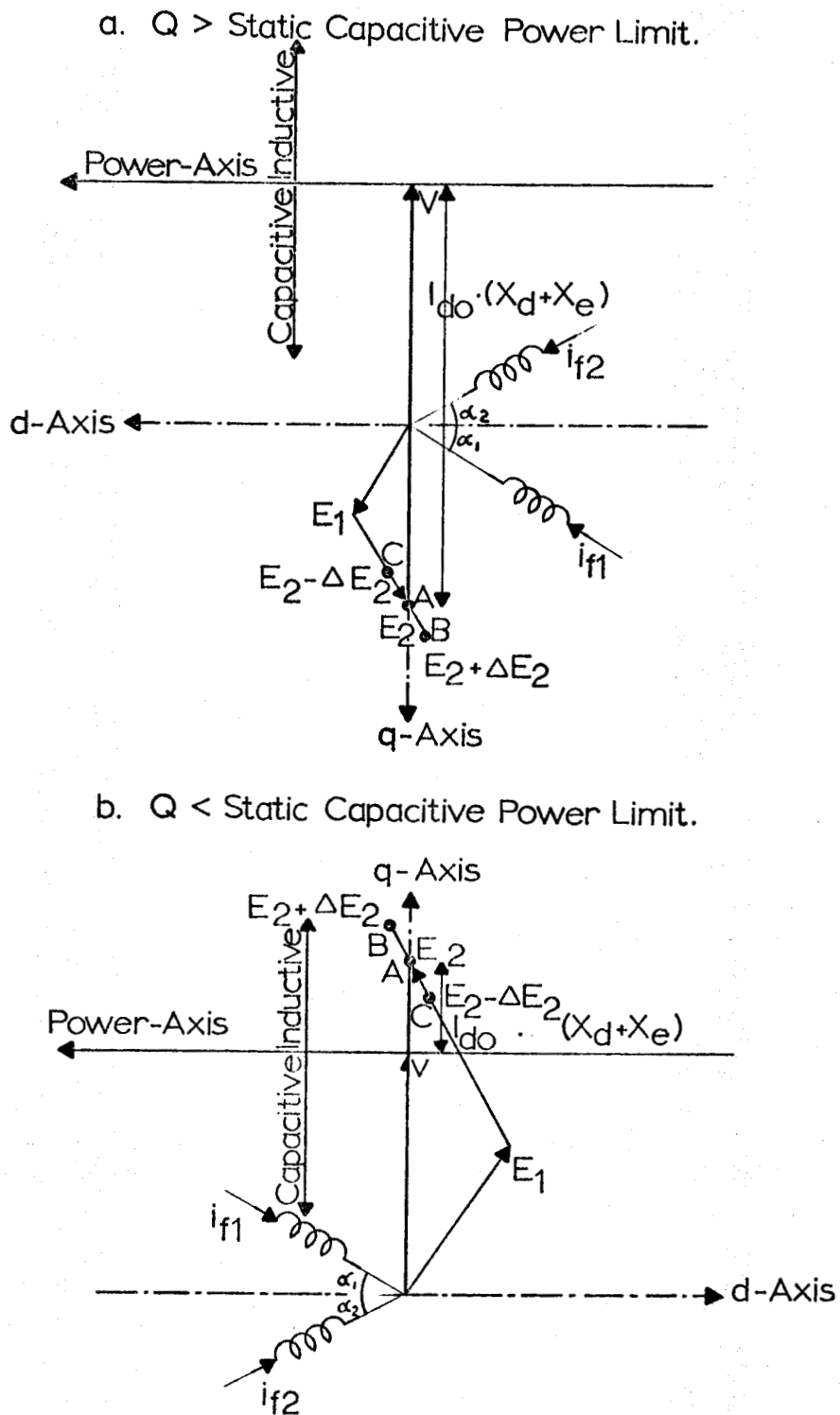


Fig. 5.13 Vector Representation of the Dual-Excited Synchronous Machine at No Load (Field Winding 2 is Controlled)

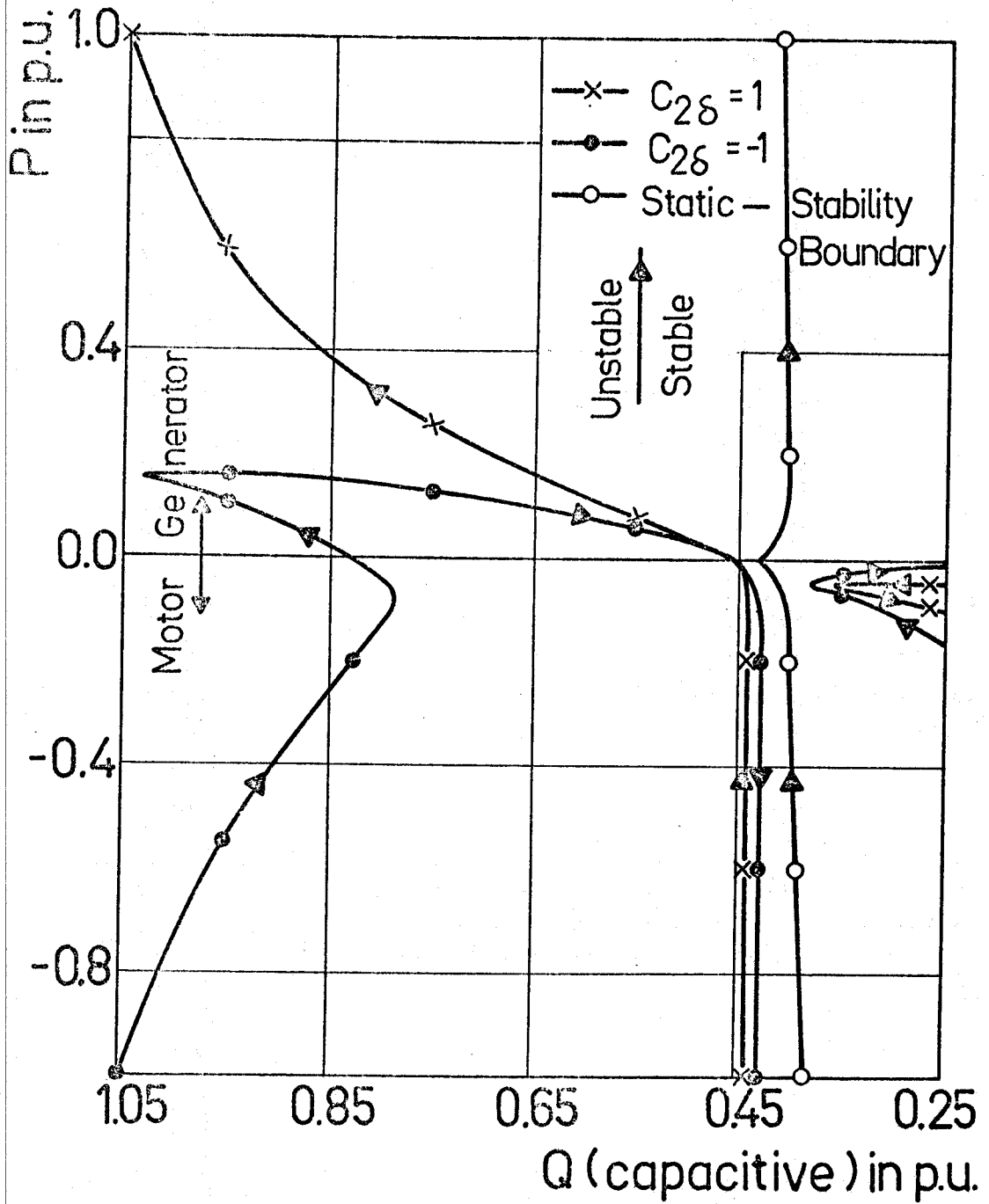


Fig. 5.14 Dynamic Stability Boundaries (P-Q) of the Dual-Excited Synchronous Generator for Operation with Equally Excited Field Windings (Field Winding 2 is Controlled by a Rotor-Angle Regulator, $\mu_a = 5$)

c) Control of both field windings

When both field windings are simultaneously controlled by identical rotor-angle regulators and with the same sign for the control signal, the machine becomes similar to a regulated conventional one. Thus the same dynamic stability limitations of conventional synchronous machines hold also for this case and no improvement can be achieved at no load.

5.4.3 Operation with fixed rotor-angle

From the preceding investigation of the dual-excited synchronous generator with equally excited field windings, it is clear that the control of either of them using a rotor-angle regulator fails to stabilize the generator over the whole loading range. The proper sign of the control signal which extends the dynamic stability region at full load creates instability within certain operating regions. These unstable regions occur approximately when the rotor-angle is less than α_1 for the case of controlling the excitation of field winding 1 and greater than $180-\alpha_2$ for the case of controlling the excitation of field winding 2.

This problem could be overcome by fixing the position of the two field windings with respect to the resultant flux for all loading conditions. To achieve this, the excitation of both field windings have to be adjusted so as to keep the rotor-angle δ fixed at a certain specified value. Fixing the rotor-angle at a value equal to α_1 makes field winding 1 magnetic-axis in the direction of the resultant flux and hence it controls only the reactive power (if saliency and resistance are neglected). This can be explained by the following simple analysis.

Considering the vector diagram of Fig. 5.15, the following equations can be written:

$$E_d = V \cdot \sin\delta - I_{qo} \cdot (x_q + x_e) \quad 5.11$$

$$E_q = V \cdot \cos\delta + I_{do} \cdot (x_d + x_e) \quad 5.12$$

$$I_p = I_{do} \cdot \sin\delta + I_{qo} \cdot \cos\delta \quad 5.13$$

$$I_v = I_{do} \cdot \cos\delta - I_{qo} \cdot \sin\delta \quad 5.14$$

where I_p and I_v are the active and reactive components of the armature current respectively.

E_d and E_q depend on the field currents as follows:

$$E_d = x_{aq} \cdot i_{f1o} \cdot \sin\alpha_1 - x_{aq} \cdot i_{f2o} \cdot \sin\alpha_2 \quad 5.15$$

$$E_q = x_{ad} \cdot i_{f1o} \cdot \cos\alpha_1 + x_{ad} \cdot i_{f2o} \cdot \cos\alpha_2 \quad 5.16$$

From equations 5.11 - 5.12

$$I_p = \frac{1}{x_d + x_e} \cdot (E_q - V \cdot \cos\delta) \cdot \sin\delta + \frac{1}{x_q + x_e} \cdot (-E_d + V \cdot \sin\delta) \cdot \cos\delta \quad 5.17$$

$$I_v = \frac{1}{x_d + x_e} \cdot (E_q - V \cdot \cos\delta) \cdot \cos\delta - \frac{1}{x_q + x_e} \cdot (-E_d + V \cdot \sin\delta) \cdot \sin\delta \quad 5.18$$

Substituting from equations 5.15 and 5.16 in 5.17 and 5.18, then:

$$I_p = \frac{1}{x_d + x_e} \cdot (x_{ad} \cdot i_{f1o} \cdot \cos\alpha_1 + x_{ad} \cdot i_{f2o} \cdot \cos\alpha_2 - V \cdot \cos\delta) \cdot \sin\delta + \frac{1}{x_q + x_e} \cdot (-x_{aq} \cdot i_{f1o} \cdot \sin\alpha_1 + x_{aq} \cdot i_{f2o} \cdot \sin\alpha_2 + V \cdot \sin\delta) \cdot \cos\delta$$

5.19

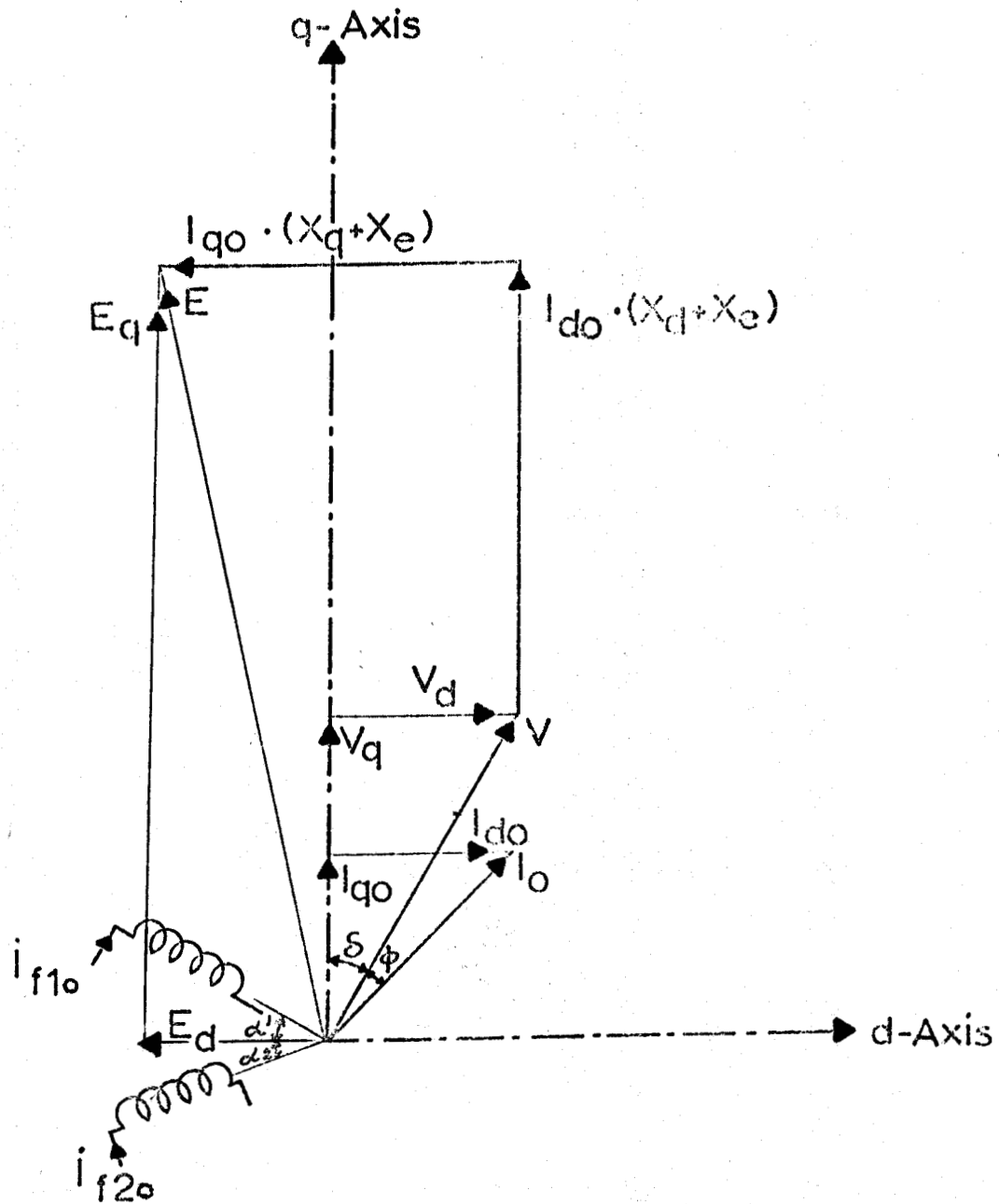


Fig. 5.15 Steady-State Vector Diagram of the Dual-Excited Synchronous Generator ($\delta = \alpha_1$, resistance neglected)

$$I_v = \frac{1}{x_d + x_e} \cdot (x_{ad} \cdot i_{f10} \cdot \cos\alpha_1 + x_{ad} \cdot i_{f20} \cdot \cos\alpha_2 - V \cdot \cos\delta) \cdot \cos\delta$$

$$\frac{1}{x_q + x_e} \cdot (-x_{aq} \cdot i_{f10} \cdot \sin\alpha_1 + x_{aq} \cdot i_{f20} \cdot \sin\alpha_2 + V \cdot \sin\delta) \cdot \sin\delta \quad 5.20$$

If $\delta = \alpha_1$ and saliency is neglected, i.e., $x_d = x_q = x_1$, $x_{ad} = x_{aq} = x_2$ then the following expressions can be obtained:

$$I_p = \frac{x_2}{x_1} \cdot \sin(\alpha_1 + \alpha_2) \cdot i_{f20} \quad 5.21$$

$$I_v = \frac{x_2}{x_1} \cdot \cos(\alpha_1 + \alpha_2) \cdot i_{f20} + \frac{x_2}{x_1} \cdot i_{f10} - \frac{V}{x_1} \quad 5.22$$

It is obvious that the active component of the current depends only on the excitation of field winding 2. So, the control of this winding by a rotor-angle regulator can improve the machine stability. Field winding 1 current controls only the reactive power and thus it makes no contribution to the stability of the machine in this case.

a) Control of field winding 2

Fig. 5.16 gives the dynamic stability boundaries of the dual-excited synchronous generator when its field winding 2 is controlled by a rotor-angle regulator. In this case, the excitation of field winding 1 is adjusted but unregulated. It is noticed that the stable under-excited region is extended at any loading condition far beyond the static stability boundary.

Such extension of the dynamic stable region can be also achieved when the rotor-angle is fixed at values other than α_1 as shown in Fig. 5.17 and Fig. 5.18. It appears from these figures that keeping δ fixed at the

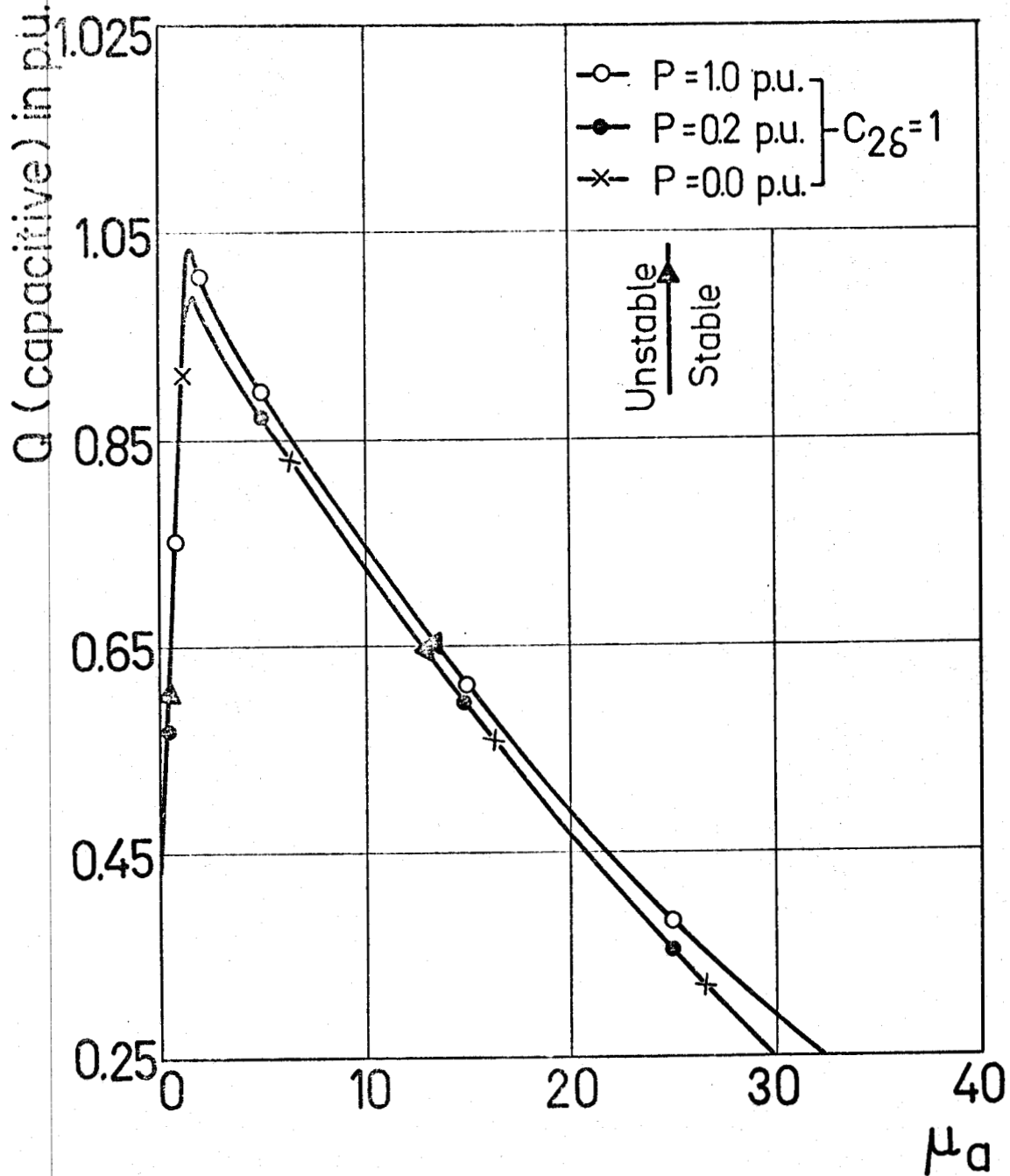


Fig. 5.16 Dynamic Stability Boundaries of the Dual-Excited Synchronous Generator for Operation with Fixed Rotor-Angle (Field Winding 2 is Controlled by a Rotor-Angle Regulator, $\delta = \alpha_1$)

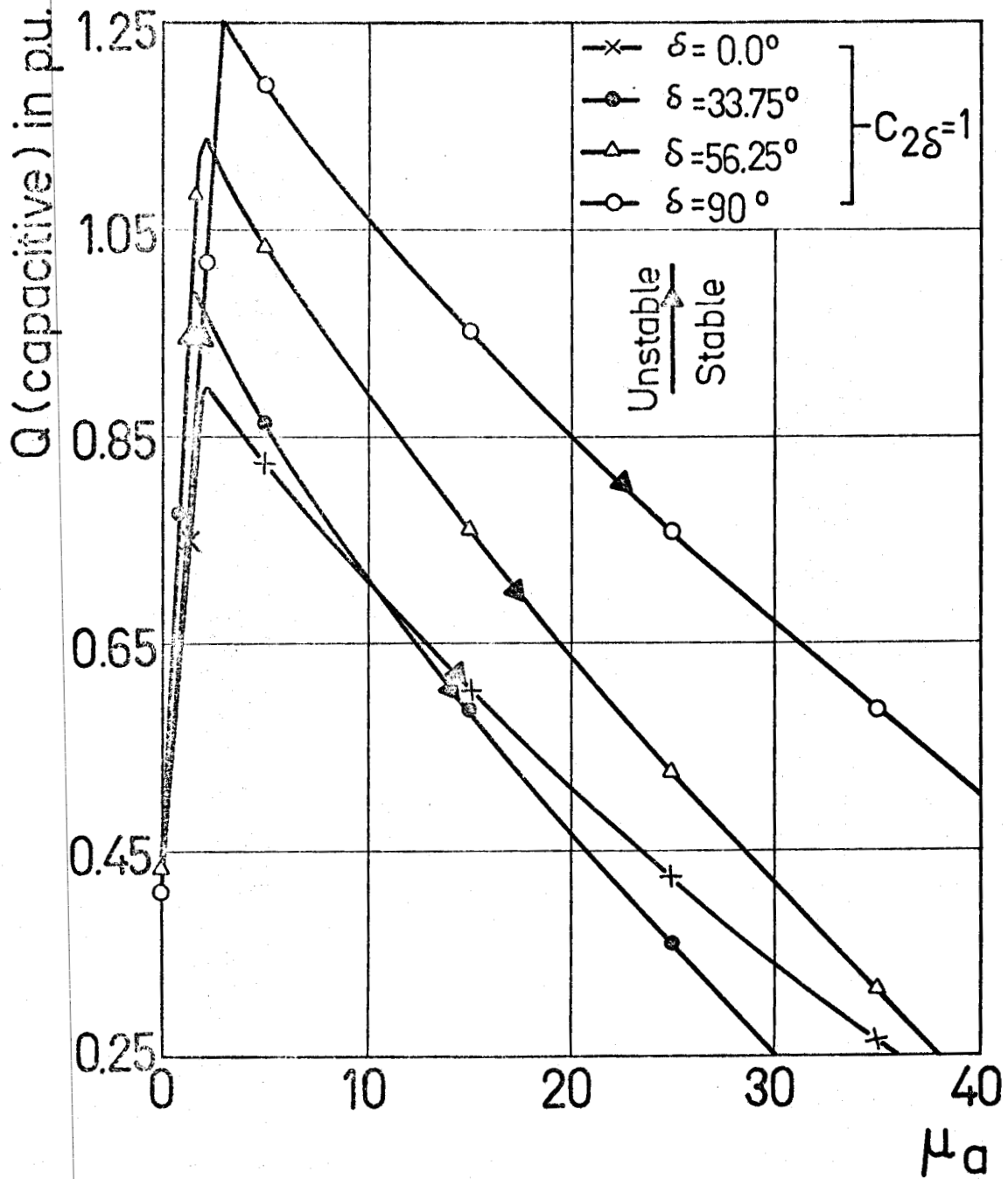


Fig. 5.17 Dynamic Stability Boundaries of the Dual-Excited Synchronous Generator for Operation with Fixed Rotor-Angle ($P=0.0$, Field Winding 2 is Controlled by a Rotor-Angle Regulator)

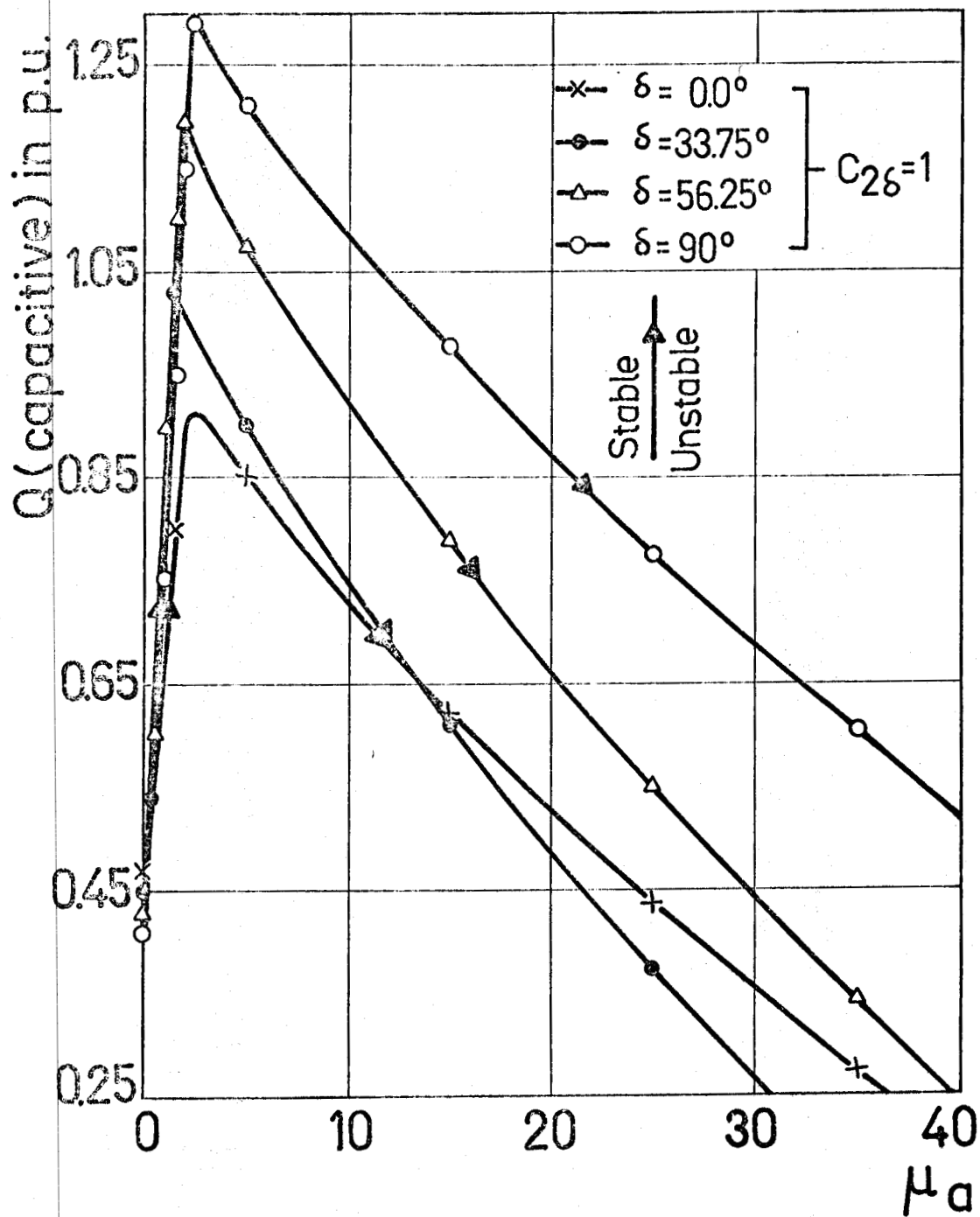


Fig. 5.18 Dynamic Stability Boundaries of the Dual-Excited Synchronous Generator for Operation with Fixed Rotor-Angle ($P=1.0$ p.u., Field Winding 2 is controlled by a Rotor-Angle Regulator)

value α_1 does not provide the maximum stable region.

It is noticed that the total copper loss and its distribution between the two field windings varies widely from one reference angle to another as shown in Figs. 5.19 and 5.20. The values may exceed the rotor safe heating limits and thus may affect the choice of the reference angle. For lagging power factors, the operation with rotor angle fixed at the value α_1 results in minimum rotor copper losses. However, equal excitation of the two field windings still produces minimum rotor copper losses. Moreover, it results in an even distribution of copper losses between the two field windings and so prevent the overheating of either of them.

b) Control of field winding 1

It has been already proved that when the rotor-angle is fixed at the value α_1 , no stability improvement can be achieved by controlling the excitation of field winding 1. This fact is confirmed by Fig. 5.21. However, the situation is different if the rotor-angle is fixed at values other than α_1 and considerable extension of the dynamic stable region in this case is also achieved (Fig. 5.21).

c) Control of both field windings

As explained before, if the rotor angle is fixed at the value α_1 , field winding 1 controls only the reactive power and so it does not contribute to the stability of the machine. This field winding could be utilized in regulating the terminal voltage of the machine by providing it with a voltage regulator. The extension of the dynamic stable region in this case can still be achieved by controlling field winding 2 with a rotor-angle regulator. As shown in Fig. 5.22, the addition of the

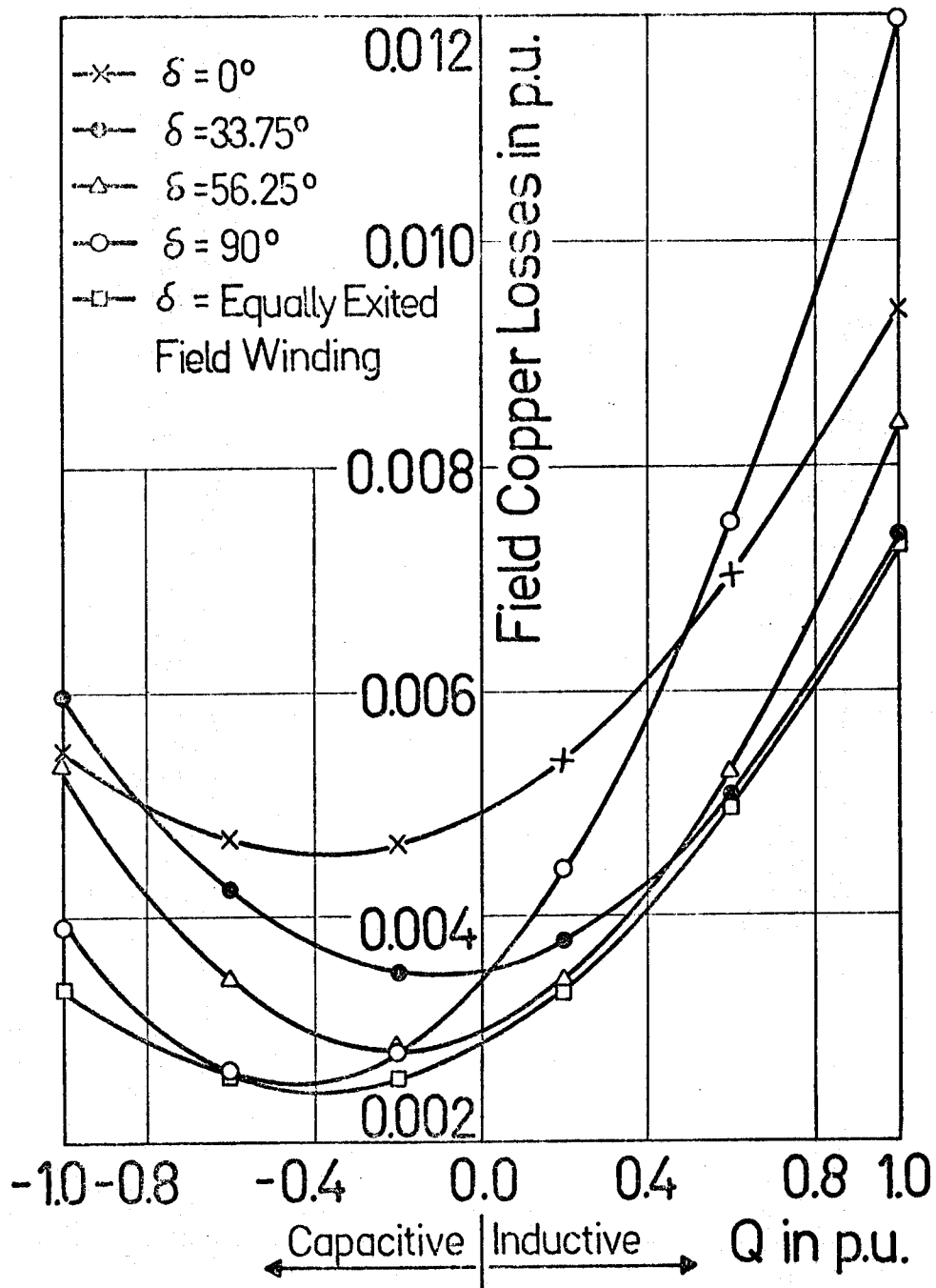


Fig. 5.19 Total Field Copper Losses of the Dual-Excited Synchronous Generator for Different Rotor-Angles. (P=1.0 p.u.)

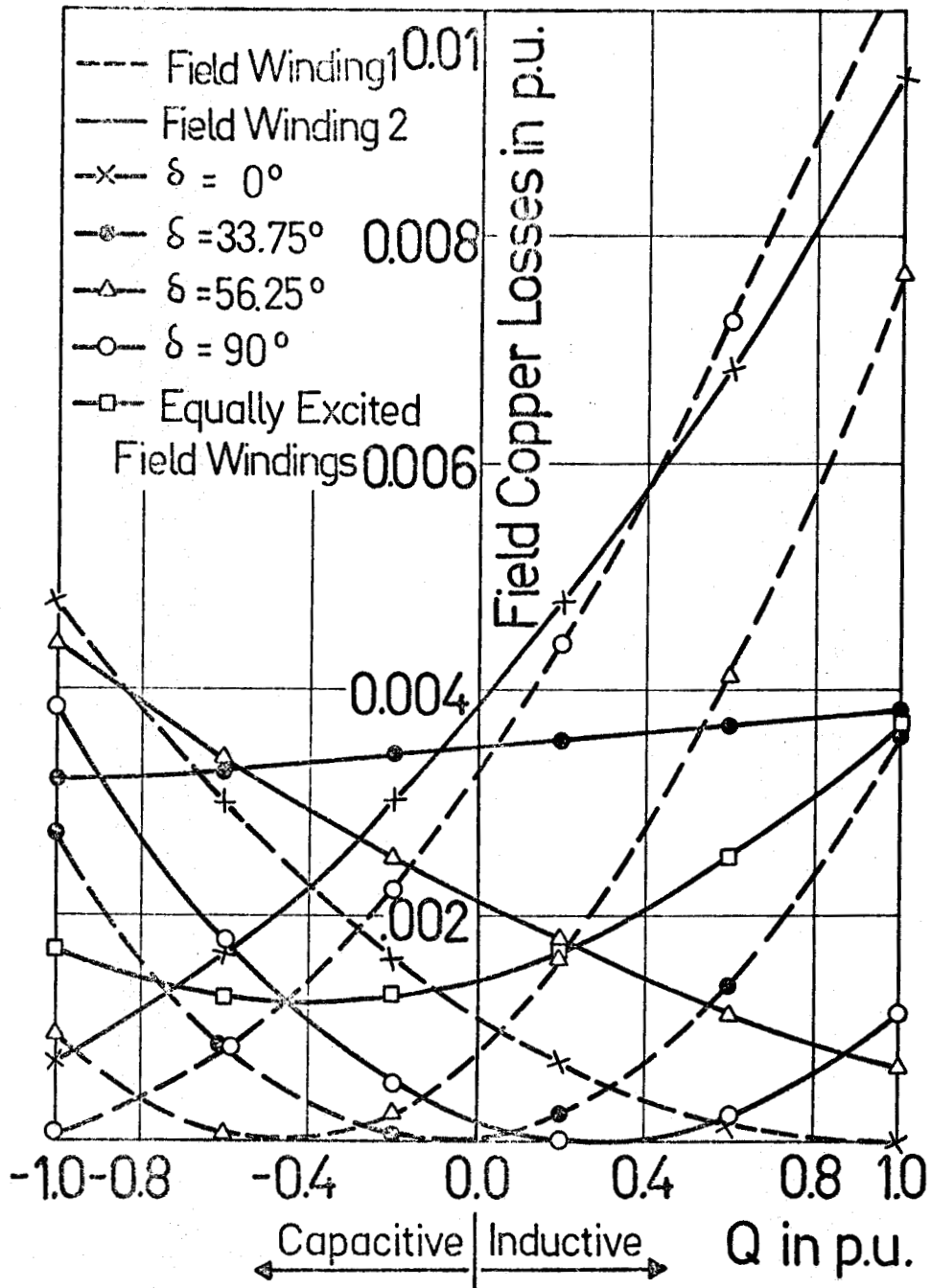


Fig. 5.20 Distribution of Copper Losses between the two Field Windings of the Dual-Excited Synchronous Generator for Different Rotor Angles ($P=1.0$ p.u.)

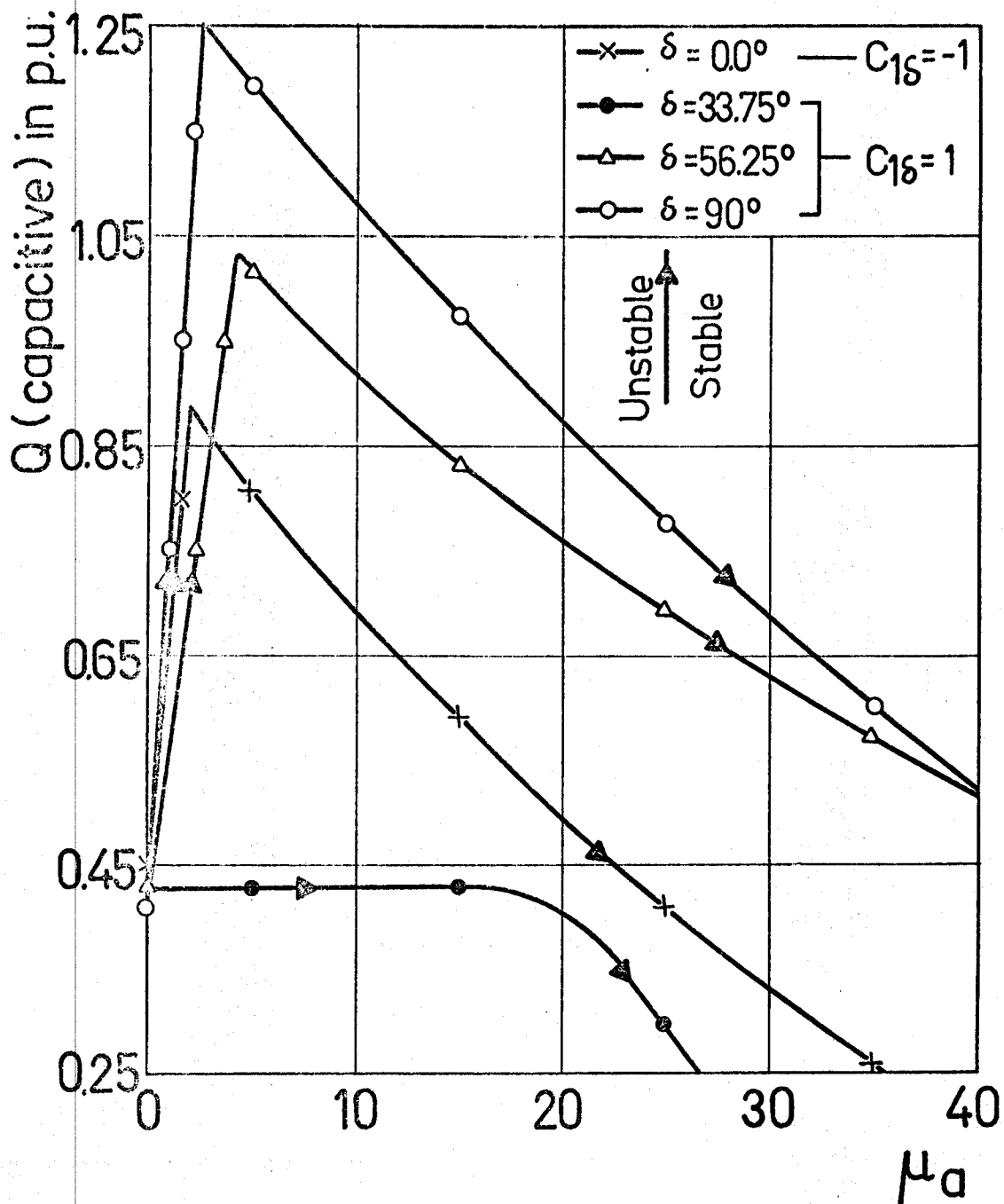


Fig. 5.21 Dynamic Stability Boundaries of the Dual-Excited Synchronous Generator for Operation with Fixed Rotor-Angle ($P=0.0$, Field Winding 1 is Controlled by a Rotor-Angle Regulator)

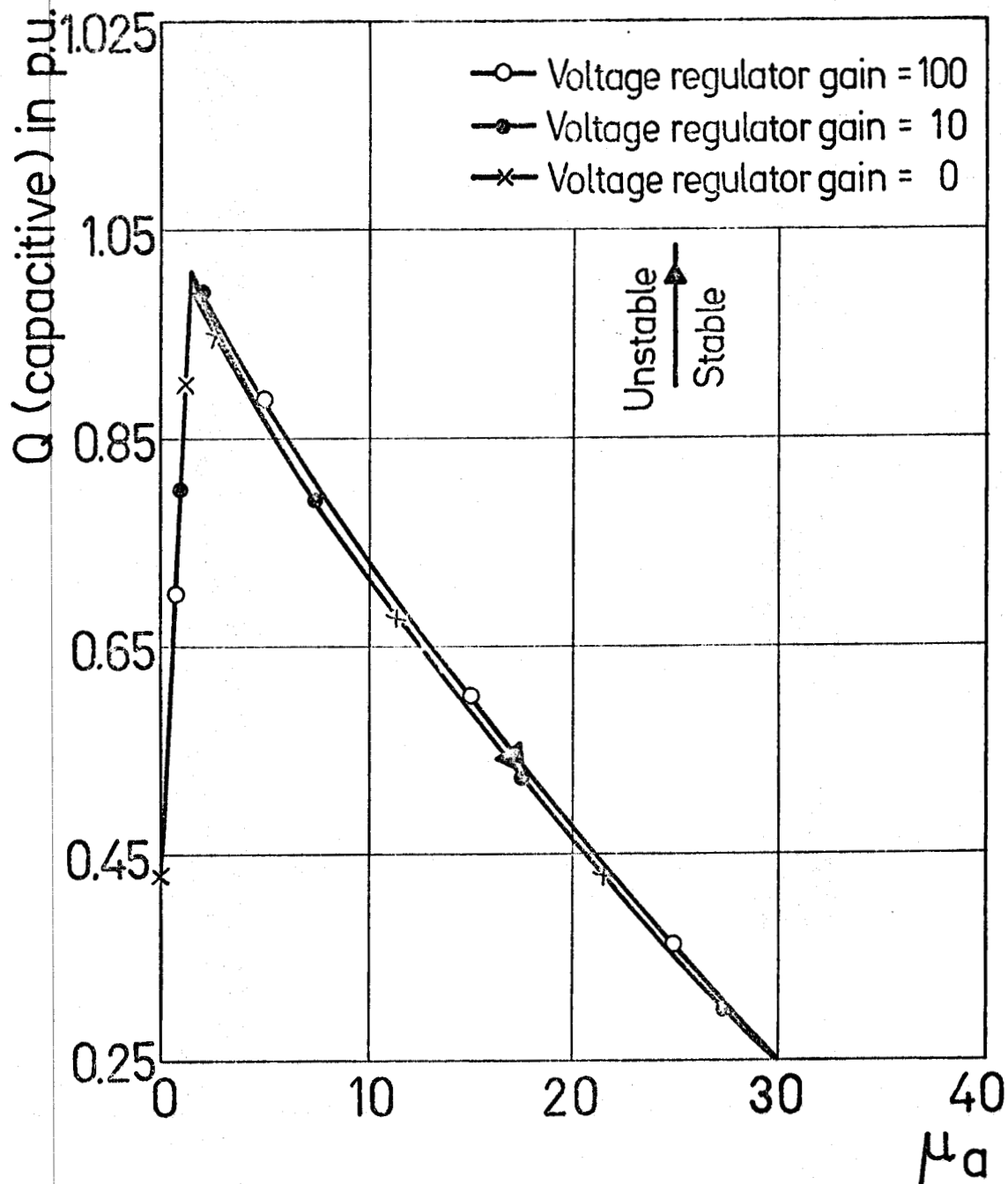


Fig. 5.22 Dynamic Stability Boundaries of the Dual-Excited Synchronous Generator for Operation with Fixed Rotor-Angle ($P=0.0$, Field Winding 1 is Controlled by a Voltage Regulator while Field Winding 2 is Controlled by a Rotor-Angle Regulator)

voltage regulator does not affect significantly the stability boundaries at no load. Moreover, the machine is stable even with very high gain for the voltage regulator.

6. CONCLUSIONS

6.1 General

The recent developments in power systems, such as the erection of long high voltage transmission lines, the widespread use of underground cables and the design of large machines with high per-unit reactances, have made the stability problem of power systems more acute. In Chapter 2, the stability problem of conventional synchronous machines both at steady-state and transient conditions is discussed briefly. It appears that, with the available methods used for improving the machine stability, a point has been reached beyond which further improvements are not seen especially for the dynamic operation at no load. Dual-exciting the rotors of synchronous machines has been recently suggested as a possible technique for achieving further extension of the stable operation of these machines.

6.2 Analysis of the Dual-Excited Synchronous Machine

In Chapter 3, a generalized analysis for the dual-excited synchronous machine has been developed. The mathematical representation obtained allows for the study of machines, in which both field windings are not necessarily located on the rotor-axis and may have different number of turns as well as different inclination angles to the direct-axis of the pole structure. This representation is also applicable to any special case such as the d-q or the conventional synchronous machine.

The equations are derived for the case of a dual-excited synchronous machine connected to an infinite-bus through a general transmission system. They are arranged in the operational form which is of interest as far as

power system analysis is concerned. Special attention has been directed in Chapter 4 towards formalizing the linearized small displacement equations taking into account the possibility of using different schemes of excitation regulation for either of the two field windings or both. In the whole analysis, no assumptions are made other than those required for deriving Park's transformation and so it offers a more exact machine representation.

The general analysis is followed in Chapter 5 by a study of the machine dynamic stability. A simple power system is considered, in which a dual-excited synchronous generator is connected to an infinite-bus via a simple tie line. The dynamic stability investigation is carried out through the application of Routh's criterion to the characteristic equation of the system as found from its linearized representation. For this, a digital computer program has been developed, which gives the stability boundaries in the plane of any two arbitrary parameters.

6.3 Static Stability and Capability Diagram of the Dual-Excited Synchronous Generator

The static stability limits of the dual-excited synchronous generator with identical and equally excited field windings are the same as those of an equivalent conventional one. This applies also for the case of differently excited field windings if there is no saliency. When saliency is present, the static stability boundary depends on the ratio of the excitation currents in both field windings. However, it does not significantly differ from that of the conventional synchronous generator.

The values of the excitation currents in both field windings are restricted at any operating point by the rotor heating limit. Not only the total field copper losses have not to exceed a safe value, but also the copper losses of each field winding should not exceed its heating limit. It has been found that equally exciting both field windings has the advantage of producing minimum total field copper losses as well as even heat distribution in the rotor. This would prevent the overheating of either of the two field windings and thus provide a wider operating range.

Hence, it can be concluded that the dual-excited synchronous generator has no advantage over the conventional one as far as the steady-state (static) operation is concerned.

6.4 Dynamic Stability of the Dual-Excited Synchronous Generator.

For investigating the dynamic stability of the dual-excited synchronous generator, two modes of operation are considered. In the first, the two field windings are always equally excited. In the second, the excitation currents of both windings are adjusted so as to keep the rotor-angle fixed at a certain specified value.

With equally excited field windings, the control of either of them by a voltage regulator extends considerably the dynamic stable region at full load. However, such an extension will be less when the machine is lightly loaded. At no load, no improvement can be achieved and the maximum capacitive power which the machine can supply for stable operation, could not exceed the static stability limit. Thus, this scheme of controlling the excitation of the dual-excited generator does not offer any further advantage in comparison with the conventional one.

However, the extension of the under-excited region beyond the static stability limits for all loading conditions can be achieved by controlling the excitation of field winding 1 by a rotor-angle regulator. In this case, instability will be created if the machine is operating within its static stable region with a rotor-angle less than α_1 . Stability within this region can then be maintained if the sign of the control signal is reversed or if the excitation control loop is out of service for this operating condition. It follows that this scheme of excitation control is not helpful unless special arrangements are used to take care of this problem. This may introduce practical difficulties, the study of which is beyond the scope of this work.

When the excitation of field winding 2 is controlled by a rotor-angle regulator, the extension of the under-excited stable region is subjected also to certain restrictions concerning the sign of the control signal. For stabilizing the machine, this sign should be positive when δ is less than $180-\alpha_2$ and negative when δ is greater than $180-\alpha_2$. It is also noticed that the improvement achieved at light loading is not satisfactory.

With both field windings equally excited and simultaneously controlled by two similar regulators, the dual-excited synchronous generator (with identical field windings) is equivalent to a conventional one. Thus, the dynamic stable region at full load can be extended considerably, while such extension is limited at light loading. At no load, no improvement can be achieved at all and the maximum capacitive power, which the generator can develop, does not exceed the static stability limit.

As the control of either of the two field windings by a rotor-angle regulator fails to stabilize the machine all over the whole generating range, the second mode of excitation has been suggested as a possible way to overcome this limitation.

If the rotor-angle is fixed at the value α_1 , the dynamic stable region can be considerably extended at any loading condition through controlling the excitation of field winding 2 by a rotor-angle regulator. Field winding 1, having in this case its magnetic-axis coinciding with the resultant flux, cannot help improve the machine stability.

The extension of the dynamic stable region can also be achieved by controlling the excitation of either of the two field windings by a rotor-angle regulator, when the rotor-angle is fixed at values other than α_1 . It is found that the largest stable region is obtained when the rotor-angle is fixed at the value 90° . However, the choice of other values than α_1 is restricted by the heating limit of each field winding. At lagging power-factors, the value α_1 gives rise to minimum rotor heating but not to the extent to be less than in the case of equally excited field windings. Further, with the rotor-angle fixed at the value α_1 , field winding 1 does not contribute to the machine stability and can be utilized to control the terminal voltage by providing it with a voltage regulator. Stability of the machine in this case can be maintained at any loading condition through controlling field winding 2 by a rotor-angle regulator. Such a scheme will allow for the use of extremely high gains for the voltage regulator without leading to instability.

In general, it can be concluded that the under-excited stable region of a properly controlled dual-excited generator can be extended

at no load as well as at low power demand far beyond its static stability limits. On the other hand, this machine at full load operation has no advantage over a properly controlled conventional one from the dynamic stability point of view.

6.5 Recommendations for Future Work

Although some effort has been directed in this thesis to study the dynamic stability of the dual-excited synchronous generator, many investigations are still to be carried out in the future to understand more its dynamic behaviour. Some of the studies suggested for future work are:

1. Studies of the effect of other control signals such as current, power, reactive power, speed, acceleration or any possible combination of them on the machine dynamic stability.
2. Finding out methods for realizing stable dynamic operation all over the whole loading range with equally excited field windings.
3. Effect of different rotor designs on the dynamic stability of this machine.
4. Optimization of the regulator parameters to achieve the best dynamic operation especially when both field windings are simultaneously controlled.
5. Enhancement of damping of synchronous machines especially at no load.
6. Investigating the machine transient stability under the effect of different schemes of excitation regulation.
7. Experimental work on the microalternator for verifying most of these theoretical studies.

7. REFERENCES

1. S.B. Crary, "Power System Stability", vol. 1, "Steady-state Stability", New York, Wiley, 1945.
2. S.B. Crary, "Power System Stability", vol. 2, "Transient stability", New York, Wiley, 1947.
3. E.W. Kimbark, "Power System Stability", vol. 1, "Elements of stability calculations", New York, Wiley, 1948.
4. E.W. Kimbark, "Power System Stability", vol. 3, "Synchronous Machines", New York, Wiley, 1956.
5. Report on the work of Study Committee No. 13, "System Planning and Operation", CIGRE, paper 330, 1964.
6. G.B. Furst, "The effect of synchronous reactances and excitation parameters on transient stability", The Institution of Engineers, Australia, Elect. Eng. Trans., pp. 135 - 140, March 1968.
7. R. W. Bruck, and H.K. Messerle, "The capability of alternators", PROC. IEE, vol. 102, pt. A, pp. 677 - 618, 1955.
8. C. Concordia, "Steady-state stability of synchronous machines as affected by voltage regulator characteristics", AIEE Trans., vol. 63, pp. 215 - 220, 1944.
9. C. Concordia, "Steady-state stability of synchronous machines as affected by angle-regulator characteristics", AIEE Trans., vol. 67, pt. I, pp. 687 - 690, 1948.
10. W.G. Heffron, and R.A. Phillips, "Effect of modern amplidyne voltage regulator on under-excited operation of large turbine generators", AIEE Trans., vol. 71, pt. III, pp. 692-697, 1952.
11. H.K. Messerle, and R.W. Bruck, "Steady-state stability of synchronous generators as affected by regulators and governors", Proc. IEE, vol. 103, pt. C, pp. 24-34, 1956.
12. H.K. Messerle, "Relative dynamic stability of large synchronous generator", Proc. IEE, vol. 103, pt. C, pp. 234-242, 1956.
13. A.S. Aldred, and G. Shackshaft, "The effect of a voltage regulator on the steady-state and transient stability of a synchronous generator", Proc. IEE, vol. 105, pt. A, pp. 420-427, 1958.
14. H.K. Messerle, "Dynamic stability of alternators as affected by machine reactances and transmission links", CIGRE, paper 315, 1958.

15. P. Langer, and K.E. Johansson, "The influence of a load-angle-dependant signal on the voltage regulation of synchronous machines", CIGRE, paper 315, 1960.
16. C.J. Goodwin, "Voltage regulator requirements for steady-state stability of water-wheel generators connected to a system through long transmission lines", CIGRE, paper 301, 1962.
17. H.E. Cales, "Effect of prime-mover governing and voltage regulation on turboalternator performance", Proc. IEE, Vol. 112, pp. 1395 - 1405, July, 1965.
18. R.R. Booth, "The effect of regulating devices on the steady-state stability of a synchronous machine", Proc. 2nd Power Systems Computation Conf., pt. 3, paper 5.4 (Stockholm, Sweden, June/July 1966).
19. Y.N. Yu, and K. Vangsuriya, "Steady-state stability limits of a regulated synchronous machine connected to an infinite system", IEEE Trans. Power Apparatus and Systems, vol. 85, pp. 759-767, July, 1966.
20. P.L. Dandeno, A.N. Karas, K.R. McClymont, and W. Watson, "Effect of high-speed rectifier excitation systems on generator stability limits". IEEE Trans. Power Apparatus and Systems, vol. 87, pp. 190-201, January, 1968.
21. F.P. Demello, and C. Concordia, "Concepts of synchronous machine stability as affected by excitation control", IEEE Trans. Power Apparatus and Systems, vol. 88, pp. 316-329, April, 1969.
22. L.J. Jacovides and B. Adkins, "Effect of excitation regulation on synchronous-machine stability", Proc. IEE, vol. 113, pp. 1021-1034, June, 1966.
23. C.A. Stapleton, "Root-Locus study of synchronous machine regulation", Proc. IEE, vol. III, pp. 761, April, 1964.
24. A.M. El-Serafi, "Optimization of excitation systems of synchronous machines for maximum possible capacitive loading", paper No. 70CP202-PWR, presented at the 1970 IEEE Winter Power Meeting, New York, N.Y., January 25-30, 1970.
25. Hamdi-Sapen, "Process for increasing the transient stability power limits on a.c. transmission system", CIGRE, paper 305, 1962.
26. Hamdi-Sapen, "Process for increasing transient stability power limits on A.C. Transmission systems, (part 2)", CIGRE, paper 304, 1964.

27. J.A. Soper and A.R. Fagg, "Divided-winding synchronous generator", Proc. IEE, Vol. 116, pp. 113 - 126, January, 1969.
28. S.C. Kapoor, S.S. Kalsi and B. Adkins. "Improvement of alternator stability by controlled quadrature excitation", Proc. IEE, Vol. 116, pp. 771 - 780, May 1969.
29. R.G. Hareley and B. Adkins. "Stability of synchronous machines with divided-winding rotor", Proc. IEE, Vol. 117, pp. 933 - 947, May, 1970.
30. M. Rama Murthi, M. Williams and B.W. Hogg, "Stability of synchronous machines with 2-axis excitation systems", Proc. IEE, Vol. 117, pp. 1799 - 1808, September, 1970.
31. B.W. Rankin, "Per-unit impedances of synchronous machines". Part 1, Transactions AIEE, Vol. 64, pp. 569 - 573, 1945. Part 2, Transactions AIEE, Vol. 64, pp. 839 - 841, 1945.
32. M.R. Harris, P.J. Lawrenson and J.M. Stephenson, "Per-unit systems: with special reference to electrical machines", IEE Monograph Series 4. (1970).
33. R.H. Park, "Two-reaction theory of synchronous machines", Part 1, AIEE Trans., Vol. 48, pp. 716 - 727, July 1929; Part 2, AIEE TRANS., Vol. 52, pp. 352 - 355, June 1933.
34. C. Concordia. "Synchronous machines", Wiley, 1951.
35. B. Adkins, "The general theory of electrical machines", Chapman and Hall, London, 1964.
36. V. Bush, "Operational circuit analysis", Wiley, 1929.

8. APPENDICES

Appendix A - Limitations of the Conventional Synchronous Machine Excitation Control At No Load.

Theoretical and experimental studies^{22,28} showed that the possible capacitive power, which a conventional synchronous generator can develop at no load, cannot be increased through the use of voltage or load-angle regulators. In this appendix, it will be proved that, no matter what signal is fed-back from the output of the generator to the direct-axis field winding, this limitation still holds.

The equations describing the performance of a conventional synchronous generator connected to an infinite-bus through a series reactance x_e are:

$$v_d = v \cdot \sin \delta = p \Psi_d - (p\theta_o + p\Delta\delta) \cdot \Psi_q - r \cdot i_d \quad 8.1$$

$$v_q = v \cdot \cos \delta = p \Psi_q + (p\theta_o + p\Delta\delta) \cdot \Psi_d - r \cdot i_q \quad 8.2$$

$$T_i = i_q \cdot \Psi_d - i_d \cdot \Psi_q + \textcircled{H} \cdot p^2 \Delta\delta \quad 8.3$$

where:

$$\Psi_d = -(x_e + x_d(p)) \quad i_d + G(p) \quad v_{fd} \quad 8.4$$

$$\Psi_q = -(x_e + x_q(p)) \quad i_q \quad 8.5$$

Since the speed changes during a small disturbance are small, the voltage terms $p\Delta\delta \cdot \Psi_q$ and $p\Delta\delta \cdot \Psi_d$ can be neglected. Also, the voltages $p\Psi_d$ and $p\Psi_q$ induced in the armature by the rate of change of armature flux linkages are negligible compared with the rotational voltages.

Neglecting $p\Psi_d$, $p\Psi_q$, $p\Delta\delta$ and substituting $p\theta_o=1$, equations 8.1 - 8.3 can be rewritten as follows:

$$v_d = v \cdot \sin\delta = (x_e + x_q(p)) i_q - r \cdot i_d \quad 8.6$$

$$v_q = v \cdot \cos\delta = -(x_e + x_d(p)) i_d + G(p)v_{fd} - r \cdot i_q \quad 8.7$$

$$\begin{aligned} T_i = & i_q \cdot (-(x_e + x_d(p)) i_d + G(p) v_{fd}) \\ & + i_d \cdot (x_e + x_q(p)) i_q + \textcircled{H} \cdot p^2 \Delta\delta \end{aligned} \quad 8.8$$

Following the procedure explained in Chapter 4, the small displacement equations can be written as follows:

$$\Delta v_d = v_{qo} \cdot \Delta\delta = (x_e + x_q(p)) \Delta i_q - r \cdot \Delta i_d \quad 8.9$$

$$\Delta v_q = -v_{do} \cdot \Delta\delta = -(x_e + x_d(p)) \Delta i_d - r \cdot \Delta i_q + G(p) \Delta v_{fd} \quad 8.10$$

$$\begin{aligned} \Delta T_i = & -i_{qo} \cdot (x_e + x_d(p)) \Delta i_d + i_{qo} \cdot (x_e + x_q) \Delta i_d \\ & + i_{do} \cdot (x_e + x_q(p)) \Delta i_q + (e - i_{do} \cdot (x_e + x_d)) \Delta i_q \\ & + i_{qo} \cdot G(p) \Delta v_{fd} + \textcircled{H} \cdot p^2 \Delta\delta \end{aligned} \quad 8.11$$

Using equations 8.9 and 8.10, equation 8.11 can be reduced to:

$$\Delta T_i = (v_{do} + i_{do} \cdot r) \cdot \Delta i_d + (v_{qo} + i_{qo} \cdot r) \cdot \Delta i_q + (Q + \textcircled{H} \cdot p^2) \cdot \Delta\delta \quad 8.12$$

where Q is the reactive power delivered to the infinite-bus and is equal to $(i_{do} \cdot v_{qo} - i_{qo} \cdot v_{do})$

Equations 8.9, 8.10, and 8.12 can be rewritten in the following matrix form:

$G(p) \Delta v_{fd}$

$$=$$

$x_e + x_d(p)$	r	$-v_{do}$
$-r$	$x_e + x_q(p)$	$-v_{qo}$
$v_{do} + i_{do} \cdot r$	$v_{qo} + i_{qo} \cdot r$	$\oplus \cdot p^2 + Q$

Δi_d
Δi_q
$\Delta \delta$

8.13

At no load:

$$v_{do} = 0 \tag{8.14}$$

$$v_{qo} = +v \tag{8.15}$$

The positive sign applies when $\delta=0^\circ$, while the negative sign when $\delta=180^\circ$. Substituting from equations 8.14 and 8.15 and neglecting the armature resistance, equation 8.13 becomes:

$G(p) \Delta v_{fd}$
0
0

$$=$$

$x_e + x_d(p)$		
	$x_e + x_q(p)$	$\frac{+v}{-}$
	$\frac{+v}{-}$	$\oplus \cdot p^2 + Q$

Δi_d
Δi_q
$\Delta \delta$

8.16

From equation 8.16, the transfer functions of the conventional synchronous generator (Fig. 8.1) can be written as follows:

$$F_{id}(p) = \frac{\Delta i_d}{\Delta v_{fd}} = \frac{x_{ad}}{r_{fd} \cdot (x_d + x_e)} \cdot \frac{(1 + T_{kd}' \cdot p) \cdot [(Q + \oplus \cdot p^2) \cdot (1 + T_q'' \cdot p) + (v^2 / (x_q + x_e)) \cdot (1 + T_{qo}'' \cdot p)]}{(1 + T_d' \cdot p) \cdot (1 + T_d'' \cdot p) \cdot [(Q + \oplus \cdot p^2) \cdot (1 + T_q'' \cdot p) + (v^2 / (x_q + x_e)) \cdot (1 + T_{qo}'' \cdot p)]} \tag{8.17}$$

$$F_{iq}(p) = \frac{\Delta i_q}{\Delta v_{fd}} = 0 \tag{8.18}$$

$$F_\delta(p) = \frac{\Delta \delta}{\Delta v_{fd}} = 0 \tag{8.19}$$

Variation in reference

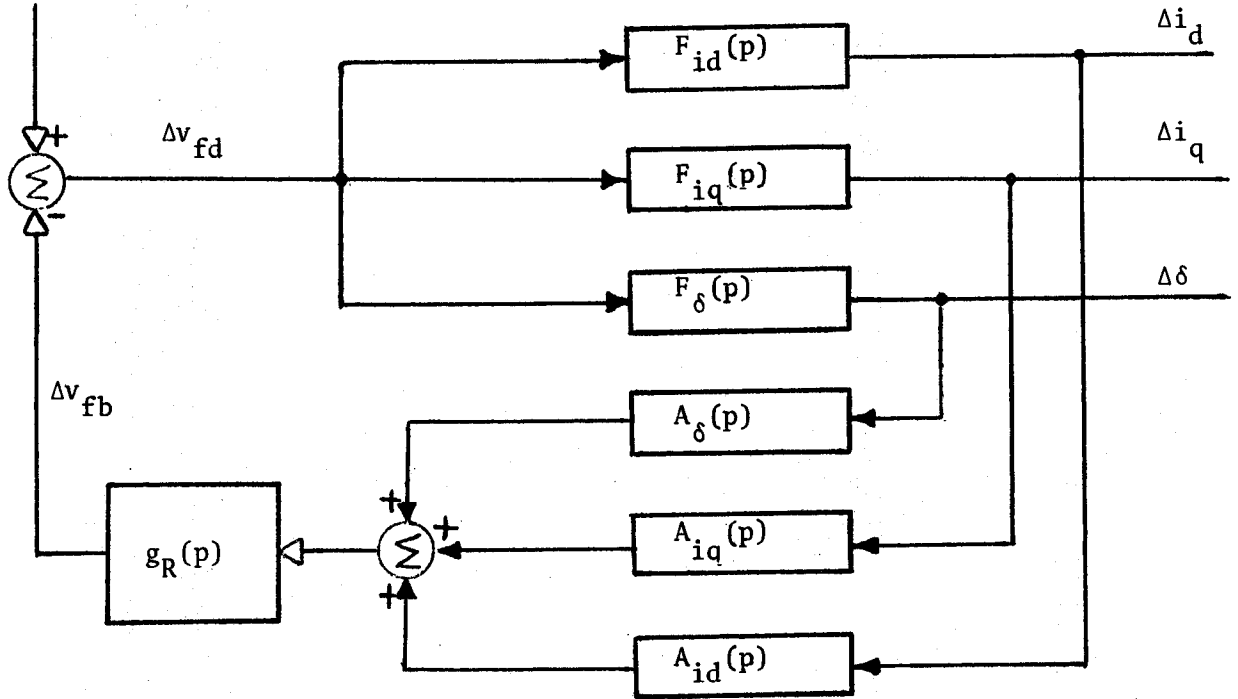


Fig. 8.1 Transfer Functions of the Conventional Synchronous Machine

where:

T_d' = direct-axis transient short-circuit time constant.

T_d'' = direct-axis subtransient short-circuit time constant.

T_{kd} = direct-axis damper leakage time constant.

T_{qo}'' = quadrature-axis subtransient open-circuit time constant.

T_q' = quadrature-axis subtransient short-circuit time constant.

Whatever feed-back signals or regulator transfer functions are used, the complete open-loop transfer function $\Delta v_{fb}/\Delta v_{fd}$ will be:

$$F_o(p) = A_{idt}(p) \cdot F_{id}(p) \quad 8.20$$

$A_{idt}(p)$ can have the following general form:

$$A_{idt}(p) = k \cdot \frac{a_n \cdot p^n + a_{n-1} \cdot p^{n-1} + \dots + \dots + 1}{b_m \cdot p^m + b_{m-1} \cdot p^{m-1} + \dots + \dots + 1} \quad 8.21$$

where $a_n, a_{n-1}, \dots, b_m, b_{m-1}, \dots$ and k are always positive. Hence, the characteristic equation of the system becomes:

$$\begin{aligned} r_{fd} \left(\frac{x_d + x_e}{x_{ad}} \right) \cdot (b_m \cdot p^m + b_{m-1} \cdot p^{m-1} + \dots + \dots + 1) \cdot (1 + T_d' \cdot p) \cdot (1 + T_d'' \cdot p) \cdot [(Q + H) \cdot p^2] \cdot \\ (1 + T_q'' \cdot p) + (v^2 / (x_q + x_e)) \cdot (1 + T_{qo}'' \cdot p) + k(a_n \cdot p^n + a_{n-1} \cdot p^{n-1} + \dots + \dots + 1) \cdot (1 + T_{kd} \cdot p) \cdot \\ [(Q + H) \cdot p^2] \cdot (1 + T_q'' \cdot p) + (v^2 / (x_q + x_e)) \cdot (1 + T_{qo}'' \cdot p) = 0 \end{aligned} \quad 8.22$$

According to Routh's Criterion, the system will be unstable if any of the polynomial terms of equation 8.22 disappears or becomes negative.

The only terms of this equation which can be zero or negative are those including the quantity $(Q+v^2/(x_q+x_e))$. It can be seen that the first term to become negative with the change of Q is the constant term of the polynomial. This occurs when $Q=-v^2/(x_q+x_e)$. Hence, the machine cannot be stable when the capacitive power exceeds its value at the static stability limit.

Appendix B - Limitations of the Dual-Excited Synchronous Machine
Excitation Control at No Load

Equations 8.1 - 8.3 are valid for any synchronous machine. Hence, it represents also the dual-excited synchronous one. The expressions for the flux linkages in both the direct- and the quadrature-axis are given by equations 3.60 and 3.61. The special case of a generator with two identical field windings having equal inclination angles to the direct-axis of the rotor and equally excited is considered. The generator is assumed to be connected to an infinite bus through a series reactance x_e . For this case, the flux linkage equations can be written as:

$$\Psi_d = -(x_e + x_d(p)) i_d + G_{f1d}(p) v_{f1} + G_{f2d}(p) v_{f2} \quad 8.23$$

$$\Psi_q = -(x_e + x_q(p)) i_q + G_{f1q}(p) v_{f1} + G_{f2q}(p) v_{f2} \quad 8.24$$

Substituting for Ψ_d and Ψ_q in equations 8.1 - 8.3 and applying the same approximations considered for deriving equations 8.6 - 8.8, the following equations are obtained:

$$v \sin \delta = -r \cdot i_d + (x_e + x_q(p)) i_q - G_{f1q}(p) v_{f1} - G_{f2q}(p) v_{f2} \quad 8.25$$

$$v \cos \delta = -r \cdot i_q - (x_e + x_d(p)) i_d + G_{f1d}(p) v_{f1} + G_{f2d}(p) v_{f2} \quad 8.26$$

$$\begin{aligned} T_i = & i_q \cdot (-x_e + x_d(p)) i_d + G_{f1d}(p) v_{f1} + G_{f2d}(p) v_{f2} \\ & - i_d \cdot (-x_e + x_q(p)) i_q + G_{f1q}(p) v_{f1} + G_{f2q}(p) v_{f2} \\ & + \textcircled{H} \cdot p^2 \Delta \delta \end{aligned} \quad 8.27$$

Hence, the small displacement equations can be written as follows:

$$\Delta v_d = v_{qo} \cdot \Delta \delta = -r \cdot \Delta i_d + (x_e + x_q(p)) \Delta i_q - G_{f1q}(p) \Delta v_{f1} - G_{f2q}(p) \Delta v_{f2} \quad 8.28$$

$$\Delta v_q = -v_{do} \cdot \Delta \delta = -r \cdot \Delta i_q - (x_e + x_d(p)) \Delta i_d + G_{f1d}(p) \Delta v_{f1} + G_{f2d}(p) \Delta v_{f2} \quad 8.29$$

$$\begin{aligned} \Delta T_i = & -i_{qo} \cdot (x_e + x_d(p)) \Delta i_d + i_{qo} \cdot G_{f1d}(p) \Delta v_{f1} + i_{qo} \cdot G_{f2d}(p) \Delta v_{f2} + \\ & i_{do} \cdot (x_e + x_q(p)) \Delta i_q - i_{do} \cdot G_{f1q}(p) \Delta v_{f1} - i_{do} \cdot G_{f2q}(p) \Delta v_{f2} + \\ & v_{qo} \cdot \Delta i_q + v_{do} \cdot \Delta i_d + \textcircled{H} \cdot p^2 \Delta \delta \end{aligned} \quad 8.30$$

If only field winding 1 excitation is controlled, then all the terms containing Δv_{f2} will disappear. Hence, equations 8.28 - 8.30 will be reduced to:

$$0 = -r \cdot \Delta i_d + (x_e + x_q(p)) \Delta i_q - v_{qo} \Delta \delta - G_{f1q}(p) \Delta v_{f1} \quad 8.31$$

$$0 = -r \cdot \Delta i_q - (x_e + x_d(p)) \Delta i_d + v_{do} \Delta \delta + G_{f1d}(p) \Delta v_{f1} \quad 8.32$$

$$\begin{aligned} 0 = & -i_{qo} \cdot (x_e + x_d(p)) \Delta i_d + i_{qo} \cdot G_{f1d}(p) \Delta v_{f1} + i_{do} \cdot (x_e + x_q(p)) \Delta i_q \\ & - i_{do} \cdot G_{f1q}(p) \Delta v_{f1} + v_{qo} \cdot \Delta i_q + v_{do} \cdot \Delta i_d + \textcircled{H} \cdot p^2 \Delta \delta \end{aligned} \quad 8.33$$

At no load, equations 8.14 and 8.15 can be also applied. Neglecting the armature resistance, equations 8.31 - 8.33 are simplified and can be arranged as follows:

$G_{f1d}(p) \Delta v_{f1}$	$x_e + x_d(p)$			Δi_d	8.34
=	$\frac{G_{f1q}(p)}{G_{f1d}(p)} \cdot (x_e + x_d(p))$	$x_e + x_q(p)$	\bar{v}	Δi_q	
		\underline{v}	$Q + \textcircled{H} \cdot p^2$	$\Delta \delta$	

where Q is the reactive power delivered to the infinite bus.

The transfer functions of the dual-excited synchronous generator (Fig. 8.2) can be written as follows:

$$F_{id1}(p) = \frac{\Delta i_d}{\Delta v_{f1}} = \frac{G_{f1d}(p) \cdot (x_e + x_q(p)) \cdot (Q + \mathbb{H} p^2) + v^2}{(x_e + x_d(p)) \cdot (x_e + x_q(p)) \cdot (Q + \mathbb{H} p^2) + v^2} \quad 8.35$$

$$F_{iq1}(p) = \frac{\Delta i_q}{\Delta v_{f1}} = \frac{G_{f1q}(p) \cdot (x_e + x_d(p)) \cdot (Q + \mathbb{H} p^2)}{(x_e + x_d(p)) \cdot (x_e + x_q(p)) \cdot (Q + \mathbb{H} p^2) + v^2} \quad 8.36$$

$$F_{\delta 1}(p) = \frac{\Delta \delta}{\Delta v_{f1}} = \frac{+v \cdot G_{f1q}(p) \cdot (x_e + x_d(p))}{(x_e + x_d(p)) \cdot (x_e + x_q(p)) \cdot (Q + \mathbb{H} p^2) + v^2} \quad 8.37$$

$x_e + x_d(p)$, $x_e + x_q(p)$, $G_{f1d}(p)$ and $G_{f1q}(p)$ can be expressed in polynomial forms as follows:

$$x_e + x_d(p) = \frac{A_4 \cdot p^4 + A_3 \cdot p^3 + A_2 \cdot p^2 + A_1 \cdot p + A_0}{A \cdot p^4 + B \cdot p^3 + C \cdot p^2 + D \cdot p + E} \quad 8.38$$

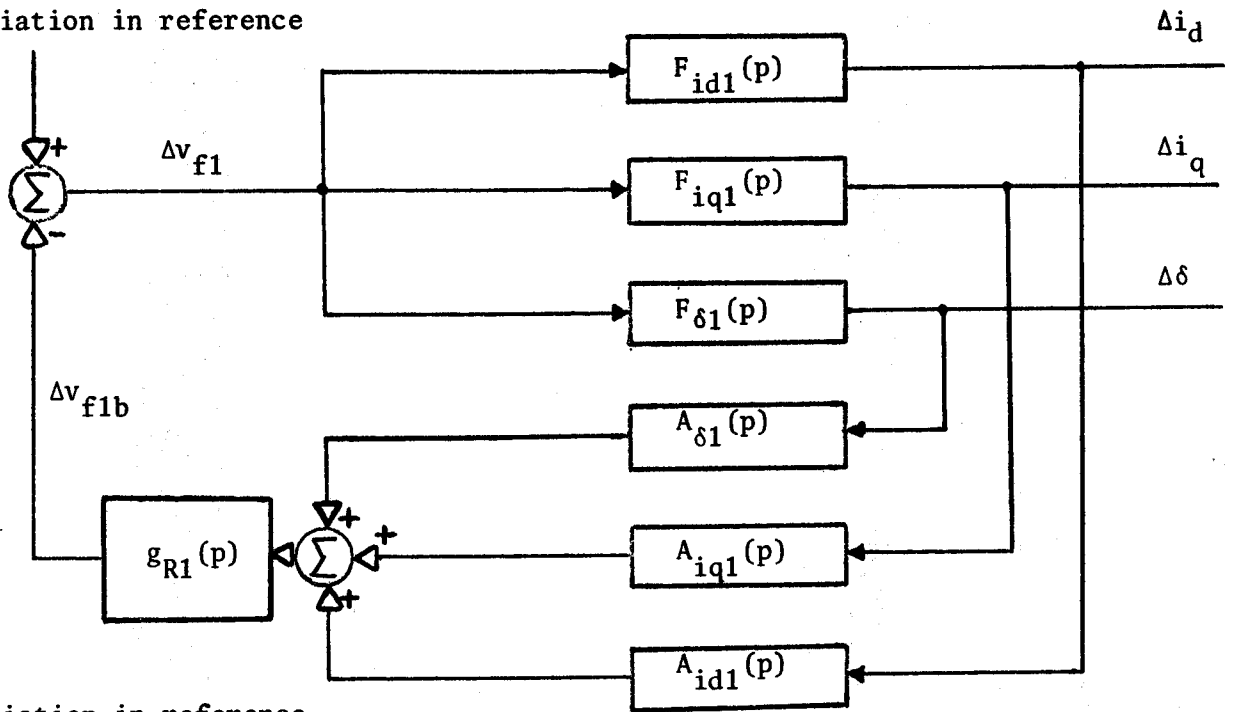
$$x_e + x_q(p) = \frac{B_4 \cdot p^4 + B_3 \cdot p^3 + B_2 \cdot p^2 + B_1 \cdot p + B_0}{A \cdot p^4 + B \cdot p^3 + C \cdot p^2 + D \cdot p + E} \quad 8.39$$

$$G_{f1d}(p) = \frac{C_3 \cdot p^3 + C_2 \cdot p^2 + C_1 \cdot p + C_0}{A \cdot p^4 + B \cdot p^3 + C \cdot p^2 + D \cdot p + E} \quad 8.40$$

$$G_{f1q}(p) = - \frac{D_3 \cdot p^3 + D_2 \cdot p^2 + D_1 \cdot p + D_0}{A \cdot p^4 + B \cdot p^3 + C \cdot p^2 + D \cdot p + E} \quad 8.41$$

It should be noted that all the values, A , B , C , D , E , A_4 , A_3 , ..., A_0 , B_4 , B_3 , ..., B_0 , C_3 , C_2 , ..., C_0 , D_3 , D_2 , ..., D_0 are positive.

Variation in reference



Variation in reference

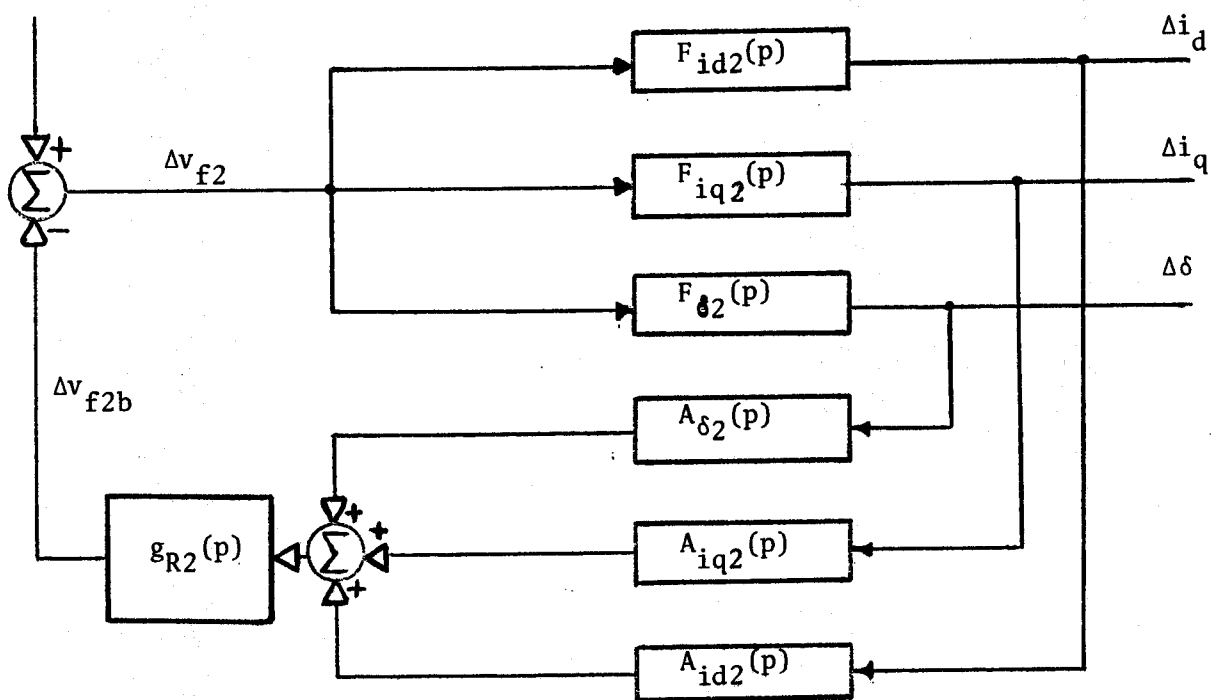


Fig. 8.2 Transfer Functions of the Dual-Excited Synchronous Machine

The effect of using the three output quantities Δi_d , Δi_q and $\Delta \delta$ individually as control signals can be studied as follows:

a) Δi_d Control signal:

The complete open loop transfer function $\Delta v_{flb}/\Delta v_{fl}$ can have the following form:

$$F_o(p) = F_{idlt}(p) \cdot F_{idl}(p) \quad 8.42$$

Assuming that $F_{idlt}(p)$ has the same form as that given by equation 8.21 for $F_{idt}(p)$, the characteristic equation of the system can be written as:

$$\begin{aligned} & (b_m \cdot p^m + b_{m-1} \cdot p^{m-1} + \dots + 1) \cdot (A_4 \cdot p^4 + A_3 \cdot p^3 + A_2 \cdot p^2 + A_1 \cdot p + A_0) \cdot ((B_4 \cdot p^4 + B_3 \cdot p^3 + \\ & B_2 \cdot p^2 + B_1 \cdot p + B_0) \cdot (Q + \textcircled{H} p^2) + (A \cdot p^4 + B \cdot p^3 + C \cdot p^2 + D \cdot p + E) \cdot v^2) + K \cdot (a_n \cdot p^n + a_{n-1} \\ & p^{n-1} + \dots + 1) \cdot (C_3 \cdot p^3 + C_2 \cdot p^2 + C_1 \cdot p + C_0) \cdot ((B_4 \cdot p^4 + B_3 \cdot p^3 + B_2 \cdot p^2 + B_1 \cdot p + B_0) \cdot \\ & (Q + \textcircled{H} p^2) + (A \cdot p^4 + B \cdot p^3 + C \cdot p^2 + D \cdot p + E) \cdot v^2) \end{aligned} \quad 8.43$$

The terms of the characteristic polynomial which can become zero or negative are those containing the quantity Q . It can be seen that the first term to become negative is the constant term of the polynomial. This term has the value $(A_0 + K \cdot C_0) \cdot (B_0 \cdot Q + E \cdot v^2)$. It is thus obvious that the machine cannot be stable when the capacitive power exceeds the value $E \cdot v^2 / B_0$. As shown, this value is independent of the control system parameters. Hence, Δi_d signal alone is useless at no load.

Inspection of the operational functions of the dual-excited synchronous machine, which are given in Appendix C, shows that

$E \cdot v^2 / B_0$ is nothing but $v^2 / (x_q + x_e)$.

b) Δi_q Control signal:

Following the same procedure as for Δi_d control signal, the characteristic equation of the system in this case may be written as:

$$\begin{aligned} & (b_m \cdot p^m + b_{m-1} \cdot p^{m-1} + \dots + 1) \cdot ((B_4 \cdot p^4 + B_3 \cdot p^3 + B_2 \cdot p^2 + B_1 \cdot p + B_0) \cdot (Q + \mathbb{H} \cdot p^2) + \\ & (A \cdot p^4 + B \cdot p^3 + C \cdot p^2 + D \cdot p + E) \cdot v^2) - K(a_n \cdot p^n + a_{n-1} \cdot p^{n-1} + \dots + 1) \cdot (D_3 \cdot p^3 + D_2 \cdot p^2 \\ & + D_1 \cdot p + D_0) \cdot (Q + \mathbb{H} \cdot p^2) = 0 \end{aligned} \quad 8.44$$

To ensure that all terms of the characteristic polynomial which do not include the quantity Q are positive, K should be negative.

In this case, the signs of the other terms depend on the value of Q .

The first term to become negative is that free from the operator p . This term has the value $(B_0 - K \cdot D_0) \cdot Q + E \cdot v^2$. Thus, stability cannot be maintained when the capacitive power exceeds the value $E \cdot v^2 / (B_0 - K \cdot D_0)$.

As K is -ve, it follows that the maximum capacitive power, which the machine can supply at no load with this scheme of control without losing its stability, is even less than the static stability limit.

c) $\Delta \delta$ Control signal:

In this case, the characteristic equation of the system becomes:

$$\begin{aligned} & (b_m \cdot p^m + b_{m-1} \cdot p^{m-1} + \dots + 1) \cdot ((B_4 \cdot p^4 + B_3 \cdot p^3 + B_2 \cdot p^2 + B_1 \cdot p + B_0) \cdot (Q + \mathbb{H} \cdot p^2) + \\ & (A \cdot p^4 + B \cdot p^3 + C \cdot p^2 + D \cdot p + E) \cdot v^2) + K \cdot v \cdot (a_n \cdot p^n + a_{n-1} \cdot p^{n-1} + \dots + 1) \cdot (D_3 \cdot p^3 + D_2 \cdot p^2 \\ & + D_1 \cdot p + D_0) = 0 \end{aligned} \quad 8.45$$

The positive sign applies when $\delta=180^\circ$ while the negative sign when $\delta=0^\circ$. Thus to ensure that all terms, which do not include the quantity Q , are positive, K should be positive when $\delta=180^\circ$ and negative when $\delta=0^\circ$. In this case, the sign of the other terms depends on the value of Q . Following the same procedure explained before for the other control signals, it can be shown that the maximum capacitive power, which the machine can supply in this case without losing its stability, is $(E \cdot V^2 + K \cdot D_o \cdot V^2) B_o$. It is thus clear that this scheme of excitation control can be effective in extending the dynamic stability of the dual-excited synchronous machine at no load.

When field winding 2 is only controlled, similar conclusions will be obtained for Δi_d and $\Delta \delta$ control signals. However, on the contrary of the case of controlling field winding 1, Δi_q control signal can extend the dynamic stable region of this machine at no load.

Appendix C - Expressions for the Operational Functions of the
Dual-Excited Synchronous Machine

The expressions for the dual-excited synchronous machine operational functions can be derived by eliminating the rotor currents from equation 3.56, 3.57. This would result in the following:

$$\begin{aligned}
 x_d(p) = x_d - \frac{x_{ad}}{\sigma} \cdot [& x_{ad} \cdot \{-r_{kd} + (2 \cdot x_{ad} - x_{kkd}) \cdot p\} \cdot \{x_{aq}^2 \cdot \sin^2(\alpha_1 + \alpha_2) p^2 \\
 & + 2 \cdot x_{f12} \cdot \cos \alpha_1 \cdot \cos \alpha_2 \cdot (r_{kq} + x_{kkq} \cdot p) \cdot p - (r_{kq} + x_{kkq} \cdot p) \cdot \\
 & \{\cos^2 \alpha_1 \cdot (r_{f2} + x_{ff2} \cdot p) + \cos^2 \alpha_2 \cdot (r_{f1} + x_{ff1} \cdot p)\} \cdot \\
 & p - 2 \cdot x_{aq}^2 \cdot x_{ad} \cdot x_{f12} \cdot \sin \alpha_1 \cdot \sin \alpha_2 \cdot p^4 - x_{ad} \cdot x_{aq}^2 \cdot \\
 & \{\sin^2 \alpha_1 \cdot (r_{f2} + x_{ff2} \cdot p) + \sin^2 \alpha_2 \cdot (r_{f1} + x_{ff1} \cdot p)\} \cdot \\
 & p^3 + x_{ad} \cdot (r_{kq} + x_{kkq} \cdot p) \cdot \{(r_{f1} + x_{ff1} \cdot p) \cdot (r_{f2} + x_{ff2} \cdot p) - \\
 & x_{f12}^2 \cdot p^2\} \cdot p] \quad 8.45
 \end{aligned}$$

$$\begin{aligned}
 x_q(p) = x_q - \frac{x_{aq}}{\sigma} \cdot [& x_{aq} \cdot \{-r_{kq} + (2 \cdot x_{aq} - x_{kkq}) \cdot p\} \cdot \{x_{ad}^2 \cdot \sin^2(\alpha_1 + \alpha_2) \cdot p^2 \\
 & - 2 \cdot x_{f12} \cdot \sin \alpha_1 \cdot \sin \alpha_2 \cdot (r_{kd} + x_{kkd} \cdot p) \cdot p - (r_{kd} + x_{kkd} \cdot p) \cdot \\
 & \{\sin^2 \alpha_1 \cdot (r_{f2} + x_{ff2} \cdot p) + \sin^2 \alpha_2 \cdot (r_{f1} + x_{ff1} \cdot p)\} \cdot p \\
 & + 2 \cdot x_{ad}^2 \cdot x_{aq} \cdot x_{f12} \cdot \cos \alpha_1 \cdot \cos \alpha_2 \cdot p^4 - x_{aq} \cdot x_{ad}^2 \cdot \\
 & \{\cos^2 \alpha_1 \cdot (r_{f2} + x_{ff2} \cdot p) + \cos^2 \alpha_2 \cdot (r_{f1} + x_{ff1} \cdot p)\} \cdot p^3 + \\
 & x_{aq} \cdot (r_{kd} + x_{kkd} \cdot p) \cdot \{(r_{f1} + x_{ff1} \cdot p) \cdot (r_{f2} + x_{ff2} \cdot p) - \\
 & x_{f12}^2 \cdot p^2\} \cdot p] \quad 8.47
 \end{aligned}$$

$$G_{f1d}(p) = \frac{x_{ad}}{\sigma} \cdot \{r_{kd} + (x_{kkd} - x_{ad}) \cdot p\} \cdot (\text{Cos}\alpha_1 \cdot (r_{kq} + x_{kkq} \cdot p) \cdot (r_{f2} + x_{ff2} \cdot p) - \text{Cos}\alpha_2 \cdot x_{f12} \cdot (r_{kq} + x_{kkq} \cdot p) \cdot p - \text{Sin}\alpha_2 \cdot \text{Sin}(\alpha_1 + \alpha_2) \cdot x_{aq}^2 \cdot p^2) \quad 8.48$$

$$G_{f2d}(p) = \frac{x_{ad}}{\sigma} \cdot \{r_{kd} + (x_{kkd} - x_{ad}) \cdot p\} \cdot (\text{Cos}\alpha_2 \cdot (r_{kq} + x_{kkq} \cdot p) \cdot (r_{f1} + x_{ff1} \cdot p) - \text{Cos}\alpha_1 \cdot x_{f12} \cdot (r_{kq} + x_{kkq} \cdot p) \cdot p - \text{Sin}\alpha_1 \cdot \text{Sin}(\alpha_1 + \alpha_2) \cdot x_{aq}^2 \cdot p^2) \quad 8.49$$

$$G_{f1q}(p) = -\frac{x_{aq}}{\sigma} \cdot \{r_{kq} + (x_{kkq} - x_{aq}) \cdot p\} \cdot (\text{Sin}\alpha_1 \cdot (r_{kd} + x_{kkd} \cdot p) \cdot (r_{f2} + x_{ff2} \cdot p) + \text{Sin}\alpha_2 \cdot x_{f12} \cdot (r_{kd} + x_{kkd} \cdot p) \cdot p - \text{Cos}\alpha_2 \cdot \text{Sin}(\alpha_1 + \alpha_2) \cdot x_{ad}^2 \cdot p^2) \quad 8.50$$

$$G_{f2q}(p) = \frac{x_{aq}}{\sigma} \cdot \{r_{kq} + (x_{kkq} - x_{aq}) \cdot p\} \cdot (\text{Sin}\alpha_2 \cdot (r_{kd} + x_{kkd} \cdot p) \cdot (r_{f1} + x_{ff1} \cdot p) + \text{Sin}\alpha_1 \cdot x_{f12} \cdot (r_{kd} + x_{kkd} \cdot p) \cdot p - \text{Cos}\alpha_1 \cdot \text{Sin}(\alpha_1 + \alpha_2) \cdot x_{ad}^2 \cdot p^2) \quad 8.51$$

$$M(p) = \frac{x_{ad} \cdot x_{aq}}{2\sigma} \cdot p \cdot (r_{kq} + (x_{kkq} - x_{aq}) \cdot p) \cdot \{r_{kd} + (x_{kkd} - x_{ad}) \cdot p\} \cdot (\text{Sin} 2\alpha_2 \cdot (r_{f1} + x_{ff1} \cdot p) - \text{Sin} 2\alpha_1 \cdot (r_{f2} + x_{ff2} \cdot p) + 2 \cdot \text{Sin}(\alpha_1 - \alpha_2) \cdot x_{f12} \cdot p) \quad 8.52$$

where

$$\begin{aligned} \sigma = & (\text{Sin}(\alpha_1 + \alpha_2) \cdot x_{ad} \cdot x_{aq} \cdot p^2)^2 - 2 \cdot \text{Sin}\alpha_1 \cdot \text{Sin}\alpha_2 \cdot x_{aq}^2 \cdot x_{f12} \cdot (r_{kd} + x_{kkd} \cdot p) \cdot \\ & p^3 + (r_{kd} + x_{kkd} \cdot p) \cdot (r_{kq} + x_{kkq} \cdot p) \cdot \{(r_{f1} + x_{ff1} \cdot p) \cdot (r_{f2} + x_{ff2} \cdot p) - x_{f12}^2 \cdot \\ & p^2\} - x_{aq}^2 \cdot (r_{kd} + x_{kkd} \cdot p) \cdot \{\text{Sin}^2\alpha_1 \cdot (r_{f2} + x_{ff2} \cdot p) + \text{Sin}^2\alpha_2 \cdot (r_{f1} + x_{ff1} \cdot p)\} \cdot \\ & p^2 + 2 \cdot \text{Cos}\alpha_1 \cdot \text{Cos}\alpha_2 \cdot x_{ad}^2 \cdot x_{f12} \cdot (r_{kq} + x_{kkq} \cdot p) \cdot p^3 - x_{ad}^2 \cdot (r_{kq} + x_{kkq} \cdot p) \cdot \\ & \{\text{Cos}^2\alpha_1 \cdot (r_{f2} + x_{ff2} \cdot p) + \text{Cos}^2\alpha_2 \cdot (r_{f1} + x_{ff1} \cdot p)\} \cdot p^2 \quad 8.53 \end{aligned}$$

It is obvious that the expression for $M(p)$ will be only equal to zero if the two field windings are identical and have equal inclination angles to the direct-axis of the rotor. This, in turn, proves that the technique of replacing the dual-excited machine by an equivalent one, which has two field windings located on the two axes of the rotor²⁹, is not valid except for this special case.

Appendix D - Steady-State Vector Diagram of the Dual-Excited Synchronous Machine*

For steady-state operation, the speed $p\theta$ is constant and if the time t is measured from the instant at which the axis of phase a is in line with the direct-axis of the rotor, then:

$$\theta = p\theta_0 \cdot t \quad 8.54$$

According to Park's transformation, the equations of the voltage and current in phase a are:

$$v_{to} = v_{tdo} \cdot \cos(p\theta_0 \cdot t) - v_{tqo} \cdot \sin(p\theta_0 \cdot t) \quad 8.55$$

$$i_{to} = i_{tdo} \cdot \cos(p\theta_0 \cdot t) - i_{tqo} \cdot \sin(p\theta_0 \cdot t) \quad 8.56$$

Now, if the voltage and current of phase a (R.M.S. values) are represented by vectors \bar{V}_{to} and \bar{I}_{to} as in Fig. 8.3,

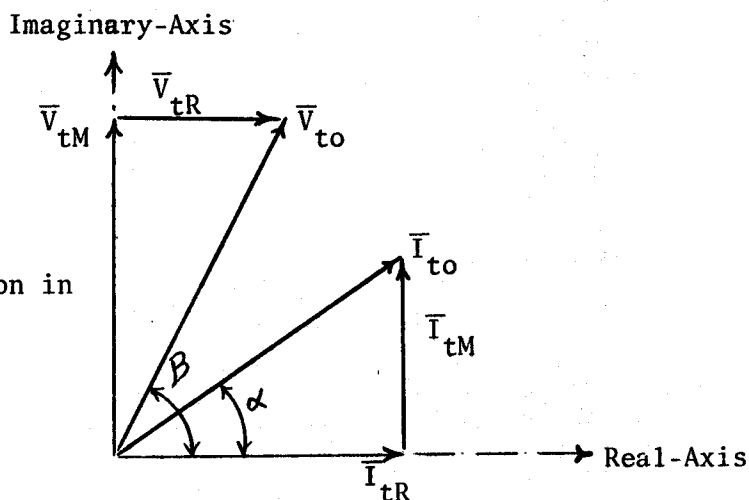


Fig. 8.3
Armature Current and
Voltage Representation in
a Complex Plane

the components of these vectors in the real and imaginary axes can be related to the phase quantities. \bar{V}_{to} is the sum of two component vectors \bar{V}_{tR} and \bar{V}_{tM} and \bar{I}_{to} is the sum of two component vectors \bar{I}_{tR} and \bar{I}_{tM} . If the magnitudes of these components are denoted by V_{tR} , V_{tM} , I_{tR} and I_{tM}

* All equations in this appendix are not normalized.

respectively, then:

$$\bar{V}_{to} = V_{tR} + jV_{tM} \quad 8.57$$

$$\bar{I}_{to} = I_{tR} + jI_{tM} \quad 8.58$$

The phase voltages and currents are known to alternate with frequency $p\theta_o/2\pi$. Hence:

$$v_{to} = \sqrt{2}|\bar{V}_{to}| \cdot \text{Cos}(p\theta_o \cdot t + B) \quad 8.59$$

$$i_{to} = \sqrt{2}|\bar{I}_{to}| \cdot \text{Cos}(p\theta_o \cdot t + \alpha) \quad 8.60$$

where $|\bar{V}_{to}|$ and $|\bar{I}_{to}|$ are the magnitudes of the vectors \bar{V}_{to} and \bar{I}_{to} respectively. Equations 8.59 and 8.60 can be rewritten as follows:

$$v_{to} = \sqrt{2} \cdot V_{tR} \cdot \text{Cos}(p\theta_o \cdot t) - \sqrt{2} \cdot V_{tM} \cdot \text{Sin}(p\theta_o \cdot t) \quad 8.61$$

$$i_{to} = \sqrt{2} \cdot I_{tR} \cdot \text{Cos}(p\theta_o \cdot t) - \sqrt{2} \cdot I_{tM} \cdot \text{Sin}(p\theta_o \cdot t) \quad 8.62$$

Equations 8.61 and 8.62 should agree with equations 8.55 and 8.56 at all instants of time. Hence:

$$v_{tdo} = \sqrt{2} \cdot V_{tR} \quad 8.63$$

$$v_{tqo} = \sqrt{2} \cdot V_{tM} \quad 8.64$$

$$i_{tdo} = \sqrt{2} \cdot I_{tR} \quad 8.65$$

$$i_{tqo} = \sqrt{2} \cdot I_{tM} \quad 8.66$$

It is seen from equations 8.63 - 8.65 that the direct- and quadrature-axis components of the voltage and current of phase a can be represented on a complex plane vector diagram. On this diagram, the real-axis corresponds to the direct-axis, while the imaginary-axis corresponds to the quadrature-axis. Thus, it will be more convenient to

replace V_{tR} , V_{tM} , I_{tR} and I_{tM} by V_{tdo} , V_{tqo} , I_{tdo} and I_{tqo} respectively.

It should be also noted that when working with per-unit quantities, there is no differentiation between maximum and R.M.S. values since both have the same per-unit value. The factor $\sqrt{2}$ will disappear from all the equations.

As it can be deduced from equations 8.63 - 8.66 and also from Park's transformation, the axis components of the voltage and current are constant values independant of time. Moreover, the induced e.m.fs and currents are constant and the damper winding voltage and current are zero. The general equations 3.23 and 3.24 can therefore be simplified as follows:

$$v_{f1o} = r_{f1} \cdot i_{f1o} \quad 8.67$$

$$v_{f2o} = r_{f2} \cdot i_{f2o} \quad 8.68$$

$$v_{tdo} = -r \cdot i_{tdo} + x_q \cdot i_{tqo} - e_d \quad 8.69$$

$$v_{tqo} = -r \cdot i_{tqo} - x_d \cdot i_{tdo} + e_q \quad 8.70$$

where:

$$e_d = \sqrt{2} E_d \quad 8.71$$

$$e_q = \sqrt{2} E_q \quad 8.72$$

Hence:

$$\begin{aligned} \bar{V}_{to} &= V_{tdo} + jV_{tqo} \\ &= \frac{1}{\sqrt{2}} \cdot (v_{tdo} + jv_{tqo}) \\ &= \frac{1}{\sqrt{2}} (-r \cdot i_{tdo} + x_q \cdot i_{tqo} - e_d - jr \cdot i_{tqo} - jx_d \cdot i_{tdo} + je_q) \end{aligned} \quad 8.73$$

Substituting 8.65, 8.66, 8.71 and 8.72 in 8.73:

$$\bar{E} = \bar{V}_{to} + r \cdot \bar{I}_{to} + jx_q \cdot I_{tqo} + jx_d \cdot I_{tdo} \quad 8.74$$

where

$$\bar{E} = -E_d + jE_q \quad 8.75$$

From equation 8.74, the steady-state vector diagram of the dual-excited synchronous machine can be constructed as shown in Fig. 8.4.

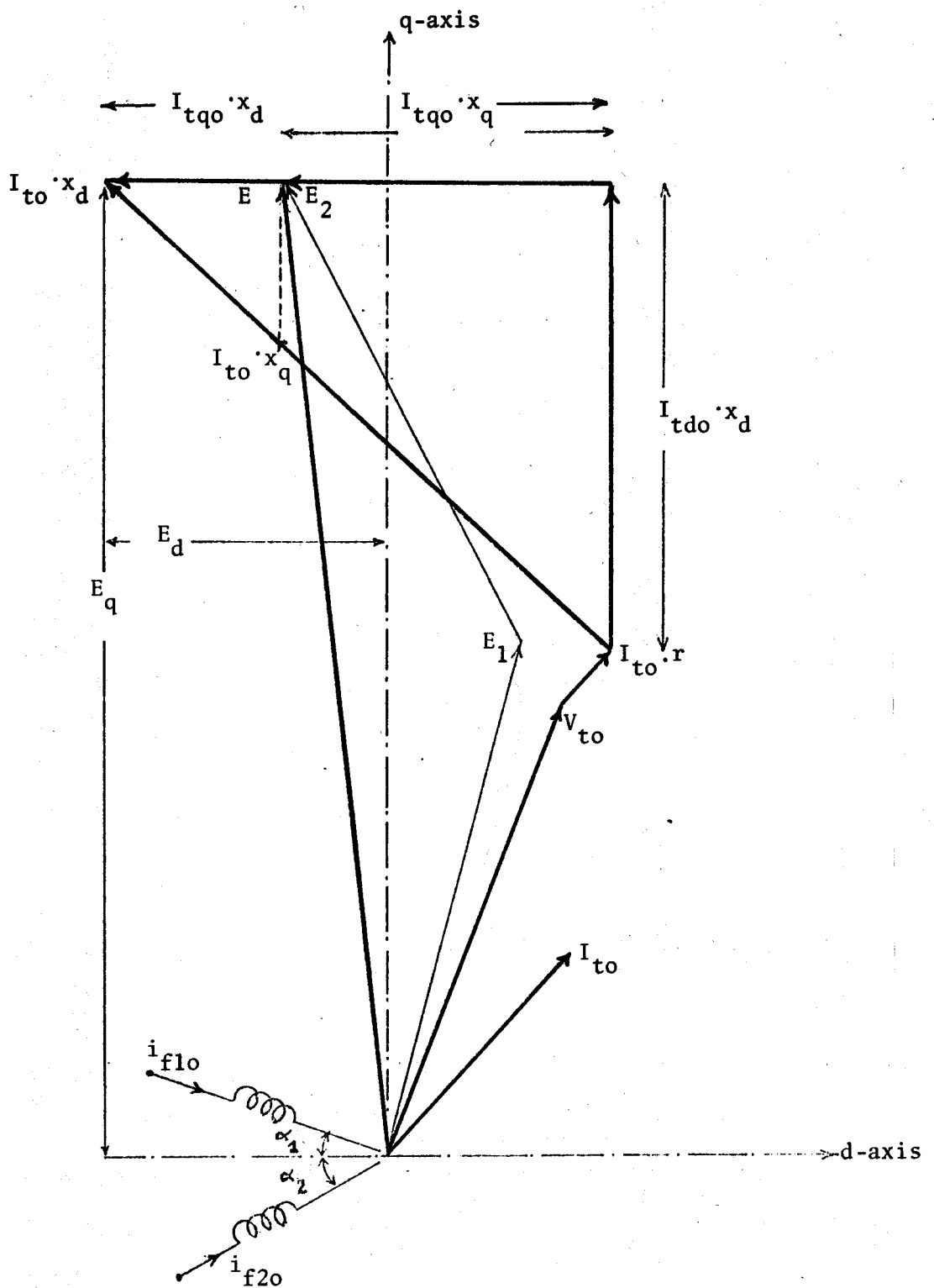


Fig. 8.4 Steady-State Vector Diagram of the Dual-Excited Synchronous Machine.

Appendix E - Power/Angle Characteristics of the Dual-Excited Synchronous Machine

The power-angle is defined as the displacement of the magnetic-axis of the exciting field from its ideal no load (no current) position. In a conventional synchronous machine, the magnetic-axis of the exciting field coincides always with the direct-axis of the rotor. Hence, the power-angle in this case is always equal to the rotor-angle. The latter is defined as the displacement of the direct-axis of the rotor from its ideal no load position.

On the other hand, the magnetic-axis of the resultant exciting field in a dual-excited synchronous machine is no longer attached to the direct-axis of the pole structure. Thus, the power-angle is not necessarily equal to the rotor-angle. In Fig. 8.5, which represents the vector diagram of a dual-excited synchronous machine connected to an infinite-bus through a simple tie line, the power-angle is denoted by δ_e while the rotor-angle by δ .

Neglecting the armature and tie-line resistances, the steady-state output power of the dual-excited synchronous generator is given by:

$$P = V_{do} \cdot I_{do} + V_{qo} \cdot I_{qo} \quad 8.75$$

From Fig. 8.5

$$V_{do} = V \cdot \sin \delta \quad 8.77$$

$$V_{qo} = V \cdot \cos \delta \quad 8.78$$

$$I_{do} = \frac{E_q - V_{qo}}{x_d + x_e} \quad 8.79$$

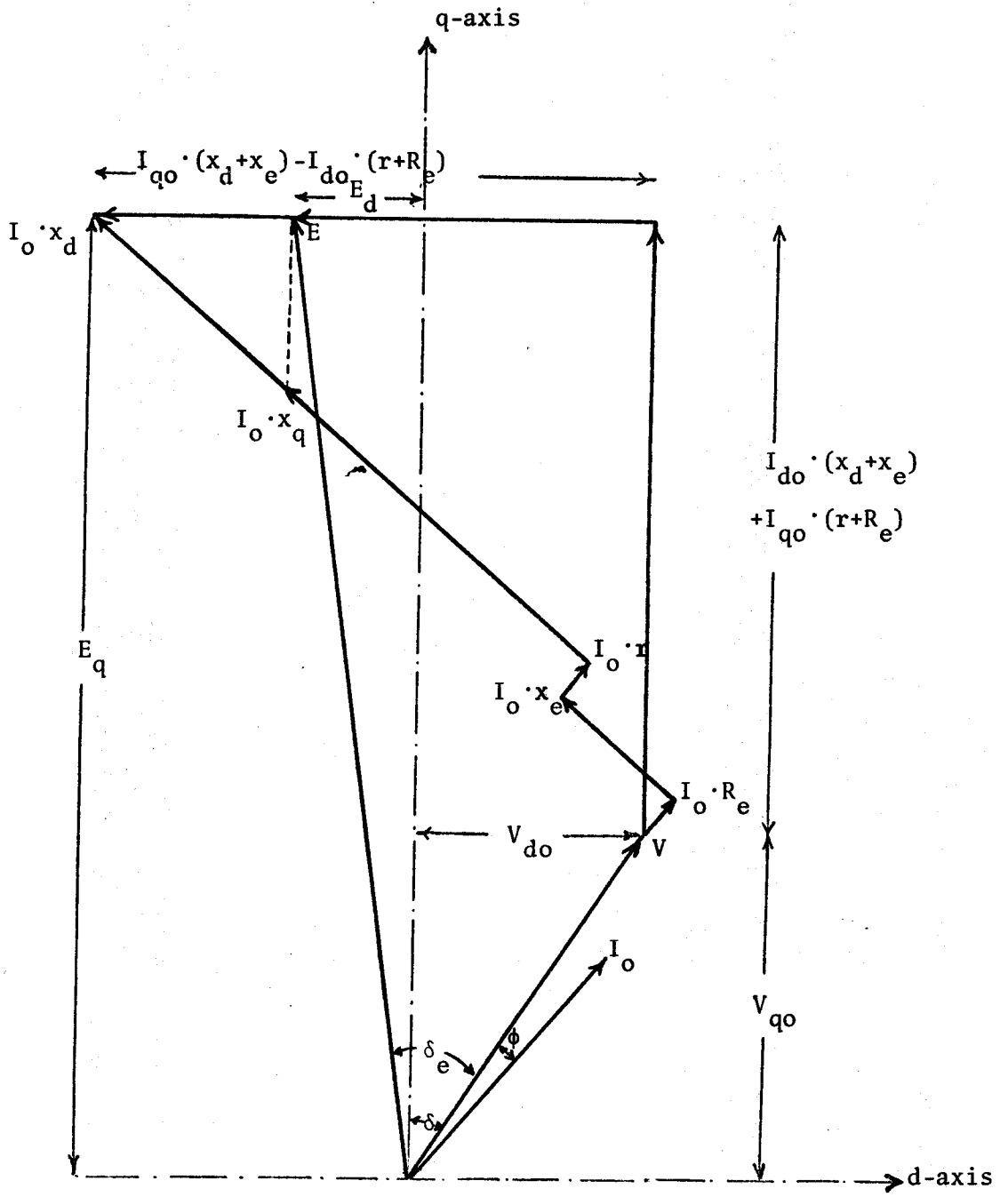


Fig. 8.5 Steady-State Vector Diagram of a Dual-Excited Synchronous Machine Connected to an Infinite-Bus Through a Simple Tie-Line

$$I_{q0} = \frac{E_d + V_{d0}}{x_q + x_e} \quad 8.80$$

Hence

$$P = \frac{V \cdot E_q}{x_d + x_e} \cdot \sin \delta + \frac{V^2}{2} \cdot \left(\frac{1}{x_q + x_e} - \frac{1}{x_d + x_e} \right) \cdot \sin 2\delta + \frac{V \cdot E_d}{x_q + x_e} \cdot \cos \delta \quad 8.81$$

Equation 8.81 shows that the only difference between the power/angle equation of the dual-excited synchronous machine and that of the conventional one is the existence of an additional term, which depends on the direct-axis component of the resultant electromotive force. A plot for this equation is given in Fig. 8.6.

The curves obtained show that the power/angle characteristics can take different shapes according to the ratio between the exciting voltages of both field windings. Moreover, the maximum output power under these conditions does not necessarily occur at $\delta=90^\circ$, as for a nonsalient-pole conventional machine, or at an angle, which depends on the ratio between the reluctance power and the exciting field power, as in the case of salient pole conventional machines. It can happen for certain ratios of the exciting voltages that the maximum power occurs at rotor angles far beyond 90° . This fact is of great interest as far as transient stability is concerned.

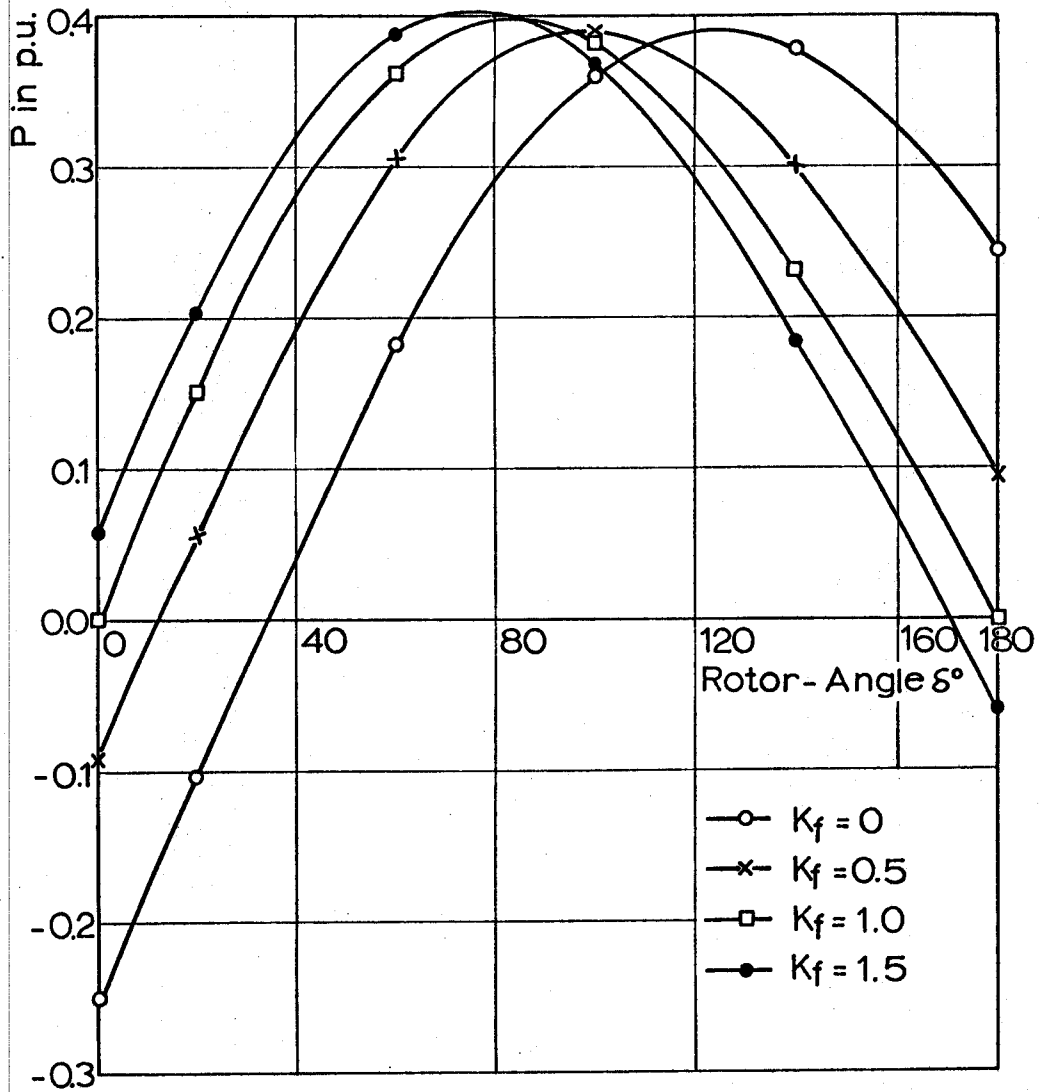
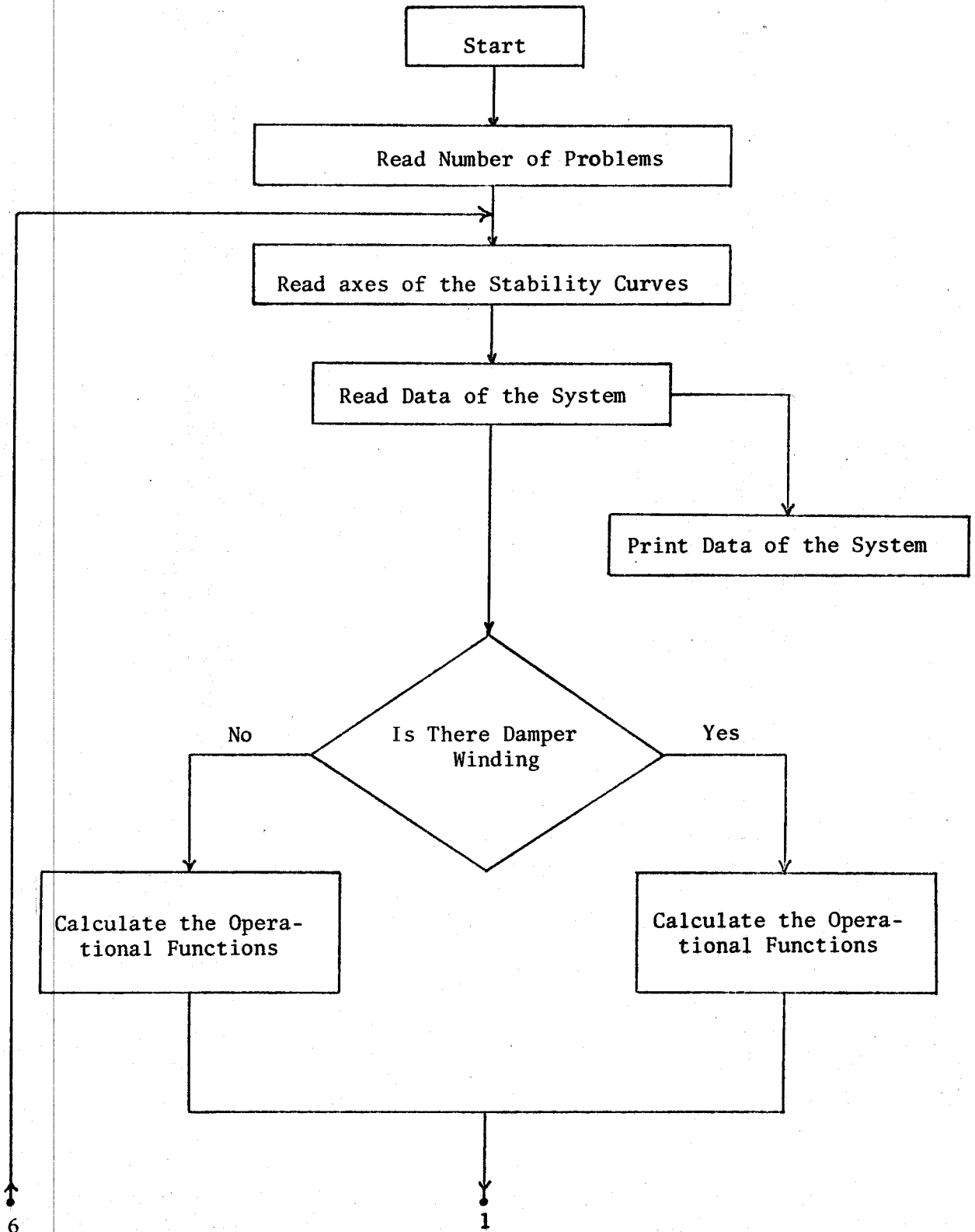
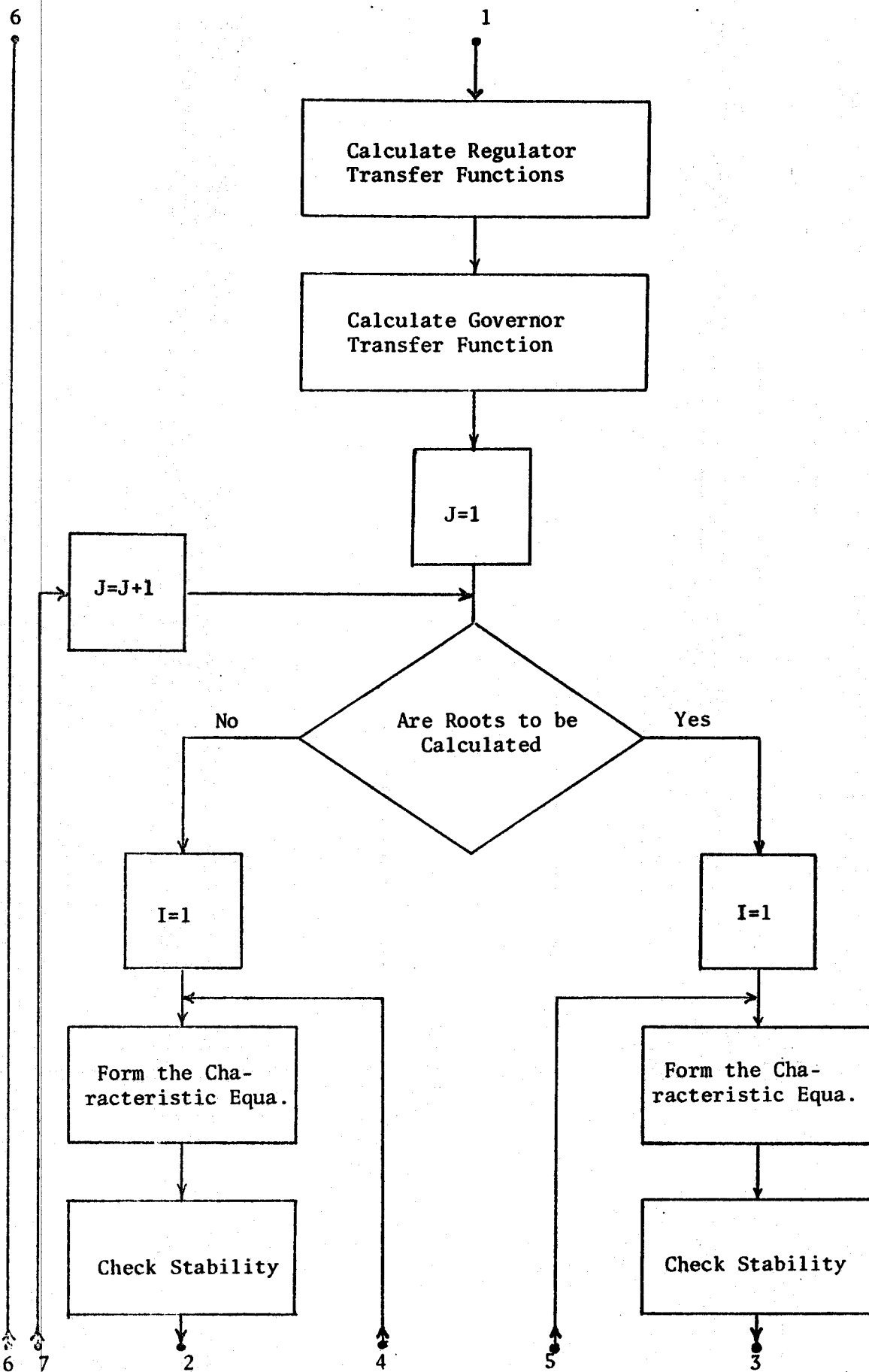
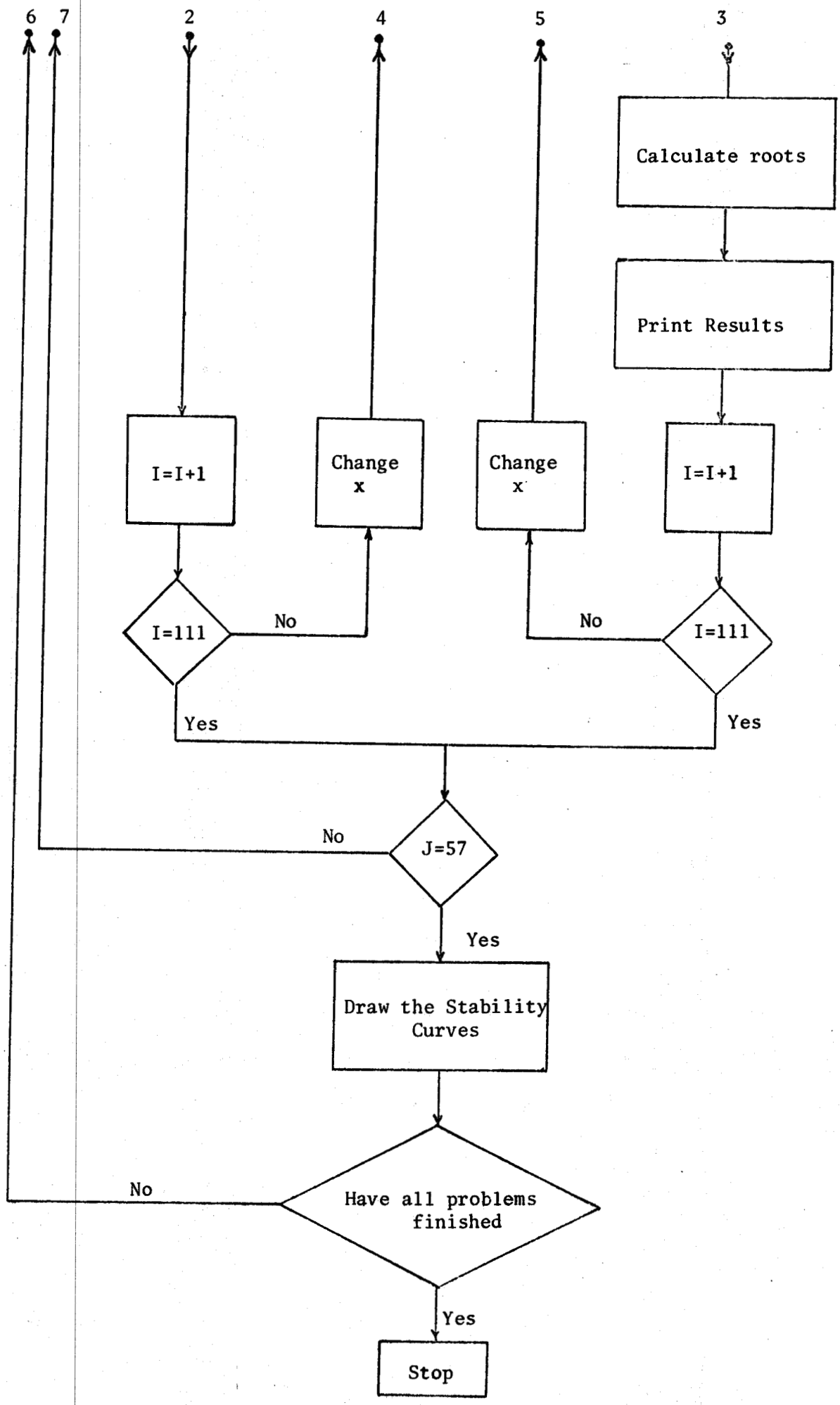


Fig. 8.6 Steady-State Power/Angle Characteristics of the Dual-Excited Synchronous Machine ($E=1.0$ p.u.)

Appendix F -- Flow Chart of the Dual-Excited Synchronous Machine Dynamic Stability Program.







Appendix G -- Typical Computer Results



Fig. 8.7 Typical Computer Results for the Dynamic Stability Boundaries (P-Q) of the Dual-Excited Synchronous Generator when Operated with Equally Excited Field Windings (Field Winding 2 is Controlled by a Rotor-Angle Regulator, C2δ=1)

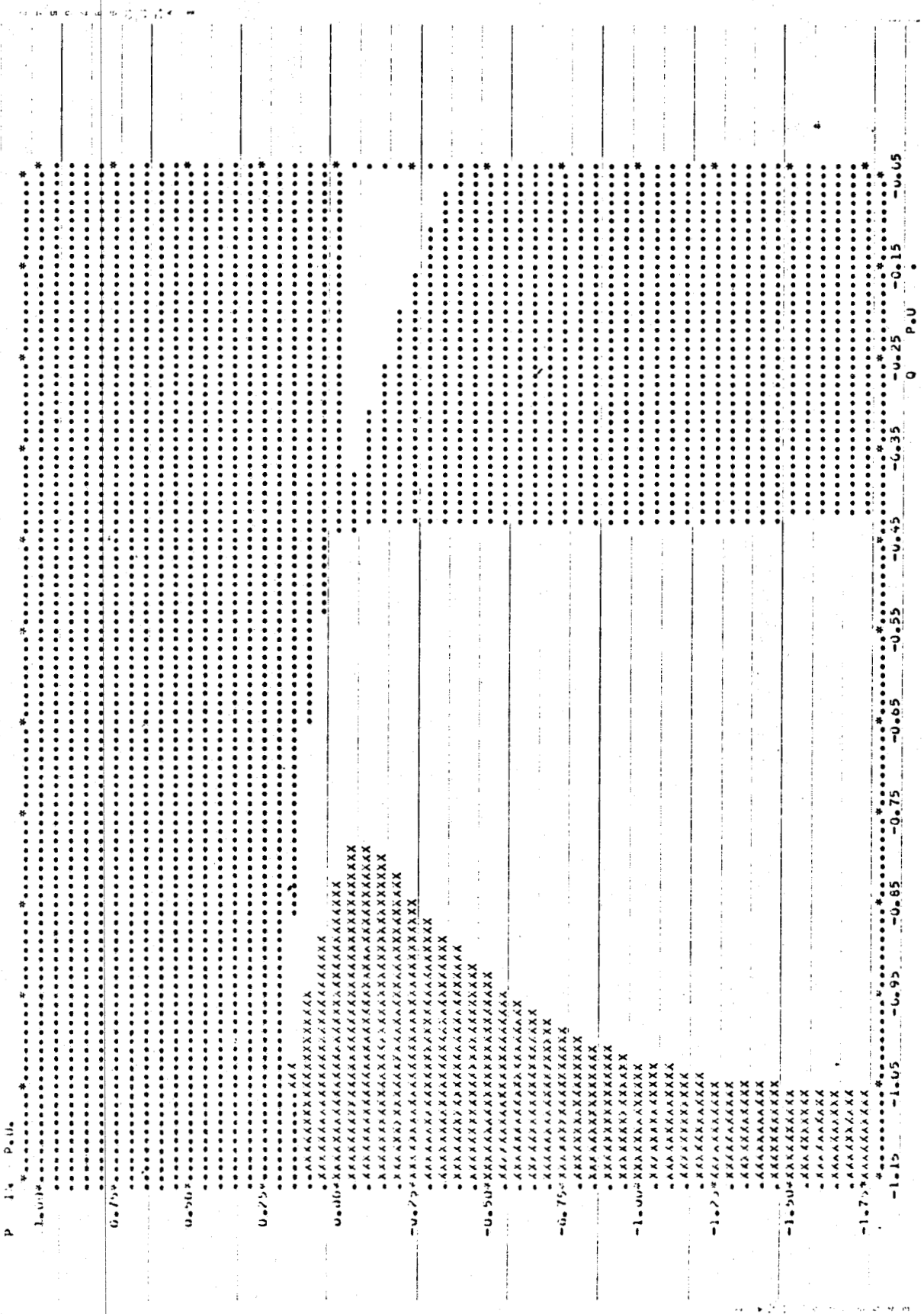


Fig. 8.8 Typical Computer Results for the Dynamic Stability Boundaries (P-Q) of the Dual-Excited Synchronous Generator when Operated with Equally Excited Field Windings (Field Winding 2 is Controlled by a Rotor-Angle Regulator, $C_{2\delta}=-1$)

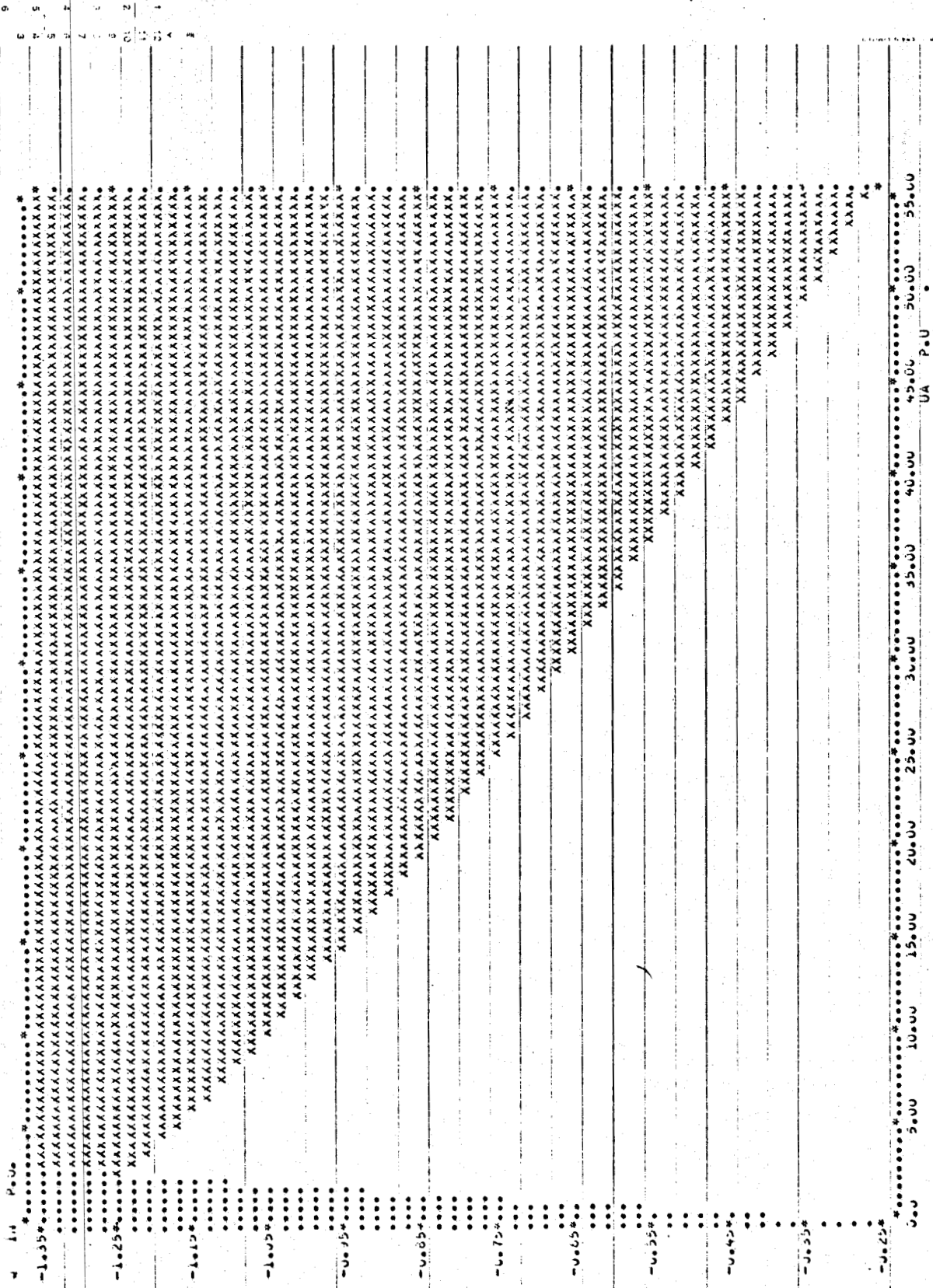


Fig. 8.9 Typical Computer Results for the Dynamic Stability Boundaries ($Q-\mu_a$) of the Dual-Excited Synchronous Generator for Operation with Fixed Rotor-Angle (Field Winding 2 is Controlled by a Rotor-Angle Regulator, $\delta=90^\circ$)